Beamforming for Performance Optimization of a Cellular Radio System

Von der Fakultät für Ingenieurwissenschaften

der Universität Duisburg-Essen

zur Erlangung des akademischen Grades eines

Doktor-Ingenieurs

genehmigte Dissertation

von

Batu Krishna Chalise

aus

Nepal

Referent: Prof. Dr.-Ing. Andreas Czylwik
Korreferent: Prof. Dr.-Ing. Armin Wittneben

Tag der mündlichen Prüfung: 21.04.2006

Abstract

In recent years, the demand for reliable transmission of high speed data and multimedia traffic in wireless communications has been growing tremendously. To alleviate the problem of scarce radio spectrum and to achieve the ambitious requirements for the existing and future generation wireless systems, attention has been recently turned into multiple antenna systems such as Smart Antenna (SA) and Multiple Input Multiple Output (MIMO) systems which may use adaptive beamforming. This dissertation aims at investigating and designing beamforming algorithms for multiple antenna wireless communication systems.

In the first part of the dissertation, the system level performance of wireless systems such as the Universal Mobile Telecommunications System (UMTS) with SAs at the Base Stations (BSs) is evaluated by using a novel and dynamic system level simulator. Compared with other investigations, the present evaluation takes into account the dynamic and stochastic behaviour of the radio propagation channel along with power control, soft handover and code management.

The second part of the dissertation is devoted to downlink beamforming based upon uplink channel parameters for UMTS Frequency Division Duplex (FDD) systems. A robust transformation of uplink to downlink spatial covariance matrices is proposed in order to overcome the adverse effect of uplink channel estimation errors into downlink beamforming. This method performs better than the previous approaches and can be efficiently implemented for realistic wireless networks.

Robust uplink and downlink beamforming algorithms based upon an outage probability criterion have been proposed in the third part of the dissertation. These algorithms reduce the degradation in system level performance caused by the uncertainty of the uplink and downlink spatial covariance matrices. Compared with the earlier robust methods based on worst-case performance optimization, the proposed algorithms do not need the knowledge of the upper bound of the uncertainty.

In the last part of this dissertation, a new stochastic approach is proposed for the design of a single user robust MIMO transmitter which has only partial Channel State Information (CSI). The proposed transmitter enhances the robustness of the MIMO system against erroneous CSI. A power control optimization problem for a multiuser MIMO system is also solved in order to minimize the BS transmit power while maintaining a minimum level of Quality of Service (QoS) for all Mobile Stations (MSs).

Acknowledgements

I would like to express my heartfelt gratitudes to Prof. Dr.-Ing. Andreas Czylwik for his valuable guidance and suggestions which have made this task possible. His encouragement and enthusiasm throughout my PhD studies helped me a lot to overcome the challenges related with research topics. I remember that I used to have open and fruitful discussions with him regardless of his busy schedule. I would also like to extend my sincere gratitude to him for providing financial support for attending various conferences. I am very much thankful to Prof. Dr.-Ing. Armin Wittneben of ETH, Zurich, for kindly agreeing to act as a second reviewer of this dissertation. Many thanks to Prof. Dr.-Ing. Peter Jung, Prof. Dr.-Ing. Axel Hunger and Prof. Dr.-Ing. Joachim Herbertz, who have been the members of my PhD examination committee.

I am deeply indebted to the members of Smart Antenna Research Team headed by Prof. Dr.-Ing. Alex Gershman for suggesting me on various issues of adaptive and robust beamforming methods. I would also like to appreciate all the distinguished lecturers who helped me to have deeper insights into the research topics. During my stay at the Department of Communication Systems, University of Duisburg-Essen, I did have very fruitful discussions with Prof. Mohammed Gharavi-Alkansari, Dr. Mehrzad Biguesh, Dr. Shahram Shahbazpanahi, Dr. Sergiy Vorobyov and many others. I am very much thankful for their time and encouragement.

I would like to extend my special thanks to my colleague Lars Häring for his cooperation during development of the MATLAB simulator. I would like to thank my other colleagues; Stefan Bieder, Kevan Zarifi and Yue Rong for giving me their time and suggestions throughout my studies. At this moment I am very much thankful to all the members of Department of Communications Engineering, especially Mrs. Petra Hoetger and Prof. Dr.-Ing. Peter Laws for providing me the overwhelming support and care during my work as a PhD student.

Recently, me and my wife have been blessed with a baby girl. She has been a major source of my satisfaction during the hectic months of thesis writing. I would like

to thank my wife, parents and brothers who have always encouraged me in my work with utmost love and care. Finally, I would like to dedicate this work to A. C. Bhaktivedanta Swami Prabhupada, founder spiritual master of the International Society of Krishna Consciousness (ISKCON), the Vaishnavas and devotees of Lord Krishna, who have inspired me to understand the science of self-realization through devotional practice.

Duisburg, April, 2006.

List of Abbreviations

2G	Second Generation
3G	Third Generation
4G	Fourth Generation
3GPP	Third Generation Partnership Project
ACM	Adaptive Modulation and Coding
AMPS	Advanced Mobile Phone System
BCH	Broadcast Channel
BOD	Bandwidth on Demand
BPSK	Binary Phase Shift Keying
BS	Base Station
CCI	Co-channel Interference
CDMA	Code Division Multiple Access
CSI	Channel State Information
DCH	Dedicated Channel
DECT	Digital European Cordless Telephony
DPDCH	Dedicated Physical Data Channel
EDGE	Enhanced Data Rates for GSM Evolution
EGC	Equal Gain Combining
FDD	Frequency Division Duplex
FDMA	Frequency Division Multiple Access
FM	Frequency Modulation
GSM	Global System of Mobile Communications
HARQ	Hybrid Automatic Request
HSDPA	High Speed Downlink Packet Access

IMT	International Mobile Telephony
IS-95	U.S. Digital Cellular Standard
ISI	Inter Symbol Interference
ITU	International Telecommunications Union
LP	Linear Programming
LSMI	Loaded Sample Matrix Inversion
MATLAB	Matrix Laboratory, Simulation software from Mathworks
M-QAM	M-ary Quadrature Amplitude Modulation
MRC	Maximum Ratio Combining
MRT	Maximum Ratio Transmission
ML	Maximum Likelihood Estimate
MIMO	Multiple Input Multiple Output System
MMSE	Minimum Mean Square Error
MS	Mobile Station
MTSO	Mobile Telephone Switching Office
MVDR	Minimum Variance Distortionless Response
NAMPS	Narrow Band Advanced Mobile Phone System
NMT-900	Nordic Mobile Telephone System
OFDMA	Orthogonal Frequency Division Multiple Access
OSTBC	Orthogonal Space-Time Block Code
OVSF	Orthogonal Variable Spreading Factor
PDC	Pacific Digital Cellular
PHS	Personal Handyphone System
QoS	Quality of Service
QP	Quadratic Program
QCLP	Quadratically Constrained Linear Program
QCQP	Quadratically Constrained Quadratic Program
QPSK	Quadrature Phase Shift Keying
RLS	Robust Least Squares
SA	Smart Antenna
SAS	Smart Antenna System
SD	Selection Diversity
SDP	Semidefinite Programming
SIR	Signal-to-Interference Ratio

SINR	Signal-to-Interference-Plus-Noise Ratio
SMI	Sample Matrix Inversion
SNR	Signal-to-Noise Ratio
SOC	Second-Order Cone
SOCP	Second-Order Cone Program
TACS	Total Access Cellular System
TDD	Time Division Duplex
TLS	Total Least Squares
ULA	Uniform Linear Array
UCA	Uniform Circular Array
UMTS	Universal Mobile Teleccomunication Services
WCDMA	Wide Band Code Division Multiple Access
WiMAX	Worldwide Interoperability for Microwave Access
ZMCSCG	Zero Mean Circularly Symmetric Complex Gaussian

List of Mathematical Symbols

$\mathbf{w}$	Beamforming weight vector
$\mathcal{C}^{M\times 1}$	Complex vector space
$(\cdot)^T$	Stands for transpose
$(\cdot)^H$	Stands for Hermitian
$s(t)$	Desired information bearing signal
$i(t)$	Interfering signal
d	Spacing between adjacent antenna elements
θ	Direction of Arrival
λ_{c}	Carrier wavelength
τ	Time delay
v_{w}	Velocity of plane wave
c	Speed of light in vacuum
ϕ	Phase shift
$\mathbf{R}_{\mathrm{Tx}}$	Spatial correlation matrix for transmitter side
$\mathbf{R}_{\mathrm{Rx}}$	Spatial correlation matrix for receiver side
$\mathbf{H}$	$n_r \times n_t$ MIMO channel matrix
$\mathbf{H}_w$	$n_r \times n_t$ MIMO channel matrix with i.i.d. Gaussian elements with unit variance
ρ	Correlation coefficient
σ_s^2	Signal power
$\mathbf{a}(\theta)$	Array response or steering vector for direction θ
$\mathbf{R}_{i+n}^d$	Interference-plus noise covariance matrix
$\hat{\mathbf{R}}$	Sample covariance matrix
$\hat{\mathbf{R}}_{\mathrm{dl}}$	Diagonally loaded data covariance matrix
$\mathbf{w}_{\mathrm{LSMI}}$	Weight vector for LSMI scheme
$\mathbf{I}$	Identity Matrix
M	Number of receive/transmit antenna elements for smart antenna systems

Q	Number of multipaths
K	Number of users in the system
$\alpha_l(t)$	Complex envelope of the path fading
$\mathbf{h}_d(t,\tau)$	Time variant vector-channel impulse response for desired user
$\tau_{d,l}$	Delay of l-th path of the desired user d
$\psi_{d,l}$	Phase offset of the l-th path of the desired user
$f_{d,l}$	Doppler frequency
$A_{d,l}$	Path transfer factor (amplitude) of l-th path of the user d
f_{up}	Uplink frequency
$\mathbf{R}_d$	Spatial covariance matrix for desired user d
$\mathbf{R}_I$	Cumulative spatial covariance matrix for interfering users
σ_θ	Standard deviation of angular spread
$\mathbf{R}_{m,n}$	Spatial fading correlation between m and n-th elements of antenna array
r	Radius of UCA
$f_\Theta(\theta)$	Probability density function of DoA
$J_n(x)$	Modified Bessel function of the first kind
C	Convex set/Convex cone
$\mathcal{R}^n$	Real vector space
$\mathbf{S}_+^n$	Set of positive semidefinite matrices
$\text{tr}(\mathbf{A})$	Trace of the matrix $\mathbf{A}$
T	Sampling period
$v(kT)$	Velocity of the MS at the time instant kT
$\mathbf{r}(kT)$	Position vector of MS at k-th snapshot
$f_v(v)$	Probability density function of MS speed
$\varphi(t)$	Direction of the movement of MS
$\Delta\varphi$	Swing angle with probability density function $f_{\Delta\varphi}(\Delta\varphi)$
$\Delta\varphi_{\max}$	Maximum swing angle
$f_A(a)$	Discrete probability density function of random variable A
λ_{r}	Average call arrival rate
$\tilde{\mu}$	Mean call duration
t_H	Holding time
ϵ	Spatial correlation between two points separated by distance D

$L_l(k_0)$	Path loss in dB for l-th path
$L_d(k_0$	Distance attenuation according to COST-HATA model
σ_{sf}	Standard deviation of log-normal fading $L_{\text{sf}}(k_0)$
σ_{pf}	Standard deviation of log-normal fading of reflected paths $L_{\text{pf},l}(k_0)$
α_{ijl}^2	Medium term expectation of transmission factor $\alpha_{ijl}^2(t)$
P_{CPICH}	Pilot channel power
$P_{\text{Intra},i}$	Intra-cell interference power
$P_{\text{Inter},i}$	Inter-cell interference power
$G_{\text{p},i}$	Spreading factor for i-th MS
λ_{up}	Uplink wavelength
λ_{dl}	Downlink wavelength
f_{dl}	Downlink frequency
$\mathbf{a}(\theta_{ijl}, \lambda_{\text{up}})$	Uplink steering vector
$\mathbf{a}(\theta_{ijl}, \lambda_{\text{dl}})$	Downlink steering vector
$\mathbf{a}'(\theta_{ijl}, \lambda_{\text{up}})$	Erroneous uplink steering vector
$\mathbf{R}'_{ij}(\lambda_{\text{up}})$	Uplink spatial covariance matrix based on $\mathbf{a}'(\theta_{ijl}, \lambda_{\text{up}})$
$\mathbf{R}_{ij}(\lambda_{\text{up}})$	Uplink spatial covariance matrix based on $\mathbf{a}(\theta_{ijl}, \lambda_{\text{up}})$
$\hat{\mathbf{R}}_{ij}(\lambda_{\text{dl}})$	Estimate of downlink covariance matrix $\mathbf{R}_{ij}(\lambda_{\text{dl}})$
$\hat{\mathbf{a}}(\theta_{ijl}, \lambda_{\text{up}})$	Estimated uplink steering vector
$\mathbf{T}$	Transformation matrix
$P(\theta_{ijl})$	Power for l-th path of the channel between i-th MS and j-th BS
$\mathbf{T}_{\text{R}}$	Transformation matrix for robust method
$\mathbf{A}_{\text{Up}}$	Matrix of uplink steering vectors
$\mathbf{A}_{\text{DL}}$	Matrix of downlink steering vectors
$\text{vec}(\mathbf{A})$	Vectored form of the matrx $\mathbf{A}$
$\|\|\mathbf{A}\|\|$	Frobenius norm of the matrix $\mathbf{A}$
$\mathbf{E}$	Perturbation or error matrix
δ, ϵ_i	Norm bounds for Frobenius norm of perturbation matrix
γ	Regularisation parameter
$\mathbf{R}_i^a$	Actual spatial covariance matrix

γ_{th}	SINR/SIR threshold value
$\mathbf{W}$	Rank 1 beamforming matrix
P_{out}	Outage probability
$N_c(\mu_x, \sigma_x^2)$	Complex Gaussian distribution with mean μ_x and variance σ_x^2
$\text{erf}(x)$	Error function with parameter x
$\tilde{P}_{\text{out}}$	Non-outage probability
p_i	Target for non-outage probability
$\hat{\mathbf{H}}$	Channel estimate available at the MIMO transmitter
$\mathbf{P}$	Diagonal matrix with power factor $\sqrt{p_n}$ for each eigenmode
$\mathbf{X}'$	Orthogonal Space-Time Block Code
$\mathbf{A}^M$	Modulation matrix
$\mathbf{A}'_q, \mathbf{B}'_q$	General complex matrices used to design OSTBC
$\mathbf{B}^M$	Receiver or matched filter matrix response
$\mathbf{C}_n$	Matrix of orthonormal temporal signatures
$\hat{\mathbf{U}}$	Matrix of eigenvectors of $\hat{\mathbf{H}}^H\hat{\mathbf{H}}$
$\mathbf{D}$	Diagonal matrix with the eigenvalues of $\hat{\mathbf{H}}^H\hat{\mathbf{H}}$
$\otimes$	Kronecker's product
γ_0	Threshold value for SNR
$\mathbf{n}(t)$	Additive Gaussian noise vector
$\mathbf{y}_i(t)$	Received signal vector at the i-th user
$\mathbf{w}_i^{\text{b}}$	Weight vector used at the base station for the i-th user
$\mathbf{w}_i^{\text{m}}$	Weight vector used at the i-th MS
σ_i^r	Singular values of the matrix $\mathbf{H}_i$
$\mathbf{u}_i^r$	Left singular values for singular value decomposition of $\mathbf{H}_i$
$\mathbf{v}_i^r$	Right singular values for singular value decomposition of $\mathbf{H}_i$
$f_{\rho_k}(x)$	Probability density function of $\rho_k = \lvert(\mathbf{v}_i^1)^H\mathbf{v}_k^1\rvert$
q_i	Target outage probability
$\lvert\lvert \cdot \rvert\rvert_l$	l-th norm
$\lvert\lvert \cdot \rvert\rvert_2$	Euclidean norm
$\lvert\lvert \cdot \rvert\rvert$	Frobenius norm

Contents

List of Tables

List of Figures

Chapter 1

Introduction

The field of wireless mobile communications is growing at an unprecedented rate, covering many technical areas. The proliferation of cellular phones, cordless phones, pagers and many other wireless communication devices indicate that the demand for wireless communications is anticipated to grow steadily and quickly. As an example, from 1990 to 1999, the number of mobile telephone users in the US has increased from 5.1 million to 65 million subscribers. Today, the penetration of cellular phones to US population is close to 50%. In Europe, South Korea and Singapore about 60-70% of the population has access to mobile phones. In Taiwan, the number of cellular phones exceeds the number of people. It is estimated, that the number of cellular phone users worldwide will reach about 2 billion by 2006 from approx. 1.6 billion existing subscribers. The worldwide research and experimental activities show the importance of this ever-growing industry. However, the problem of limited channel bandwidth is a major obstacle for satisfying the ever growing number of mobile users in a wireless mobile communication system. The radio spectrum is scarce and expensive.

The first generation wireless systems were introduced in the early 1980s in order to provide voice traffic services to mobile subscribers over a wide area. They mainly employed Frequency Modulation (FM) as a modulation scheme and Frequency Division Multiple Access (FDMA) as a multiple access method. Low spectrum efficiency, requirement of high transmission power, less interference rejection capability and a poor set of service types have been the limitations of the first generation public cellular wireless communication networks. These systems employed different frequency reuse ratios and supported the movement of mobile users from one cell or area to another. The first generation systems include Advanced Mobile Phone Systems (AMPS) in North America, Nordic Mobile

Telephone/Total Access Cellular System (NMT/TACS) in Europe and Nippon-Telephone and Telegraph-800/Japanese Total Access Communication System (NTT-800/JTACS) in Japan.

The capacity limited first generation wireless systems could not cover up the increasing number of mobile subscribers. They are generally incompatible because of different frequencies and communication protocols used. The advancements in digital signal processing have paved the path for the development of Second Generation (2G) wireless systems. In order to increase the capacity of the overall system, compression and coding methods associated with digital technology are employed. Almost all 2G wireless systems have used digital modulation techniques. The multiple access schemes like Time/Code Division Multiple Access (TDMA/CDMA) along with FDMA have been used in these systems. The advanced speech coding methods with voice activity detection have reduced the required transmission data rate and also the battery drain by the mobile transmitter. The employment of TDMA has enabled the number of users to share the same channel bandwidth in time. Similarly, because of the inherent interference resistance properties of CDMA, the systems can operate at much larger interference levels than compared to first generation counterparts. Since CDMA systems can operate with much smaller SNR, they can use the same set of frequencies in every cell which provides a large improvement in capacity [83]. 2G systems that were successfully deployed worldwide are the Global System for Mobile Communications (GSM) and the Interim Standard (IS) systems based on TDMA (IS-136) and CDMA (IS-95), respectively.

The Third Generation (3G) systems are required to have voice services of wire line quality, and provide high bit rate data services of 144 kbits/s to 2 Mbits/s depending on the radio environment. The capability to provide reliable services irrespective of the type of radio environment has made 3G systems more attractive. They are going to have better quality and coverage, be more power and bandwidth efficient, and be deployed in diverse environments like macro, micro, pico cellular; urban, suburban, and rural; indoor and outdoor [90].

The world organization International Telecommunications Union (ITU) has incorporated all 3G systems under a framework called International Mobile Telephony 2000 (IMT-2000). Within IMT-2000, there are several different air interfaces defined for 3G systems, based on either CDMA or TDMA. Among them, the Wide Band Code Division Multiple

Access (WCDMA) air interface is going to be widely used, from Europe to Asia including Korea and Japan, using the frequency bands allocated for 3G IMT-2000 system at around 2 GHz. In addition to WCDMA, other air interfaces that can be used to provide 3G services are EDGE (Enhanced Data Rates for GSM Evolution) and multicarrier CDMA (CDMA-2000) [54]. EDGE can provide 3G services with bit rates up to 500 kbits/s within a GSM carrier spacing of 200 KHz [83]. EDGE includes advanced features that are not part of GSM to improve the spectrum efficiency and to support new services. The multicarrier CDMA (CDMA 2000) can be used as an upgrade solution for the existing IS-95 operators, where for the downlink transmission, instead of a single wideband carrier, multiple parallel narrowband CDMA carriers are transmitted from each BS.

In 3GPP standards, Release 5 specifications introduce High Speed Downlink Packet Access (HSDPA) to provide data rates up to approximately 14 Mbps to support packet-based multimedia services. HSDPA is an extension of WCDMA downlink and includes Adaptive Modulation and Coding (AMC), Hybrid Automatic Request (HARQ), fast cell search, and advanced receiver design. Recently, the Orthogonal Frequency Division Multiple Access (OFDMA) has become major topic of interest for researchers because of its capability to transmit high data rates over frequency selective wireless channels. OFDMA based WiMAX [2] system is being projected as one of the most attractive candidates for 4G wireless systems.

As the number of subscribers grows, spectral crowding and Co-channel Interference (CCI) become important issues in all types of the wireless systems overviewed above. CCI arises from frequency reuse whereby multiple cells operate at the same carrier frequency. The geographic conditions and the propagation environment induce various effects like noise, multipath and fading of the wireless channels. Multiple antennas provide a means to improve the spectral efficiency and quality of communications over wireless channels. They are capable of simultaneously estimating the channels of several co-channel sources as well as demodulating the sources themselves. Depending on the multiple number of antennas used at the transmitter and /or receiver, the multiple antenna system can be classified as SA and MIMO system. SA and MIMO systems are expected to even increase the data transmission capacity of the packet data oriented wireless systems like HSDPA and WiMAX.

1.1 Smart Antenna Wireless Communication System

Figure 1.1 shows a wireless communication system which employs multiple antennas at the BS. The idea of SA is to exploit the spatial properties of wave propagation. Because of a limitation of space, SAs are mainly used only at BSs. SAs consist of an array of

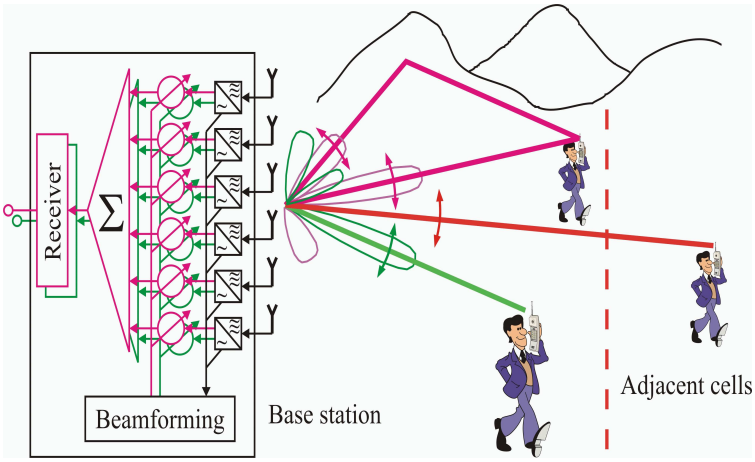

Figure 1.1: Wireless communication system with smart antenna

antenna elements and a smart processing of antenna signals. With the help of signal processing, the beam pattern of the antenna array is optimally adapted to the mobile radio channel.

In wireless communication 'uplink' is described as the transmission from MSs to BSs whereas 'downlink' is the transmission from BSs to MSs. The goal is to receive in the uplink as much power as possible from the desired MS and to attenuate as much as possible the signals from any undesired MS. In the downlink as much power as possible has to be transmitted into the direction of the desired MS and as little power as possible to undesired mobiles. By this method, CCI in a cellular system can be reduced, with the consequence that the capacity increases. It has to be mentioned that for each desired MS an individual beam pattern must be optimized. SAs can adaptively cancel interference produced by the MSs which use the same frequency band, time slots or spreading codes in nearby cells or as well as within the same cell.

Spatial processing with antenna arrays can facilitate a denser use of the available bandwidth and hence increase the system capacity. This gain in system performance which is obtained from the directional reception and transmission, can provide better coverage by

the BS. As a consequence, the number of BSs as well as the complexity of Mobile Telephone Switching Office (MTSO) can be reduced. Moreover, signal processing techniques can be used to concentrate the complexity to a centralised BS so that MS receivers can be simplified.

1.2 Summary of Related Work

Antenna array processing has found numerous applications in radar, sonar, siesmology and microphone speech processing [16, 40, 62]. It was originally developed for applications related with target tracking and anti-jamming military communications [57, 101]. The early technique used directed beams to hide transmissions from an enemy. The implementation required very large antenna structures and time-intensive processing and calculation. After a decade of extensive research (e.g. [75]) in this area coupled with rapid advances in microelectronics technology, high resolution antenna array technology can now achieve superior performance with affordable cost. Recently, Smart Antenna Systems (SASs) [4, 47, 92, 103] have been proposed to overcome some of the major difficulties in current wireless communication systems, e.g. multipath fading, Inter Symbol Interference (ISI) and CCI, coverage and capacity limitations, handoff, and battery life, by exploiting the spatial dimension. Downlink beamforming for the cellular wireless networks has been extensively investigated [30, 47, 71, 81, 99] in order to increase the downlink capacity. It will not be possible to provide a complete and thorough coverage of the enormous body of work on array applications to wireless systems. In the next few paragraphs, the major contributions on the subjects related to this dissertation are highlighted.

It has been shown by many studies that when an array is appropriately used in a mobile communications system, it helps in improving the system performance by increasing channel capacity and spectrum efficiency, extending range coverage, tailoring beam shape, steering multiple beams to track many mobiles, and compensating aperture distortion electronically. However, the improvement of the system performance obtained from antenna array can be evaluated in a proper way only by carrying out system level analysis in a realistic propagation environment. For this purpose, static system level simulations for downlink beamforming without power control and soft handover have been presented in [26] and [27]. Baumgartner investigated [6] downlink beam switching based upon static system level simulations. In this dissertation, we develop a novel method for

analyzing the system level performance of a cellular mobile communication system which uses BSs with SAs.

Downlink beamforming is difficult for practical mobile communication systems especially in case of FDD channels where the uplink and downlink channels are highly uncorrelated. In most of the previous researchs related with downlink beamforming, the frequency difference between uplink and downlink channels have been not considered and hence the uplink weights are directly used for downlink beamforming. Uplink to downlink covariance matrix transformation techniques like the Minimum Mean Square Error (MMSE) and the Minimum Variance Distortionless Response (MVDR) filter for downlink beamforming have been proposed in [5, 34] and [55], respectively. However, these methods are not robust against channel uncertainty. We develop a new transformation technique that provides robustness against such channel uncertainty. Channel uncertainty arises because of the difference between the true and the estimated spatial signatures.

Recently, many of the robust beamforming algorithms have been proposed to make the adaptive beamformers robust against perturbation errors. The robust adaptive beamformer proposed in [86] and [100] is based on explicit modeling of uncertainties in the desired signal array response and data covariance matrix as well as worst-case performance optimization. The optimum transmit beamforming methods that provide robustness against channel uncertainties have been discussed in [8] and [102]. However, all of these methods are based upon worst-case performance optimization which in communication systems is a pessimistic approach. The major drawback of these methods is that the beamformer must have a knowledge of the upper bound of the channel perturbation. Since errors in channel parameters are caused by mismatch in modelling of the propagation effects like multipaths, delay etc and noise, it is more logical to model the uncertainty with some statistical distribution and provide average robustness. In this dissertation, we propose uplink and downlink robust beamforming algorithms based on stochastic optimization methods.

The idea of SA technology has been recently extended to MIMO systems [35, 36, 95] which use multiple antennas both at the receiver and transmitter side for providing receiver as well as transmitter diversity. A very powerful transmission technology known as Space-Time Coding (STC) is proposed in [3, 93, 94] for MIMO systems. Like in SASs, linear processing or beamforming is also used in MIMO based wireless communications.

A Maxmin approach for the design of a robust MIMO transmitter is proposed in [58] where transmission scheme as a combination of Orthogonal Space-Time Block Code (OSTBC) and beamforming is used. The objective was to find optimum power loadings for the eigenmodes of the channel by maximizing the SNR at the receiver for a worst case channel estimate. Here, we propose a stochastic approach for the design of robust MIMO transmitter which combines OSTBC and beamforming.

An outage probability expression for the uplink of a multi-cellular MIMO system is provided in [96] for an arbitrary number of transmit and receive antennas. However, the closed form expression of outage probability was obtained for the case of equal power intracell interferers which is not the case in all types of cellular systems. If a cellular system uses CDMA technique, power control is essential in the uplink and the assumption of equal power intracell interferers is not a critical one. Moreover, any optimum power control method based upon this complex expression of outage probability needs a very high computational effort, especially if the wireless systems are big. In this dissertation, we develop a simple and approximate form of the outage probability expression for the downlink of a multiuser MIMO system that employs beamforming based upon a Maximum Ratio Transmission (MRT) technique. The advantage of this expression is that it can be used to efficiently solve the optimum power control problem for the downlink where the criterion is to minimize the total BS transmit power while satisfying the quality of service (in terms of outage probability) constraints for all MSs.

1.3 Contribution of the Dissertation

In previous research work, the use of beamforming was mainly confined to the link-level analysis of the wireless communication. The effect of the very random and complex nature of the wireless environment have not been taken into consideration. One of the important aspects of this dissertation is that it addresses the difficulties that arise in the practical implementation of the beamforming methods in a cellular wireless network. Another important aspect is that, it proposes robust beamforming algorithms that can be applied in a realistic radio propagation environment. A robust uplink to downlink spatial covariance transformation method is developed in order to provide robustness against imperfect estimation of the uplink spatial signature at the BS. We also provide robust beamforming methods based on an outage probability approach for both uplink and downlink communications. A new stochastic approach is developed for the design of

a MIMO transmitter that has only partial CSI. An optimum power control problem is solved for a multiuser MIMO system that employs beamforming.

Many of the results presented in this dissertation appeared in conference proceedings and in manuscripts published or submitted to refereed Book Chapter and Journals. The dynamic system level simulator developed for UMTS-FDD systems with SAs at the BSs in **Chapter 3** is based on results in

- "Smart antenna solutions for UMTS," *Smart Antennas – State-of-the-Art*, EURASIP Hindawi Book Series, Ed. T. Kaiser and A. Boudroux, 2005. (with A. Czylwik and A. Dekorsy)
- "System level simulation of WCDMA systems with smart antennas," *COST 273*, Barcelona, Spain, 15-17 Jan., 2003. (with L. Häring and A. Czylwik)
- "Dynamic system level simulations of UMTS-FDD with downlink beamforming," *In Proceedings of IEEE Globecom 2003*, SanFrancisco, USA, 1-5 Dec., 2003.(with L. Häring and A. Czylwik)

The non-robust and robust uplink to downlink spatial covariance matrix transformation methods for downlink beamforming in Chapter 4 are based on results in

- "System level performance with covariance transformation based DL beamforming," *In Proceedings of IEEE Globecom 2003*, SanFrancisco, USA, 1-5 Dec., 2003. (with L. Häring and A. Czylwik)
- "Uplink to downlink spatial covariance transformation concepts for downlink beamforming," *In Proceedings of IEEE ISSPIT 2003*, Darmstadt, Germany, 14-17 Dec., 2003.(with L. Häring and A. Czylwik)
- "Robust spatial covariance transformation techniques for downlink beamforming," *In Proceedings of International Zurich Seminar 2004*, Zurich, Switzerland, 19-21 Feb., 2003. (with L. Häring and A. Czylwik)
- "Uplink to downlink spatial covariance transformation methods for downlink beamforming of UMTS-FDD systems," *In Proceedings of IEEE VTC Spring 2004*, Milan, Italy, 17-21 May, 2004. (with L. Häring and A. Czylwik)
- "Robust uplink to downlink spatial covariance transformation for downlink beamforming," *In Proceedings of IEEE ICC 2004*, Paris, France, 20-24 June, 2004. (with L. Häring and A. Czylwik)

The algorithm and simulations of robust uplink beamforming based upon minimum outage probability in **Chapter 5** are based on results in

- "Robust uplink beamforming based upon mininum outage probability criterion," *IEEE Globecom 2004*, Dallas, Texas, 29 Nov.-3 Dec., 2004. (with A. Czylwik)

- "Uplink user capacity of UMTS-FDD with robust beamforming based upon minimum outage probability, " *COST 273, TD (04) 179*, Duisburg, Germany, 20-22 Sept., 2004. (with A.Czylwik)

The robust downlink beamforming algorithm presented in **Chapter 6** is based on results in

- "Robust downlink beamforming based upon outage probability criterion," *In Proceedings of IEEE VTC Fall 2004*, Los Angeles, USA, 26-29 Sept., 2004. (with A. Czylwik)

- "Robust downlink beamforming based on outage probability specifications," submitted to *IEEE Transactions on Wireless Communications*, Jan., 2006. (with S. Shahbazpanahi, A. Czylwik and A. Gershman)

Finally, the robust MIMO design and the optimum power control for MIMO systems with beamforming presented in **Chapter 7** are based on results in

- "Robust MIMO design with outage probability specifications," *In Proceedings of 2nd International Workshop on Smart Antennas WSA 2005*, Duisburg, Germany, 3-5 Apr., 2005.(with A. Czylwik)

- "Optimum power control for multiuser MIMO systems with beamforming," *In Proceedings of IEEE PIMRC'05*, Berlin, Germany, 11-14 Sept., 2005. (with A. Czylwik)

- "An outage probability approach for a robust MIMO transmitter design," *submitted to EURASIP Journal of Applied Signal Processing*, Nov. 2005. (with A. Czylwik)

1.4 Organization of the Dissertation

The remaining of the dissertation is organized as follows. **Chapter 2** presents a summary of multiple antenna systems such as SA and MIMO technology. Basics of SA principles

and algorithms along with spatio-temporal channels of the radio propagation environment are dealt in this chapter. A brief introduction of convex optimization problems like Second-Order Cone Programming (SOCP) and Semidefinite Programming (SDP) is also provided in this chapter. In **Chapter 3**, the system level performance of a UMTS-FDD system with SAs is analyzed using the dynamic system level simulator. The details of the different modules of the simulator are given in this chapter. **Chapter 4** deals with the uplink to downlink spatial covariance matrix transformation techniques along with the simulation results. We also present a new robust uplink to downlink spatial covariance matrix transformation technique in this chapter. The performance of this algorithm is compared with non-robust methods using the system level simulator. **Chapter 5** provides a robust uplink beamforming algorithm based on the minimum outage probability criterion. The performance of this algorithm is evaluated both in a deterministic as well as in probabilistic scenario. We propose an optimum robust downlink beamforming algorithm and the simulation results based on the outage probability criterion in **Chapter 6**. Single as well as multiuser MIMO systems are analyzed in **Chapter 7**. A modified algorithm for a robust MIMO transmitter in case of partial CSI is proposed in this chapter along with an optimum power control scheme for multiuser MIMO systems with beamforming. Finally, the dissertation concludes with summary and description of future research in **Chapter 8**.

Chapter 2

Principles and Concepts

This chapter deals with the fundamentals of multiple antenna systems (Section 2.1) namely SA and MIMO systems. As the major focus of this dissertation is the use of spatial filtering or beamforming for wireless cellular communications, we give a brief overview of the beamforming or SA algorithms in Section 2.2. Because channel models play a vital role in wireless communications, the basics of channel models, especially the vector channel model along with the spatial fading correlation of a Uniform Circular Antenna Array (UCA) are presented in Section 2.3. Moreover, as we emphasize on non-robust and robust beamforming for the UMTS-FDD systems, we give a brief introduction of WCDMA which is an air interface technology for UMTS-FDD systems. Most of the optimization problems that are proposed in this dissertation are convex and can be solved efficiently to find the global optimum. Therefore, the theory of convex optimization and some well known convex problems such as SOCP and SDP problems are presented in Section 2.5.

2.1 Introduction to Multiple Antenna Systems

A multi-antenna communication system is shown in Fig. 2.1. A binary data stream from a compressed digital source is fed to a transmitter which in general introduces error control coding and mapping to complex modulation symbols (QPSK, M-QAM, etc). Several separate symbol streams produced by the modulator are then mapped onto the multiple transmit antennas. Linear spatial weighting of the antenna signals or linear antenna space-time precoding can be used for mapping. After upward frequency conversion, filtering and amplification, the signals are transmitted through a wireless

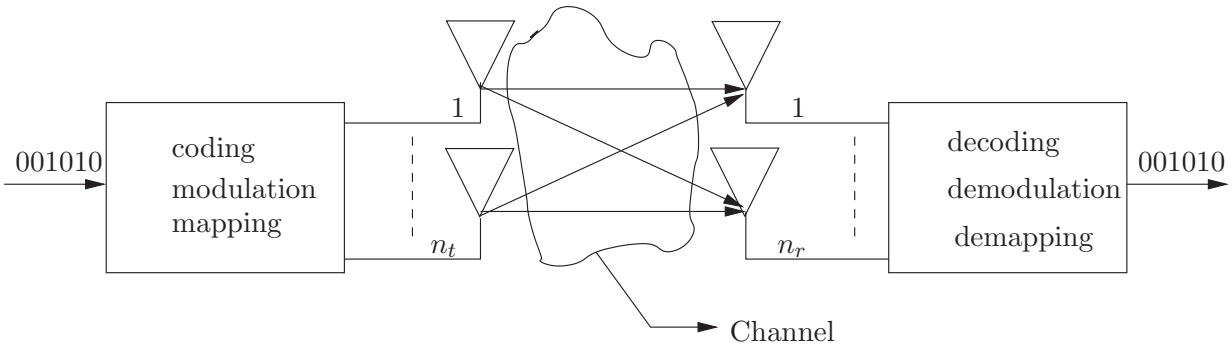

Figure 2.1: Multi-antenna wireless communication system [41]

channel. At the receiver, the signals are received by multiple antennas followed by the demodulation and demapping operations to recover the message. The selection of coding and antenna mapping algorithms depends on different factors like the availability of CSI, complexity and the application type. This determines the class and performance of the multi-antenna system that is implemented. As subscriber units are gradually evolving to become sophisticated wireless internet access devices rather than just pocket telephones, the stringent size and complexity constraints are becoming somewhat more relaxed. This makes multiple antenna transceivers a possibility at both sides of the link, although from the engineering point of view it is more logical to push most of the processing and cost to the network side like the BS or BS controller.

2.1.1 Smart Antenna Systems

If in a multi-antenna system only the transmitter or the receiver is actually equipped with more than one antenna element, being typically the BS, then such a system along with the spatial filtering method is known as a SAS. The extra cost and space that are necessary to accomodate multiple antennas have been considered more easily affordable at the BSs than on small phone handsets. The intelligence of SASs is located in the weight selection algorithm.

Signal impairments in wireless communications are mainly due to ISI and CCI. The transmitted signal arrives at the receiver with different time delays through the time-varying multipath channel. The received signal symbols are smeared and overlapped with one another. This signal distortion is called ISI [80]. Frequency reuse and multiple access cause the CCI, which are inherent features of cellular systems. Temporal and/or spatial signal processing is applied to mitigate signal impairments. Temporal signal processing reduces the ISI using an equalizer or a rake receiver. The equalizer compensates the

channel distortion and the rake receiver distinguishes each delayed signal and combines them constructively. Spatial signal processing reduces the CCI by properly combining each antenna signal. Through this operation, it is possible to extract the desired signal and to suppress interference. When spatial signal processing is combined with temporal signal processing, the space-time processing can further repair the impairments to result in higher network capacity, coverage, and quality [44, 45, 66, 76, 103]. Another powerful

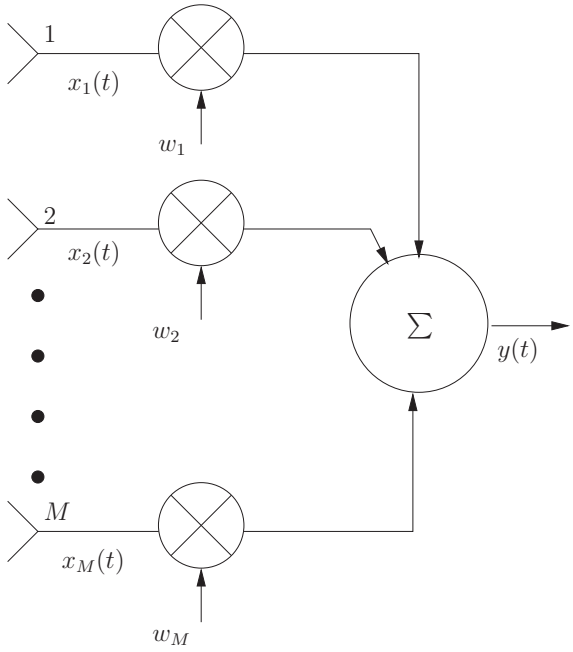

Figure 2.2: Antenna array system

effect of SA lies in the concept of spatial diversity. Spatial diversity is obtained when the separation between antenna elements is large and consequently the fading correlations among antenna elements is low [41]. In the presence of random fading caused by multipath propagation, the probability of losing the signal decreases exponentially with the increasing number of decorrelated antenna elements. This gives to a notion of diversity order which is given by the number of decorrelated spatial branches available at the receiver or transmitter. Finally, SAs provide *array gain* (improves SNR), which is obtained by combination of the signals captured by multiple antennas. When all features (*array gain*, *spatial diversity*, *interference rejection*) of SA can be combined together, it is shown that SAs improve the coverage range, and the QoS offered to the MS [77]. The *array gain* is defined as the reduction in the required received signal power for a given average output SNR, while the *diversity gain* is defined as the reduction in the required average output SNR for a given bit error rate (BER). Some antennas use horizontal and vertical polarization to achieve diversity. The angle diversity uses several narrow beam antennas.

A sector antenna in which four narrow beam antennas (each narrow beam antenna covers a section of 30°) cover a sector of 120° is an example of angle diversity.

Figure (2.2) shows a block diagram of an antenna array system, in which the signals $x_i(t),\ i = 1, \cdots, M$ received by each antenna element are weighted by complex w_i and combined to generate an output signal $y(t)$ given as

$$y(t) = \mathbf{w}^H \mathbf{x}(t), \tag{2.1}$$

where $\mathbf{w}^H = [w_1, w_2, \cdots, w_M] \in \mathcal{C}^{M\times 1}$ is the complex vector of beamforming weights, $\mathbf{x}(t) = [x_1(t), x_2(t), \cdots, x_M(t)]^T \in \mathcal{C}^{M\times 1}$ is the complex vector of array observations, and $(.)^T$ and $(.)^H$ stand for the transpose and Hermitian transpose respectively.

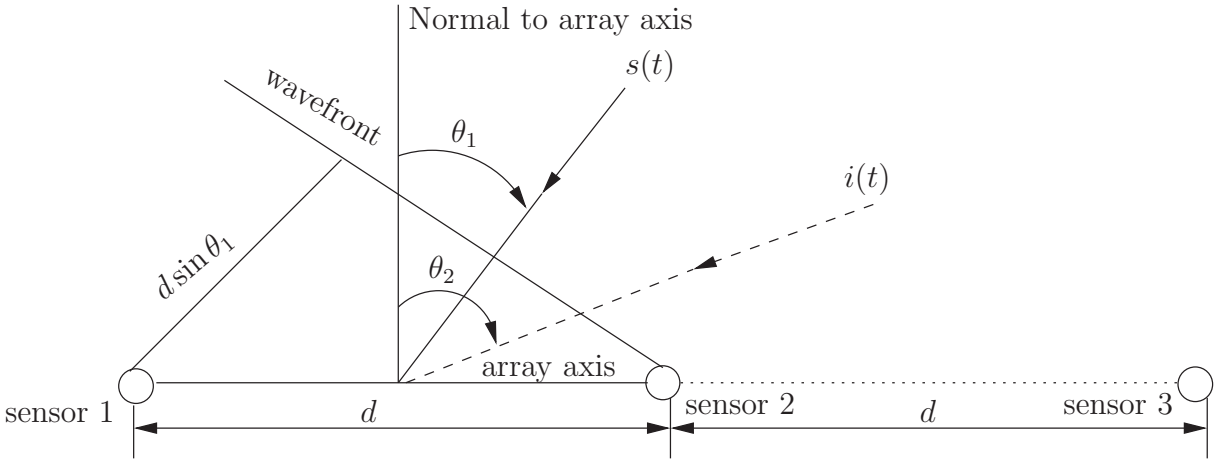

Figure 2.3: Uniform linear array

A Uniform Linear Antenna (ULA) array with three identical antenna elements is shown in Fig. 2.3. In order to achieve spatial diversity and corresponding diversity gain, the antenna elements have to be separated far enough (the separation is a few or tens of carrier wavelengths). When antennas are placed in proximity, the correlation between the antenna signals is high. In this case, the adaptive filter theory can be applied to extract the desired signal while suppressing the interference signal [57]. To extract the desired signal and to suppress the interference signal, complex antenna weights are used to change the phases and the magnitudes of the received signal.

In the following, we consider only two antenna elements of the ULA that are joined with a solid line (see Fig. 2.3). Assume that the two antenna elements (sensor 1 and sensor

2) are separated by $d = \frac{\lambda_c}{2}$, where λ_c is a carrier wavelength, and a desired signal $s(t)$ generated by a MS located in the far-field of the antenna array is incident on the antenna array with an angle of arrival θ_1 (normal to the array axis). If the direction θ_1 is different from zero, then sensor 2 experiences a time delay with respect to sensor 1 by $\tau = \frac{d \sin\theta_1}{v_w}$, where v_w is the velocity of the plane wave. If $s(t)$ is a narrowband signal with carrier frequency f, then the time delay τ corresponds to a phase shift of $\phi = \frac{2\pi d \sin\theta_1}{\lambda_c}$, where $\lambda_c = \frac{v_w}{f}$ is the wavelength corresponding to the carrier frequency. Now assume that an interference signal $i(t)$ with the same carrier frequency impinges on the array with an angle of arrival $\theta_2 = \frac{\pi}{6}$ radian. Let us consider the direction of arrival θ_1 of $s(t)$ to be 0 radian. The task of a SAS is to null out the interfering signal $i(t)$ such that the output becomes $s(t)$. The only difference between the interference signal $i(t)$ received at antenna 1 and the interference signal $i(t)$ received at antenna 2 is the phase difference, which is $\frac{\pi}{2}$ radian for $d = \frac{\lambda_c}{2}$ of this configuration. Similarly, the phase difference between the desired signal $s(t)$ received at antenna 1 and antenna 2 is 0 radian. With the help of Fig. 2.2, the output of the SA network due to desired signal $s(t)$ can be written as

$$\begin{aligned} & s(t)w_1 + s(t)w_2 \\ = \; & s(t)\left\{(w_{1,1} + w_{2,1}) + \mathrm{j}(w_{1,2} + w_{2,2})\right\}, \end{aligned} \tag{2.2}$$

where $w_1 = w_{1,1} + \mathrm{j}w_{1,2}$ and $w_2 = w_{2,1} + \mathrm{j}w_{2,2}$ are complex values. Similarly the array output for undesired signal $i(t)$ can be written as

$$\begin{aligned} & i(t)w_1 + i(t)w_2 \\ = \; & i(t)\left(w_{1,1} + \mathrm{j}w_{1,2}\right) + i(t)\mathrm{e}^{\frac{-\mathrm{j}\pi}{2}}\left(w_{2,1} + \mathrm{j}w_{2,2}\right) \\ = \; & i(t)\left(w_{1,1} + w_{2,2}\right) + \mathrm{j}\left(w_{1,2} - w_{2,1}\right). \end{aligned} \tag{2.3}$$

To extract the desired signal and to suppress the interference signal, the antenna weights should satisfy the following equations.

$$\begin{aligned} w_{1,1} + w_{2,1} &= 1 \\ w_{1,2} + w_{2,2} &= 0 \\ w_{1,1} + w_{2,2} &= 0 \\ w_{1,2} - w_{2,1} &= 0. \end{aligned} \tag{2.4}$$

The above equations are derived from the following two conditions; the unity gain to the desired signal and the zero gain to the interference signal. The antenna weights, $w_{1,1} = \frac{1}{2}$, $w_{1,2} = \frac{1}{2}$, $w_{2,1} = \frac{1}{2}$ and $w_{2,2} = -\frac{1}{2}$ are found if the angles of arrival are 0 and $\frac{\pi}{6}$, respectively. The antenna beam pattern for this case is shown in Fig. 2.4, in which

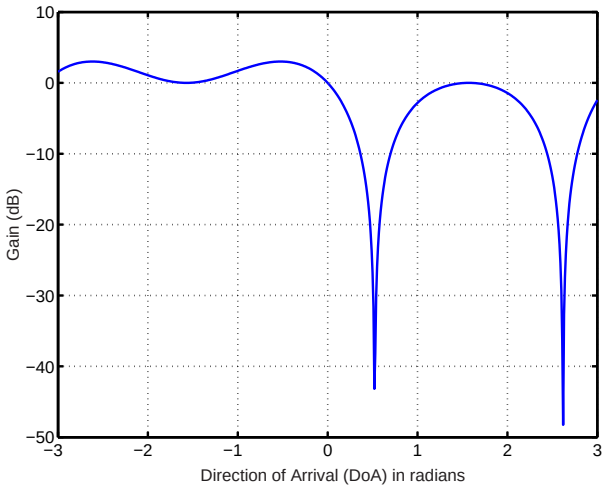

Figure 2.4: Normalized directional pattern of an adaptive antenna array

the antenna beam pattern provides much larger gain toward the direction ($\theta = 0$) of the desired signal than compared to the gain toward the direction ($\theta = \frac{\pi}{6}$) of the interference signal. Thus it can be said, that the adaptive antenna array is capable of separating the desired signal $s(t)$ from the interfering signal $i(t)$.

2.1.2 MIMO Systems

Any arbitrary wireless communication system with a link equipped with multiple antennas both at the transmitter and the receiver is called *Multiple Input and Multiple Output* (MIMO) system. The idea behind MIMO is that the signals on the transmit antennas at one end and the signals on the receive antennas at other end are combined in such a way that the quality or the data rate of the communication for each MIMO user is improved. Like SASs, MIMO systems also use the space-time signal processing in which time is complemented with the spatial dimension inherent in the use of multiple spatially distributed antennas. Thus MIMO systems can be viewed as an extension of SASs. Moreover, the benefits of SASs are retained since the optimization of multi-antenna signals is carried out in a larger space, thus providing additional degrees of freedom. MIMO systems can provide a joint transmit-receive diversity gain, as well as an array gain upon coherent combining of the antenna element signals.

One of the important features of MIMO systems is the ability to turn multipath propagation, traditionally a pitfall of wireless transmission system into a benefit of the user. MIMO effectively takes benefits of random fading [35, 36, 95] and when available, multipath delay spread [13, 82] for multiplying transfer rates. The average capacity (bit/s/Hz)

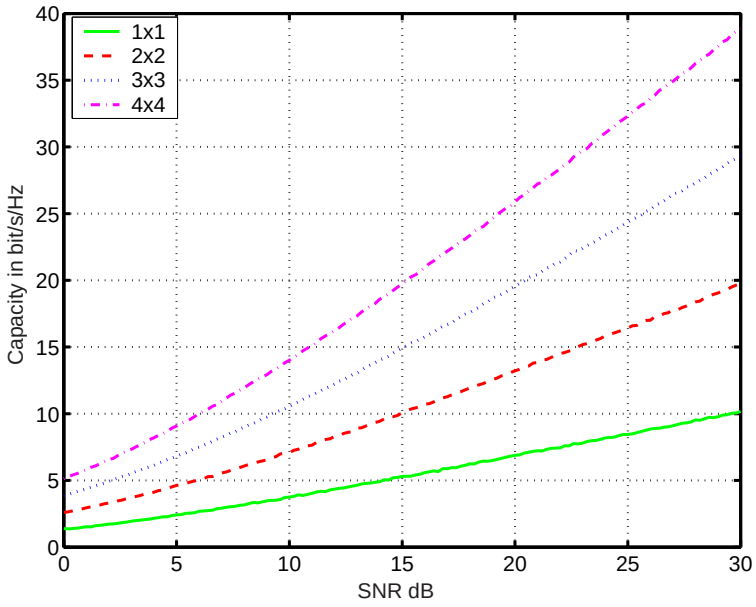

Figure 2.5: Ergodic capacity of a spatially uncorrelated flat fading MIMO system

of a MIMO system with a spatially uncorrelated Rayleigh flat fading channel is shown in Fig. 2.5, for the different numbers of transmit and receive antennas. Capacity results are computed using Monte-Carlo simulations using 2000 random channel realizations. For a given value of SNR, as the number of transmit and receive antenna increases, the capacity of the MIMO link increases significantly.

As shown in Fig. 2.6, as the correlation between channels increases, the MIMO channel capacity decreases. The spatial correlation among the transmitter antenna elements and that among the receiver antenna elements are modeled using Kronecker's model [23]

$$\mathbf{H} = (\mathbf{R})_{\mathrm{Rx}}^{\frac{1}{2}} \mathbf{H}_w (\mathbf{R})_{\mathrm{Tx}}^{\frac{1}{2}}, \tag{2.5}$$

where $\mathbf{H}_w \in \mathcal{C}^{n_r \times n_t}$ is the channel matrix with i.i.d. zero mean complex Gaussian random elements having unit variance, $(\mathbf{R})_{\mathrm{Rx}}^{\frac{1}{2}} \in \mathcal{C}^{n_r \times n_r}$ and $(\mathbf{R})_{\mathrm{Tx}}^{\frac{1}{2}} \in \mathcal{C}^{n_t \times n_t}$ are the receive and transmit correlation matrices, respectively. Moreover, a simple exponential correlation model [105] is used to build the transmit and receive correlation matrices. According to this model, the correlation between ith and jth elements of the transmit or receive antenna is given by

$$\mathbf{R}(i,j)_{\mathrm{Tx/Rx}} = \rho^{|i-j|}. \tag{2.6}$$

As we go from a perfectly uncorrelated case ($\rho = 0$) to a highly correlated case ($\rho = 0.95$), the MIMO channel capacity decreases significantly.

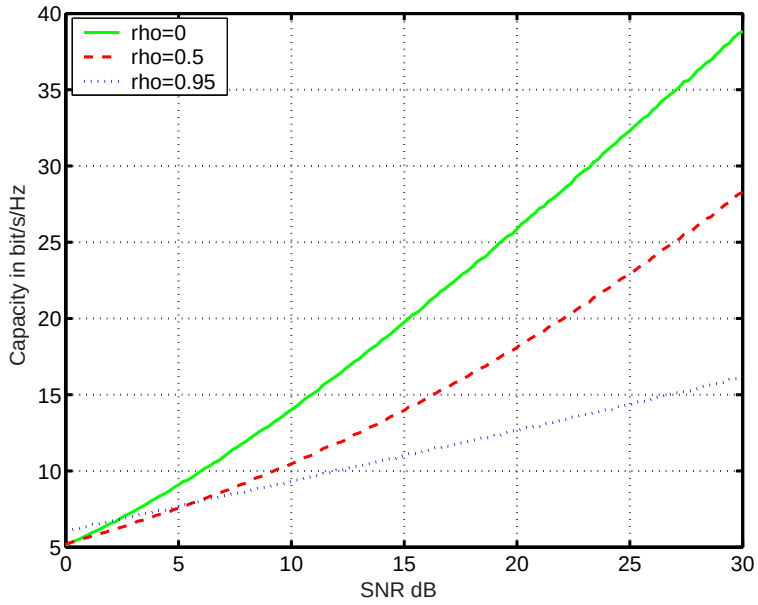

Figure 2.6: Ergodic capacity of a MIMO system for uncorrelated and correlated spatial fading

2.2 Smart Antenna Algorithms

The SA technology consists of mainly two schemes, computation of antenna weights known as diversity combining and combination of antenna signals known as adaptive combining. In diversity combining, antenna signals are combined to maximize the output SNR. In adaptive combining, also known as beamforming, the antenna weights are dynamically adjusted to enhance the desired signal while suppressing interference signals to maximize the Signal-to-Interference-plus-Noise Ratio (SINR). The performance of the adaptive combining is sometimes limited under certain circumstances, such as when the angular separation between desired signal and interference is small or if some of the exploited assumptions on the environment, sources or antenna array become imprecise [39]. There are three basic schemes in the diversity combining technique: Selection Diversity (SD), Equal Gain Combining (EGC), and Maximum Ratio Combining (MRC) [70]. SD is the simplest method of all, in which a diversity branch having the highest SNR is selected and directed to the output. It is also called Selection Combining (SC). The MRC scheme weights each antenna signal by its SNR before combining. The MRC provides the maximum output SNR. The MRC achieves high performance, but it is difficult to accurately compute the SNR of each antenna signal. The EGC scheme simply adds each antenna signal with an equal weight. For example, each antenna signal is weighted by $\frac{1}{M}$ for an M element antenna array.

An adaptive antenna array continuously adjusts its antenna weights by means of a feedback control. Sometimes, it is called a SA in a narrow sense. Several criteria can be used to compute antenna weights for the adaptive combining. The criteria include maximum SINR, MMSE, minimum variance, and Least Squares (LS) [57]. All criteria intend to maximize the output SINR under various assumptions. When only noise is considered, the adaptive antenna performs the same task as the diversity antenna with the MRC. In the presence of strong interference, the adaptive antenna shows a better performance compared with the diversity antenna with the MRC even if the number of interferences is greater than the number of antennas [104]. There are two kinds of beamforming systems: multibeam antenna and adaptive combining (in a narrow sense). The multibeam antenna system selects one fixed beam among the multiple pre-defined beams, which offers the maximum output SINR. Even though multibeam antenna system adaptively selects the beam pattern, it provides non-uniform gain and limited interference suppression [103] since the beam pattern is pre-defined and the number of beam patterns is limited. On the other hand, the adaptive combining system adaptively and freely changes its antenna beam pattern by tracking the antenna weights. The adaptive combining system with M antennas can form up to $M-1$ independent nulls to cancel up to $M-1$ interference signals [87]. The antenna weights must adapt fast enough to track the fading of the desired and interfering signals. However, the antenna weights must also change much more slowly than the data rate.

The output of the narrowband beamformer is given by equation (2.1). The observation vector $\mathbf{x}(t)$ can be defined as

$$\begin{aligned} \mathbf{x}(t) &= \mathbf{s}(t) + \mathbf{i}(t) + \mathbf{n}(t) \\ &= s(t)\mathbf{a} + \mathbf{i}(t) + \mathbf{n}(t), \end{aligned} \tag{2.7}$$

where $\mathbf{s}(t)$, $\mathbf{i}(t)$ and $\mathbf{n}(t)$ are the desired signal, interference and noise components respectively. Here, $s(t)$ is the signal waveform, and $\mathbf{a}$ is the signal steering vector. The optimum weight vector can be computed from the maximum of the SINR [72]

$$\text{SINR} = \frac{\sigma_s^2 |\mathbf{w}^H \mathbf{a}|^2}{\mathbf{w}^H \mathbf{R}_{i+n}^d \mathbf{w}}, \tag{2.8}$$

where

$$\mathbf{R}_{i+n}^d = E\left\{(\mathbf{i}(t) + \mathbf{n}(t))(\mathbf{i}(t) + \mathbf{n}(t))^H\right\} \tag{2.9}$$

is the $M \times M$ interference-plus noise covariance matrix, σ_s^2 is the signal power and $\mathbf{a}$ is the $M \times 1$ steering vector. It is easy to find the solution to the weight vector by

maintaining a distortionless response toward the desired signal and minimizing output interference-plus-noise power [72]. Thus, the maximization of (2.8) is equivalent to [72]

$$\min_{\mathbf{w}} \mathbf{w}^H \mathbf{R}_{i+n}^d \mathbf{w} \quad \text{subject to} \quad \mathbf{w}^H \mathbf{a} = 1. \tag{2.10}$$

From (2.10), the following well-known solution can be found for the optimal vector [72]

$$\mathbf{w}_{\text{opt}} = \alpha (\mathbf{R}_{i+n}^d)^{-1} \mathbf{a}, \tag{2.11}$$

where $\alpha = (\mathbf{a}^H (\mathbf{R}_{i+n}^d)^{-1} \mathbf{a})$ is the normalization constant and does not affect the output SINR (2.8). The solution (2.11) is commonly known as MVDR beamformer [72, 109]. In practical applications, the exact interference plus noise covariance matrix $\mathbf{R}_{i+n}^d$ is not available. In such a case a sample covariance matrix $\hat{\mathbf{R}}$ [100] is used instead of $\mathbf{R}_{i+n}^d$. The solution to this problem is commonly referred to as the Sample Matrix Inversion (SMI) algorithm, whose weight vector is given by

$$\mathbf{w}_{\text{SMI}} = \hat{\mathbf{R}}^{-1} \mathbf{a}. \tag{2.12}$$

A robust modification of the SMI algorithm is well-known as loaded SMI (LSMI) algorithm, which is based on the diagonal loading of the sample covariance matrix [100]. The essence of this approach is to replace the sample covariance matrix $\hat{\mathbf{R}}$ by the so-called diagonally loaded covariance matrix

$$\hat{\mathbf{R}}_{\text{dl}} = \delta \mathbf{I} + \hat{\mathbf{R}} \tag{2.13}$$

in the SMI algorithm (2.12). Using (2.13), the LSMI weight vector can be written as

$$\mathbf{w}_{\text{LSMI}} = \hat{\mathbf{R}}_{\text{dl}}^{-1} \mathbf{a} = (\delta \mathbf{I} + \hat{\mathbf{R}})^{-1} \mathbf{a}, \tag{2.14}$$

where δ is the diagonal loading factor and $\mathbf{I}$ is the identity matrix. The main problem of LSMI method is how to choose the diagonal loading factor δ.

2.3 Channel Models

Channel modeling is an important aspect for proper evaluation of a SAS because it influences the design of receivers and their performance. In the uplink of 3G systems, signals from different MSs arrive at the BS through different paths, each associated with a random time delay and fading gain. Besides multipath fading, there are interference coming from other users signals either of the same cell (intra-cell interference) or other cells (inter-cell interference). In the downlink of the 3G systems, the signal transmitted

from the BS is the superposition of all active users signals and common control signals. The desired user signal and multiple access interference signals traverse the same paths, but they are inherently orthogonal with each other. Another source of interference in the downlink is coming from adjacent cells (inter-cell interference), which can have a substantial impact on the performance. Note that the latter case becomes manifest when the soft handover occurs. Since the number of adjacent BSs and hence the number of interference signals from these BSs is small, a dual antenna system is a good candidate to combat such interference. As shown in Fig. 2.7, the signal transmitted from a MS

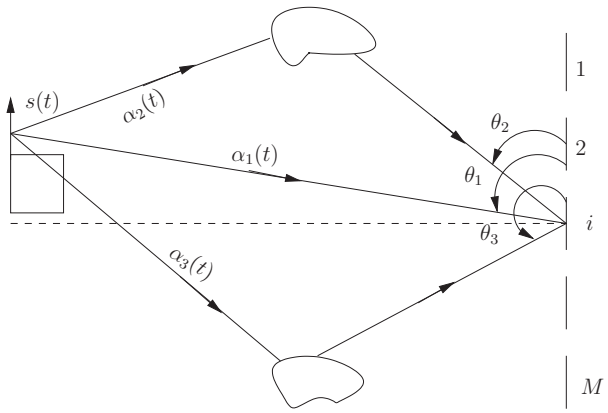

Figure 2.7: Multipath scenario in a SAS

traverses through different paths and arrives at the antenna elements of the BS. Each signal of a single path is effectively an interference signal to any other single path signal. However, a rake receiver manages to utilize multipath signals to improve the quality of received signal. For a wireless channel model, three components are considered for a typical variation in the received signal level [83]. The three components are mean path loss, lognormal fading (or slow fading), and Rayleigh fading (or fast fading), as shown in Figure 2.8. Both theoretical and measurement based models indicate that an average received signal level decreases according to a power law with distance [89]. The difference in path loss at different locations at the same transmitter-receiver distance is modeled as a lognormal random variable (lognormal fading). Reflections due to many scatterers in the vicinity of the receiver cause the received signal to be time varying, in which the envelope of a multipath signal follows a Rayleigh distribution (Rayleigh fading) [83, 89]. A channel model also needs to consider the delay spread due to multipath propagation, the Doppler spread due to motion of the MS, and the anglular spread due to scattering.

To obtain the channel profile (such as delay, average power, and angle of arrival of each multipath signal), not only a channel model based on statistical properties of the channel,

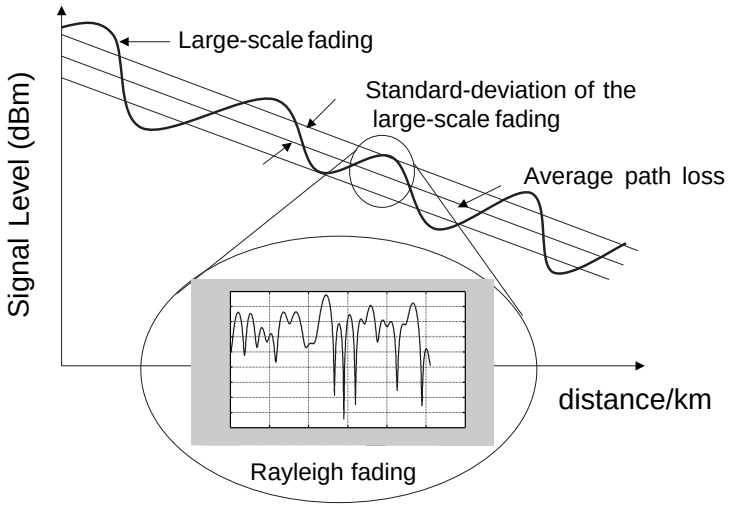

Figure 2.8: Variation of the received signal level

but also a channel model based on measurement data should be considered.

2.3.1 Vector Channel Model

To understand the operation of a SAS, we need to first introduce spatial signatures. Consider uplink transmission with an M-element antenna array at a BS receiving signals from different users at different spatial locations. The array output contains both direct path and delayed path signals. Radio propagation environments exhibit a multipath effect when the received signal consists of multiple replicas of the transmitted signal, arriving from various directions. The steering vector to a transmitting signal $s(t)$ from a direction of arrival θ has the form

$$\mathbf{a}(\theta) = [1,\ a_1(\theta),\ \cdots,\ a_M(\theta)], \tag{2.15}$$

where $a_i(\theta)$ is a complex number denoting the amplitude gain and phase shift of the signal at the ith antenna relative to that of the first antenna. For a uniform linear array

$$a_i(\theta) = \mathrm{e}^{\mathrm{j}\frac{2\pi d(i-1)\sin\theta}{\lambda_\mathrm{c}}},\ i = 1, \cdots, M, \tag{2.16}$$

where d is the spacing between adjacent antennas and λ_c is the wavelength of the carrier. In a typical wireless scenario, an antenna array with omni-directional elements not only receives signals from a direct path but also from many reflected paths with different Direction of Arrivals (DoA). Therefore, the total signal received by the ith antenna element

can be written as

$$x_i(t) = \sum_{l=1}^{Q} a_i(\theta_l)\,\alpha_{i,l}(t)\,s(t-\tau_l), \tag{2.17}$$

where $a_i(\theta_l)$ represents the response of i-th element of the array for an l-th path with DoA θ_l, $\alpha_{i,l}(t)$ is the complex envelope of the path fading, τ_l is the path delay, Q is the number of multipath signals and $s(.)$ is the transmitted signal that depends upon modulation method and the information data stream. The signal complex envelope received by each element of array is identical except of phase differences that depend on the DoA. Usually the inverse of the signal bandwidth is large in comparison to the travel time across the array. This leads to: $\alpha_{1,l}(t) = \alpha_{2,l}(t) = \cdots \alpha_{M,l}(t) = \alpha_l(t)$, where M is the number of array elements. The spacing among the array elements is generally $< \left(\frac{\lambda_c}{2}\right)$, in order to have strong correlation between the antenna elements. Strong correlation between antenna elements is suitable for beamforming, whereas weak correlation is required for obtaining diversity. Since there are M array elements, the array response or steering vector $\mathbf{a}(\theta_l)$ for a DoA of l-th multipath is

$$\mathbf{a}(\theta_l) = [a_1(\theta_l)\ \ a_2(\theta_l)\cdots\ a_M(\theta_l)]^T. \tag{2.18}$$

Including all the multipaths, the received base band signal for the k th user is

$$\mathbf{x}^k(t) = \sum_{l=1}^{Q} \mathbf{a}(\theta_{k,l})\,\alpha_{k,l}(t)\,s_k(t-\tau_{k,l}), \tag{2.19}$$

where $\mathbf{x}^k(t) = \left[x_1^k(t)\,x_2^k(t)\cdots x_M^k(t)\right]^{\mathbf{H}}$ and $\tau_{k,l}$ are not absolute values but are defined with respect to the path with shortest propagation delay. In a multiuser system, if $k = 0, 1\cdots K-1$ users are transmitting signals, the received baseband signal at the BS can be expressed as

$$\begin{aligned}\mathbf{x}(t) &= \sum_{k=0}^{K-1}\sum_{l=1}^{Q_k} \mathbf{a}(\theta_{k,l})\,\alpha_{k,l}(t)\,s_k(t-\tau_{k,l}) \\ &= \sum_{l=1}^{Q_d} \mathbf{a}(\theta_{d,l})\,\alpha_{d,l}(t)\,s_d(t-\tau_{d,l}) + \sum_{k=0,\ k\neq d}^{K-1}\sum_{l=1}^{Q_k} \mathbf{a}(\theta_{k,l})\,\alpha_{k,l}(t)\,s_k(t-\tau_{k,l}).\end{aligned} \tag{2.20}$$

The first term in the right hand side of (2.20) indicates the signal received corresponding to the desired user. The second term indicates the interference signal from $K-1$ interferers. Let us consider the signal received from the desired user for which the beamforming

vector is $\mathbf{w}_d^H$. The output of the beamformer (2.1) is given by

$$\begin{aligned} y_d(t) &= \sum_{l=1}^{Q_d} \mathbf{w}_d^H \mathbf{a}(\theta_{d,l})\, \alpha_{d,l}(t)\, s_d(t-\tau_{d,l}) \\ &= \mathbf{w}_d^H \int_{\tau=-\infty}^{\infty} \mathbf{h}_d(t,\tau_d) s_d(t-\tau_d)\, d\tau_d, \end{aligned} \tag{2.21}$$

where the time-variant vector channel between the BS and the desired MS is given by the impulse response

$$\begin{aligned} \mathbf{h}_d(t,\tau_d) &= \sum_{l=1}^{Q_d} A_{d,l} \exp(\mathrm{j}2\pi f_{d,l} t + \psi_{d,l}) \mathbf{a}(\theta_{d,l}) \delta(\tau - \tau_{d,l}) \\ &= \sum_{l=1}^{Q_d} \alpha_{d,l}(t) \mathbf{a}(\theta_{d,l}) \delta(\tau - \tau_{d,l}). \end{aligned} \tag{2.22}$$

In equation (2.22), Q_d, $A_{d,l}$, $f_{d,l}$, $\psi_{d,l}$, $\theta_{d,l}$ and $\tau_{d,l}$ are the number of propagation paths, the path transfer factor (amplitude), Doppler frequency, phase offset, DoA and the delay of lth path, respectively. The gain function $\alpha_{d,l}(t)$ (2.22) is the fading associated with each path. According to Jake's model [59], as shown in Fig. 2.9 a circular group of

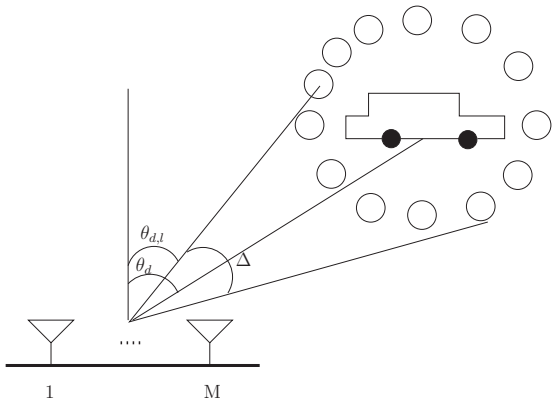

Figure 2.9: Jake's model with angular spread

scatterers is considered, where each scatterer generates different Doppler shifts, phase offsets and the azimuth directions or DoAs. The sum of all the rays arriving from each scatterer generates the lth path in equation (2.22). In this model, the angular spreading is represented by a notion of a cone that contains all the incoming rays from this group of scatterers. Assuming that the azimuth angle of the lth path is $\theta_{d,l}$, when the speed of the desired mobile is used as a reference, the Doppler frequency $f_{d,l}$ is given by

$$f_{d,l} = \frac{f_{\mathrm{up}} \cos(\theta_{d,l}) v}{c}, \tag{2.23}$$

where f_{up}, v and c are the uplink carrier frequency, the mobile speed and the speed of light, respectively. The Doppler frequency $f_{d,l}$ and the phase offset $\psi_{d,l}$ remain unchanged practically during a time slot. Similarly, the number of paths Q_d, the path transfer factors $\alpha_{d,l}$, DoA $\theta_{d,l}$ and the delays $\tau_{d,l}$ can be assumed to be fixed for a number of time slots. The average power of the desired signal after beamforming at the BS is

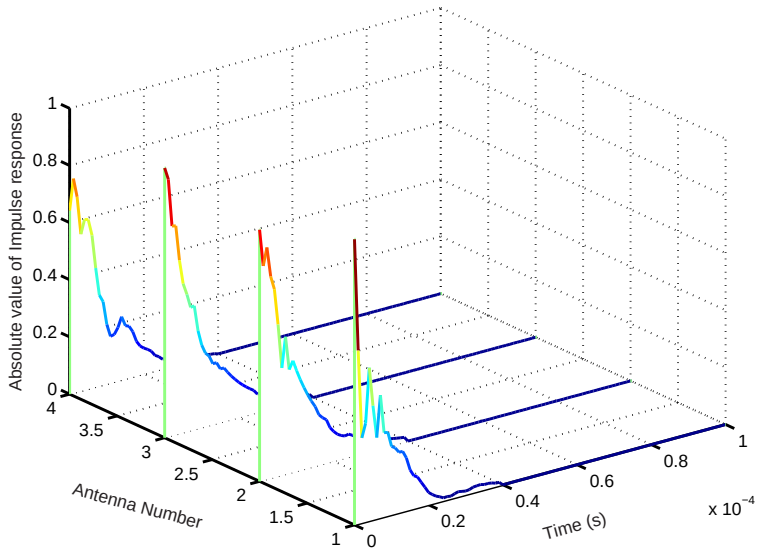

Figure 2.10: Impulse response of a spatio-temporal channel

$$P_d \;=\; E\left\{y_d(t)y_d^*(t)\right\}. \tag{2.24}$$

Substituting equation (2.21) into (2.24), we get the average power of the desired signal as

$$P_d = \mathbf{w}_d^H \left(\sum_{l=1}^{Q_d} |A_{d,l}|^2 \mathbf{a}(\theta_{d,l})\mathbf{a}(\theta_{d,l})^H \right) \mathbf{w}_d, \tag{2.25}$$

where $|A_{d,l}|^2$ is the average power of fading $\alpha_{d,l}(t)$ and the following normalization was considered

$$E\left\{s(t)s^*(t)\right\} \;=\; 1. \tag{2.26}$$

The spatial covariance matrix (see eqn. 2.25) of the desired signal received at the BS is thus given by

$$\mathbf{R}_d = \sum_{l=1}^{Q_d} |A_{d,l}|^2 \mathbf{a}(\theta_{d,l})\mathbf{a}^H(\theta_{d,l}). \tag{2.27}$$

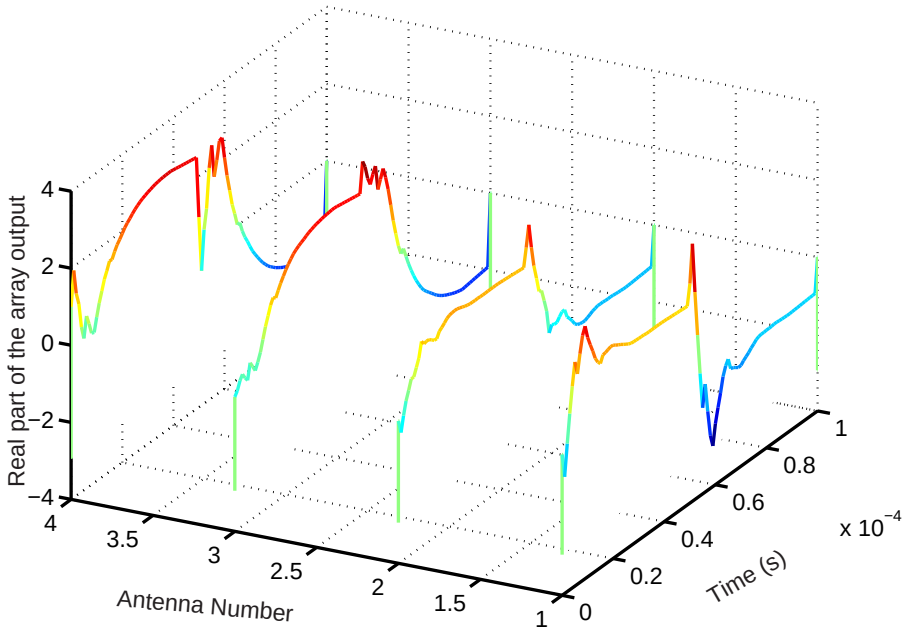

Figure 2.11: Output of a spatio-temporal channel

Similar derivations can be carried out to find the spatial covariance matrix for the interferers. The cumulative spatial covariance matrix of the interferers can be written as

$$\mathbf{R}_I = \sum_{k=1,k\neq d}^{K-1} \sum_{l=1}^{Q_k} |A_{k,l}|^2 \mathbf{a}(\theta_{k,l}) \mathbf{a}^H(\theta_{k,l}), \tag{2.28}$$

where $K-1$ indicates the number of interferers. The impulse response for an arbitrary realization of a time-variant vector channel is depicted in Fig. 2.10 where a truncated exponential power delay profile with a maximum delay of $40\mu s$ and a delay spread of $10\mu s$ is considered. The fading associated with each path $\alpha_{d,l}(t)$ (2.22) is modeled as a Rayleigh fading with time correlation described by a Jake's spectrum [59]. The speed of the MS is assumed to be 400 km/hr, the carrier frequency is 2 GHz, and the direction of arrival is Laplacian distributed with a variance of 20°. A ULA with a spacing of $\frac{\lambda_c}{2}$ and size $M = 4$ is used at the BS. The response of an arbitrary realization of such a spatio-temporal channel to an input bit sequence of $[1, 0]$ is shown in Fig. 2.11 for an observation interval of $100\mu s$. The output of the antennas are different because of the different multipath fading processes at each antenna element.

2.3.2 Spatial Fading Correlation of UCA

In wireless communications, the wave propagation effects result in delay spread, angle spread and Doppler spread. The antenna arrays are used to mitigate these channel

impairments thereby helping to improve signal quality. Among antenna array systems, the ULA is probably the most common form employed in cellular systems. Ideally, the antenna elements in a space diversity scheme should be spaced far enough apart so that the randomly fading signal at each diversity branch is independent and uncorrelated. However, this may be difficult to achieve in practice due to space limitations. Recently, an analysis of fading correlation as a function of antenna spacing and DoA distribution (uniform and cosine shaped) was carried out for UCA in [97]. We provide a closed form solution of the signal fading correlation for a UCA system with the assumption of Laplacian distributed DoA [28]. The Laplacian distribution of DoA is described as

$$f_{\Theta}(\theta) = \frac{1}{\sqrt{2}\sigma_{\theta}} \mathrm{e}^{\left(-\frac{\sqrt{2}|\theta-\mu|}{\sigma_{\theta}}\right)}, \tag{2.29}$$

where μ is the average DoA and σ_{θ}^2 is the variance of DoA. The steering vector for an M element UCA is

$$\mathbf{a}\left(\theta, \lambda_{\mathrm{c}}\right) = \left[\mathrm{e}^{-\mathrm{j}2\pi\frac{r}{\lambda_{\mathrm{c}}}\cos\theta}, \mathrm{e}^{-\mathrm{j}2\pi\frac{r}{\lambda_{\mathrm{c}}}\cos\left(\theta-\frac{1}{M}2\pi\right)}, \ldots, \mathrm{e}^{-\mathrm{j}2\pi\frac{r}{\lambda_{\mathrm{c}}}\cos\left(\theta-\frac{M-1}{M}2\pi\right)}\right]^T. \tag{2.30}$$

Dropping the index λ_{c} from $\mathbf{a}\left(\theta, \lambda_{\mathrm{c}}\right)$ of (2.30), we can write the spatial correlation [97] between the mth and nth antenna element as (also refer to eqn. 2.7 without noise and interference)

$$\begin{aligned}
\mathbf{R}_s(m,n) &= E\left\{x_m(t)x_n^*(t)\right\} \\
&= E\left\{a_m(\theta)s(t)a_n^*(\theta)s^*(t)\right\} \\
&= |s^2(t)| \cdot \int_{\theta} a_m(\theta)a_n^*(\theta)f_{\Theta}(\theta)\,d\theta \\
&= \int_{-\pi+\mu}^{\pi+\mu} \mathrm{e}^{-\mathrm{j}2\pi\frac{r}{\lambda_{\mathrm{c}}}\cos(\theta-\phi_m)}\mathrm{e}^{\mathrm{j}2\pi\frac{r}{\lambda_{\mathrm{c}}}\cos(\theta-\phi_n)}f_{\Theta}(\theta)\,d\theta,
\end{aligned} \tag{2.31}$$

where desired signal power $|s^2(t)| = 1$. After defining the following constants

$$\begin{aligned}
Q_1 &= \frac{2\pi r}{\lambda_{\mathrm{c}}}\left(\cos\phi_m - \cos\phi_n\right) \\
Q_2 &= \frac{2\pi r}{\lambda_{\mathrm{c}}}\left(\sin\phi_m - \sin\phi_n\right) \\
\sin\alpha &= \frac{Q_1}{\sqrt{Q_1^2+Q_2^2}} \\
\cos\alpha &= \frac{Q_2}{\sqrt{Q_1^2+Q_2^2}} \\
A_c &= \sqrt{Q_1^2+Q_2^2},
\end{aligned} \tag{2.32}$$

we can express (2.31) as

$$\begin{aligned}\mathbf{R}_s(m,n) &= \int_{-\pi+\mu}^{\pi+\mu} \mathrm{e}^{-\mathrm{j}A_c\sin(\alpha+\theta)} f_\Theta(\theta)\, d\theta \\ &= \int_{-\pi+\mu}^{\mu} \mathrm{e}^{-\mathrm{j}A_c\sin(\alpha+\theta)} \frac{1}{\sqrt{2}\sigma_\theta} \mathrm{e}^{\frac{\sqrt{2}(\theta-\mu)}{\sigma_\theta}}\, d\theta + \int_{\mu}^{\pi+\mu} \mathrm{e}^{-\mathrm{j}A_c\sin(\alpha+\theta)} \frac{1}{\sqrt{2}\sigma_\theta} \mathrm{e}^{\frac{\sqrt{2}(-\theta+\mu)}{\sigma_\theta}}\, d\theta.\end{aligned} \tag{2.33}$$

With further derivations (see Appendix 9.1), the spatial correlation between the two elements of the UCA can be finally expressed as

$$\begin{aligned}\mathbf{R}_s(m,n) \;=\; &\left(1-\mathrm{e}^{-\frac{\sqrt{2}\pi}{\sigma_\theta}}\right) J_0(A_c) + 2\left(1+\mathrm{e}^{-\frac{\sqrt{2}\pi}{\sigma_\theta}}\right) \sum_{k=1}^{\infty} \frac{J_{2k}(A_c)}{1+2\sigma_\theta^2 k^2} \cos\left(2k(\alpha+\mu)\right) - \\ &\left(1+\mathrm{e}^{-\frac{\sqrt{2}\pi}{\sigma_\theta}}\right) 2\mathrm{j} \sum_{k=1}^{\infty} \frac{2J_{(2k-1)}(A_c)}{2+\sigma_\theta^2(2k-1)^2} \sin\left((2k-1)(\alpha+\mu)\right).\end{aligned} \tag{2.34}$$

where $J_n(x)$ is the modified Bessel function of the first kind. A 4-element UCA as shown in Figure (2.12) is used as a test case for the numerical analysis.

The fading correlations $|\mathbf{R}_s(m,n)|$ for the 4-element UCA are plotted against radius of

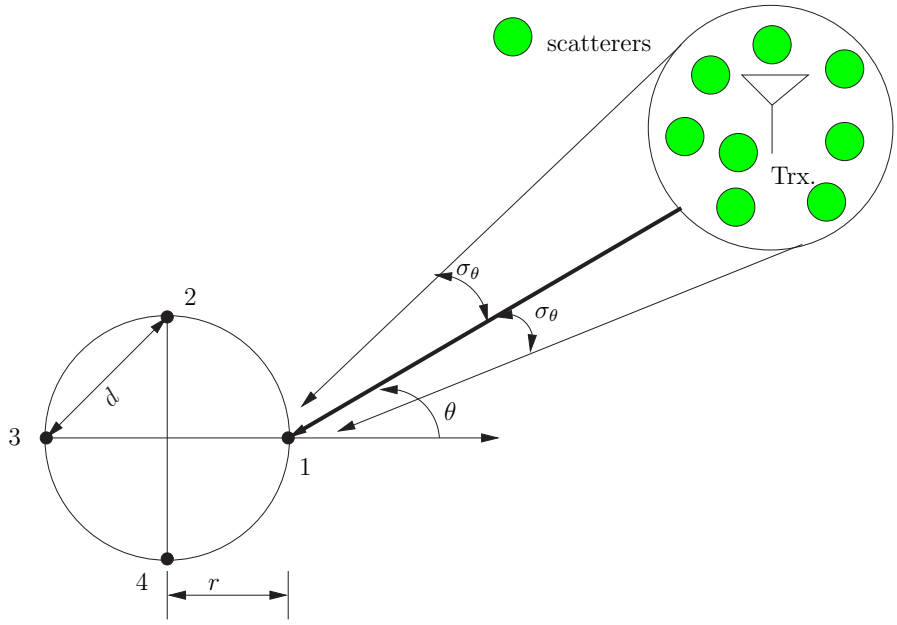

Figure 2.12: Wireless communication system employing UCA with M elements

the circular array normalized by the wavelength for different angular spreads σ_θ. Note that, the antenna spacing d is proportional to the radius r and is given by $d = \sqrt{2}r$. Because of the symmetry of the UCA, the fading correlation $|\mathbf{R}_s(1,2)| = |\mathbf{R}_s(1,4)|$. Thus

we only need to evaluate the fading correlation for $m = 1$ and $n = 2$ to 3. Figures (2.13, 2.15) show the fading correlations $|\mathbf{R}_s(1,2)|$ and $|\mathbf{R}_s(1,3)|$ with an average DoA=0° and different angle spreads, respectively. The fading correlation decreases as r and angle

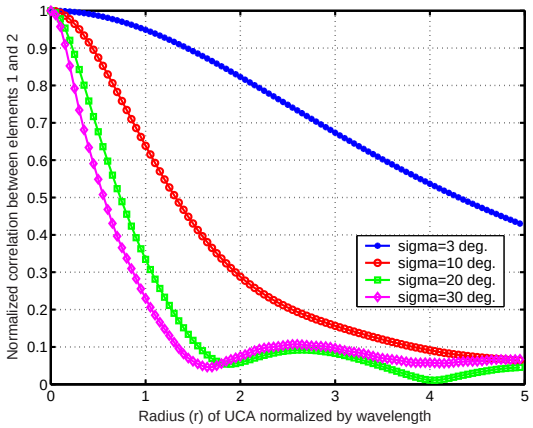

Figure 2.13: Spatial fading correlation between element 1 and 2 with average DoA= 0°

spread σ_θ increases. It is shown that $|\mathbf{R}_s(1,2)|$ gives the lowest fading correlation for the same values of σ_θ and $\frac{r}{\lambda_c}$ while $|\mathbf{R}_s(1,3)|$ gives the highest correlation. It can be observed that for all simulation cases, the spatial fading correlation decreases as the radius of the antenna r in terms of wavelength λ_c or the angular spread increases. Figures (2.14, 2.16)

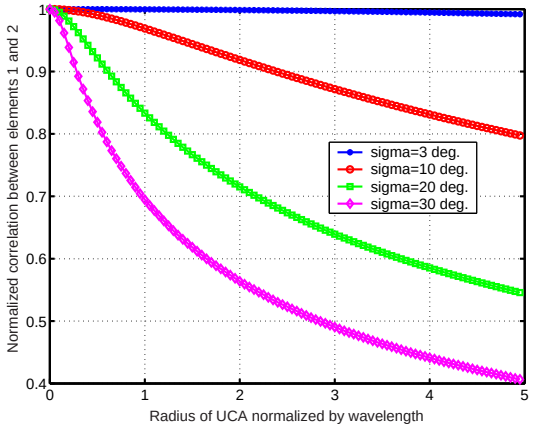

Figure 2.14: Spatial fading correlation between element 1 and 2 with average DOA= 45°

show the fading correlations $|\mathbf{R}_s(1,2)|$ and $|\mathbf{R}_s(1,3)|$ of the UCA with average DoA=45° and various angle spreads, respectively. As in previous case, the fading correlation decreases as r and angle spread σ_θ increases. For the case of average DoA=45°, $|\mathbf{R}_s(1,3)|$ gives the lowest fading correlation for the same values of σ_θ and $\frac{r}{\lambda_c}$ while $|\mathbf{R}_s(1,2)|$ gives

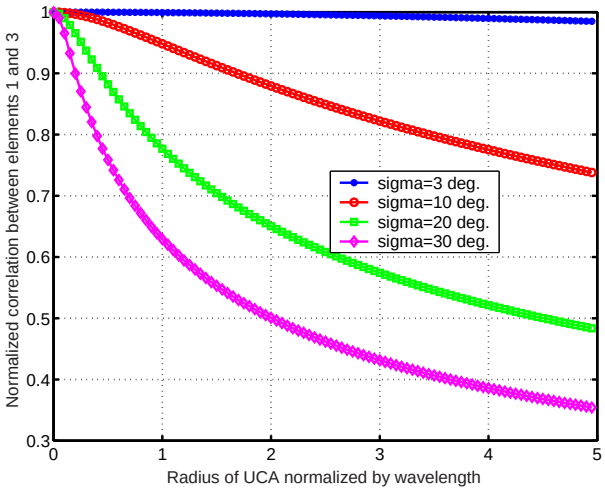

Figure 2.15: Spatial fading correlation between element 1 and 3 with average DOA= 0°

the highest correlation. Moreover, it is seen that the spatial fading correlation is a function of average DoA. For example, with same angle spread and the circle of radius r,

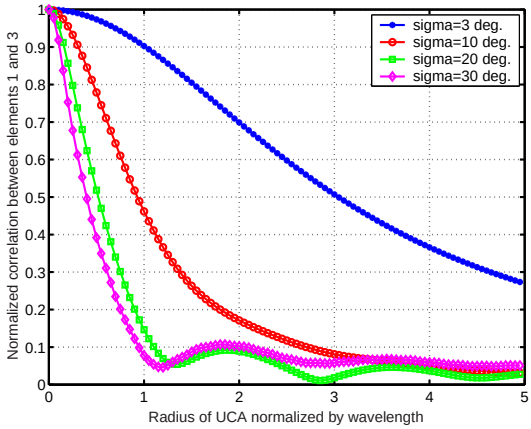

Figure 2.16: Spatial fading correlation between element 1 and 3 with average DOA= 45°

$|\mathbf{R}_s(1,2)|$ for average DoA of 0° is different from the case of average DoA of 45°. In Figure (2.17), we compare the analytical results with simulation results for the spatial fading correlation between element 1 and 2 of the 4-element UCA with average DoA of 0°. It can be observed that the simulation results exactly match with the analytical results.

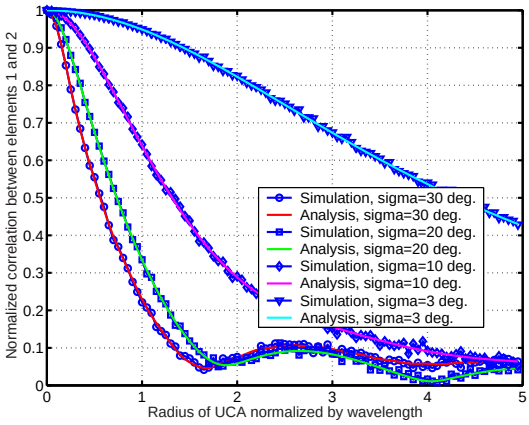

Figure 2.17: Spatial fading correlation between element 1 and 2 with average DOA= 0°

2.4 WCDMA as an Air-interface for UMTS-FDD

In the standardisation forums, WCDMA has emerged as the most widely adopted 3G air interface. The joint standardisation project of the standardisation bodies from Europe, Japan, Korea, USA and China, known as 3GPP (the 3rd Generation Partnership Project) has developed the specifications for WCDMA. Within 3GPP, WCDMA is called UTRA (Universal Terrestrial Radio Access) FDD and TDD (Time Division Duplex). Hence WCDMA covers both FDD and TDD operations. Some of the important features of WCDMA [54] are listed below:

- WCDMA-FDD mode uses direct sequence code division multiple access DS-CDMA, where the user information bits are spread over a wide bandwidth by multiplying the user data with pseudo random sequences derived from CDMA spreading codes. The use of a variable spreading factor and multicode connections is supported, so that the system can support very high bit rates up to 2 Mbit/s.

- In contrast to a carrier bandwidth of 1 MHz in narrowband CDMA systems like IS-95, WCDMA is a wideband CDMA system where the used chip rate of 3.84 Mcps leads to carrier bandwidth of approximately 5 MHz. This wide bandwidth of WCDMA is very helpful in supporting high user data rates and increased multipath diversity.

- WCDMA supports two basic modes of operation: FDD and TDD. The FDD mode uses separate carrier frequencies with 5 MHz spacing for the uplink (connection from the mobile to the BS) and downlink (connection from the BS to the mobile),

Multiple access scheme	DS-CDMA
Duplex scheme	FDD/TDD
Packet access	Dual mode: combined and dedicated channel
Multirate,variable rate scheme	Variable spreading factor and multicode
Chip rate	3.84 MHz
Frame length	10 ms
Carrier spacing	4.4−5.2 MHz
Channel coding	Convolutional coding(rate 1/2 and 1/3), Turbo coding
BS synchronization	FDD: asynchronous TDD: synchronous
Service multiplexing	Multiple services with different quality of service requirements
Multiuser detection, smart antennas	Supported by the standard, optional in the implementation

Table 2.1: The key technical parameters of WCDMA [54]

respectively. The TDD mode employs only one 5 MHz channel that is shared in time between uplink and downlink.

- WCDMA uses coherent detection on uplink and downlink by the use of pilot symbols or common pilot symbols, that is expected to result in an overall increase of coverage and capacity on the uplink.

- WCDMA supports highly variable user data rates. Frames of 10 ms duration during which the user data rate is kept constant are allocated to each user. The data capacity among the users can vary from frame to frame. Hence WCDMA supports the concept of Bandwidth on Demand (BOD).

- The WCDMA air interface has been designed in such a way that it can support the advanced CDMA receiver concepts, such as multiuser detection, and smart adaptive antennas. These features, which are not available in 2G systems have given the network operator an option to increase the capacity or coverage.

- One of the most promising features of WCDMA is that it is designed to be deployed in conjunction with GSM. Handovers between GSM and WCDMA are supported.

2.5 Convex Optimization

A convex program is an optimization problem where we seek the minimum of a convex function over a convex set. Its objective function as well as the constraints are convex. Convex optimization problems often occur in signal processing, communications, structural analysis and many other fields. Convex problems can be solved numerically with great efficiency and global optimums can be obtained. Very efficient interior-point methods are available for the solution of convex optimization problems. However, the difficulty is often to recognize convexity; convexity is harder to recognize than say, linearity. One important feature of convexity is that it is possible to address difficult, non-convex problems (such as combinatorial optimization problems) using convex approximations that are more efficient than classical linear ones. Convex optimization is especially relevant when the data of the problem at hand is uncertain, and robust solutions are sought.

2.5.1 Convex Set

A set C is convex if the line segment between any two points in C lies in C, i.e., if for any $x_1,\ x_2 \in C$ and any θ with $0 \leq \theta \leq 1$, we have

$$\theta x_1 + (1-\theta)x_2 \in C. \tag{2.35}$$

In other words, in a convex set C every point in the set can be seen by every other point, along an unobstructed straight path between them, where unobstructed means lying in the set. Some simple convex and nonconvex sets in $\mathcal{R}^2$ is shown in Figure 2.18. The

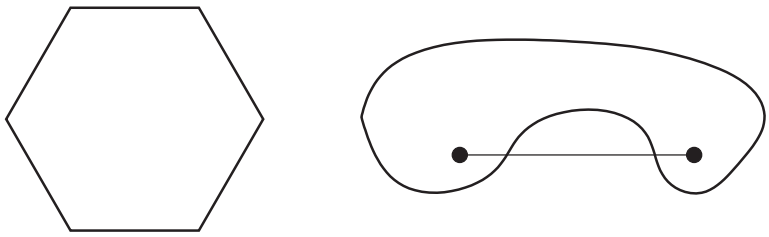

Figure 2.18: Some simple convex and nonconvex sets

hexagon including its boundary is a convex set whereas the kindney shaped set is not convex, since the line segment between the two points is partly not contained in the set.

2.5.2 Cones

A set C is called a Cone, if for every $x \in C$ and $\theta \geq 0$ we have $\theta x \in C$. The set C is called a convex cone if it is convex and a cone, which means that for any $x_1, x_2 \in C$ and $\theta_1, \theta_2 \geq 0$, we have

$$\theta_1 x_1 + \theta_2 x_2 \in C. \tag{2.36}$$

Points of this form can be described geometrically as forming the two-dimensional 'pie-slice', with apex 0 and edges passing through x_1 and x_2 as shown in Figure 2.19. The

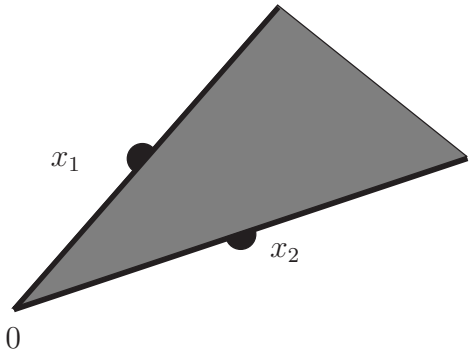

Figure 2.19: Example of a convex cone [15]

pie-slice shows all the points of the form $\theta_1 x_1 + \theta_2 x_2$, where $\theta_1, \theta_2 \geq 0$. The apex of the slice that corresponds to $\theta_1 = \theta_2 = 0$ is at 0 and its edges pass through the points x_1 and x_2.

2.5.3 Convex Functions

A function $f : \mathcal{R}^n \rightarrow \mathcal{R}$ is convex if the domain of f is convex and for all x, y that belong to the domain of f and for any $0 \leq \theta \leq 1$, we have

$$f(\theta x + (1-\theta)y) \leq \theta f(x) + (1-\theta) f(y). \tag{2.37}$$

The function f is strictly convex if strict inequality holds in (2.37) whenever $x \neq y$ and $0 < \theta < 1$. It can be said that f is concave, if $-f$ is convex, and strictly concave if $-f$ is strictly convex . Geometrically, the inequality (2.37) can be interpreted as a line segment between $(x, f(x)$ and $(y, f(y))$ that lies above the graph of f as shown in Figure 2.20. Some of the examples of convex functions are

- Exponential; e^{ax} is convex on $\mathcal{R}$, for any $a \in \mathcal{R}$.
- Powers of absolute value; $|x|^p$, for $p \geq 1$, is convex on $\mathcal{R}$.

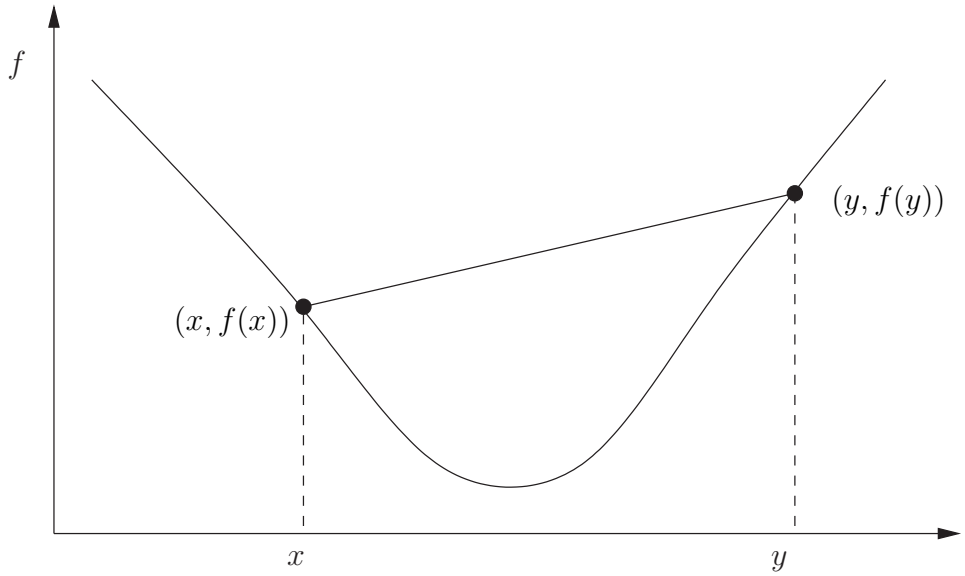

Figure 2.20: Graph of a convex function

- Powers; x^a, for $a \geq 1$ or $a \leq 0$, is convex on $\mathcal{R}_{++}$.

2.5.4 Convex Optimization Problem

An optimization problem in its standard form is

$$\begin{array}{ll} \text{minimize} & f_0(\mathbf{x}) \\ \text{subject to} & f_i(\mathbf{x}) \leq 0, \quad i = 1, \cdots, m \\ & h_i(\mathbf{x}) = 0, \quad i = 1, \cdots, p, \end{array} \tag{2.38}$$

where

- $\mathbf{x} \in \mathcal{R}^n$ is the optimization variable.
- $f_0 : \mathcal{R}^n \to \mathcal{R}$ is the objective or cost function.
- $f_i : \mathcal{R}^n \to \mathcal{R}$, $i = 1, \cdots, m$ are the inequality constraint functions.
- $h_i : \mathcal{R}^n \to \mathcal{R}$, $i = 1, \cdots, p$ are the equality constraint functions.

In its standard form, a convex optimization problem can be expressed as

$$\begin{array}{ll} \text{minimize} & f_0(\mathbf{x}) \\ \text{subject to} & f_i(\mathbf{x}) \leq 0, \quad i = 1, \cdots, m \\ & \mathbf{a}_i^T \mathbf{x} = b_i, \quad i = 1, \cdots, p, \end{array} \tag{2.39}$$

where $f_o, f_1, \cdots, f_m$ are convex and the equality constraints are affine (every affine set is a convex). A feasible set of the convex optimization problem is convex [15]. The problem is quasiconvex if f_0 is quasiconvex and $f_1, \cdots, f_m$ are convex, respectively. The most commonly used convex optimization problem is the Linear Programming (LP) problem, an optimization problem with linear objective and linear inequality constraints:

$$\begin{aligned} &\text{minimize} \quad \mathbf{f}^T\mathbf{x} \\ &\text{subject to} \quad \mathbf{c}_i^T\mathbf{x} \leq d_i, \quad i = 1, \cdots, L, \end{aligned} \tag{2.40}$$

where the optimization variable is the vector $\mathbf{x}$, and $\mathbf{c}_i \in \mathcal{R}^n$, $d_i \in \mathcal{R}$, and $\mathbf{f} \in \mathcal{R}^n$ are the problem parameters.

2.5.5 Second-Order Cone Programming (SOCP)

Suppose $||\cdot||_l$ is any norm on $\mathcal{R}^n$. From the general properties of the norms, it can be shown that a norm ball of radius r with center $\mathbf{x}_c$, given by $\{\mathbf{x}|, ||\mathbf{x} - \mathbf{x}_c||_l < r\}$, is convex. The cone associated with the norm $||\cdot||_l$ is

$$C = \{(\mathbf{x}, t)|, ||\mathbf{x}||_l < t\}. \tag{2.41}$$

The SOC is the norm cone for the Euclidean norm ($l = 2$) and is described as

$$C \;=\; \left\{(\mathbf{x}, t) \in \mathcal{R}^{n+1}|, ||\mathbf{x}||_2 < t\right\}, \tag{2.42}$$

where $n + 1$ is also known as the dimension of the cone. A convex optimization problem with SOC constraints is also known as a SOCP problem, which in general has the following form

$$\begin{aligned} &\text{minimize} \quad \mathbf{f}^T\mathbf{x} \\ &\text{subject to} \quad ||\mathbf{A}_i\mathbf{x} + \mathbf{b}_i||_2 \leq \mathbf{c}_i^T\mathbf{x} + d_i, \quad i = 1, \cdots, L, \end{aligned} \tag{2.43}$$

where $||\cdot||_2$ denotes the Euclidean norm, i.e., for any $\mathbf{z} \in \mathcal{R}^n$, $||\mathbf{z}||_2 = \sqrt{\mathbf{z}^T\mathbf{z}}$, $\mathbf{x} \in \mathcal{R}^n$ is the optimization variable, and the problem parameters are $\mathbf{f} \in \mathcal{R}^n$, $\mathbf{A}_i \in \mathcal{R}^{m_i \times n}$, $\mathbf{b}_i \in \mathcal{R}^{m_i}$, $\mathbf{c}_i \in \mathcal{R}^n$ and $d_i \in \mathcal{R}$. The constraint

$$||\mathbf{A}_i\mathbf{x} + \mathbf{b}_i||_2 \leq \mathbf{c}_i^T\mathbf{x} + d_i, \quad i = 1, \cdots, L \tag{2.44}$$

is a SOC constraint of dimension $m_i + 1$. The set of points satisfying a SOC constraint is the inverse image of the unit SOC under an affine mapping [15]:

$$||\mathbf{A}_i\mathbf{x} + \mathbf{b}_i||_2 \leq \mathbf{c}_i^T\mathbf{x} + d_i \Leftrightarrow \begin{pmatrix} \mathbf{A}_i \\ \mathbf{c}_i^T \end{pmatrix}\mathbf{x} + \begin{pmatrix} \mathbf{b}_i \\ d_i \end{pmatrix} \in C_{m_i+1}, \tag{2.45}$$

and hence it is convex. Thus, the SOCP (2.43) problem is a convex programming problem since the objective is a convex function and the constraints define a convex set. SOC constraints can be used to represent several common convex constraints. For example, when $m_i = 0$ for $i = 1, \cdots, L$, the SOCP reduces to LP

$$\begin{aligned} &\text{minimize} \quad \mathbf{f}^T\mathbf{x} \\ &\text{subject to} \quad \mathbf{c}_i^T\mathbf{x} + d_i \geq 0, \quad i = 1, \cdots, L, \end{aligned} \tag{2.46}$$

which is also given in (2.40). Another interesting special case arises when $\mathbf{c}_i = \mathbf{0}$, so the i-th SOC constraint reduces to $||\mathbf{A}_i\mathbf{x}+\mathbf{b}_i||_2 \leq d_i$, which is equivalent (assuming $d_i \geq 0$) to the (convex) quadratic constraint $||\mathbf{A}_i\mathbf{x}+\mathbf{b}_i||^2 \leq d_i^2$. Thus, when all $\mathbf{c}_i$ vanish, the SOCP problem reduces to a Quadratically Constrained Linear Program (QCLP). The (convex) Quadratic Programs (QPs), Quadratically Constrained Quadratic Programs (QCQPs), and many other nonlinear convex optimization problems can be reformulated as SOCP problems as well. Thus SOCP problems include LP problems and QPs as special cases, but can also be used to solve a variety of nonlinear, nondifferentiable problems.

2.5.6 Semidefinite Programming (SDP)

Let us consider a set of Hermitian $n \times n$ matrices represented by $\mathbf{S}^n$ as

$$\mathbf{S}^n = \left\{\mathbf{X} \in \mathcal{C}^{n\times n} | \mathbf{X} = \mathbf{X}^H\right\}, \tag{2.47}$$

which is a vector space with dimension $n(n+1)$. Using the notation $\mathbf{S}_+^n$, the set of Hermitian positive semidefinite matrices can be represented as

$$\mathbf{S}_+^n = \left\{\mathbf{X} \in \mathbf{S}^n | \mathbf{X} \succeq 0\right\}, \tag{2.48}$$

where the notation $\mathbf{X} \succeq 0$ represents that the matrix $\mathbf{X}$ is positive semidefinite. The set $\mathbf{S}_+^n$ is a convex cone; if $\theta_1\mathbf{A} + \theta_2\mathbf{B} \in \mathbf{S}_+^n$ for $\mathbf{A}, \mathbf{B} \in \mathbf{S}_+^n$ and $\theta_1, \theta_2 \geq 0$. This can be easily seen from the positive semidefiniteness; i. e., for any $\mathbf{x} \in \mathcal{C}^n$, we have

$$\mathbf{x}^H(\theta_1\mathbf{A} + \theta_2\mathbf{B})\mathbf{x} = \theta_1\mathbf{x}^H\mathbf{A}\mathbf{x} + \theta_2\mathbf{x}^H\mathbf{B}\mathbf{x} \geq 0, \tag{2.49}$$

if $\mathbf{A} \succeq 0$, $\mathbf{B} \succeq 0$, and $\theta_1, \theta_2 \geq 0$. An example of a positive semidefinite cone in $\mathbf{S}_+^2$ is given by

$$\begin{aligned} \mathbf{X} \quad &= \quad \begin{pmatrix} x & y \\ y & z \end{pmatrix} \in \mathbf{S}_+^2 \\ &\iff \quad x \geq 0, \; z \geq 0, \; xz \geq y^2. \end{aligned} \tag{2.50}$$

An SDP is a problem of minimizing a linear function over the intersection of an affine set and the cone of positive semidefinite matrices. Such a constraint is nonlinear and nonsmooth, but convex, so SDP problems are convex optimization problems. SDP unifies several standard problems (e.g., linear and quadratic programming) and finds many applications in engineering and combinatorial optimization. Although SDP problems are much more general than LP problems, they are not much harder to solve. Most interior-point methods for LP have been generalized to SDP problems. As in LP, these methods have polynomial worst-case complexity, and perform very well in practice.
In a SDP a matrix affine in the program variable $\mathbf{x}$ is constrained to be positive semidefinite and can be expressed as

$$\begin{aligned} &\text{minimize} \quad \mathbf{c}^T\mathbf{x} \\ &\text{subject to} \quad \mathbf{A}_0 + \mathbf{A}_1\mathbf{x}_1 + \cdots + \mathbf{A}_n\mathbf{x}_n \succeq 0, \end{aligned} \tag{2.51}$$

where $\mathbf{A}_i \in \mathcal{R}^{n\times n}$, and $\mathbf{A} \succeq 0$ denotes matrix inequality, i.e., $\mathbf{z}^T\mathbf{A}\mathbf{z} \geq 0;\ \forall\ \mathbf{z} \in \mathcal{R}^n$. SDP can also be regarded as an extension of LP where the componentwise inequalities between vectors are replaced by matrix inequalities, or, equivalently, the first orthant is replaced by the cone of positive semidefinite matrices. In general, a SDP problem can be also expressed as

$$\begin{aligned} &\min_{\mathbf{X}_k} \sum_{k=1}^{K} \mathrm{tr}(\mathbf{C}_k\mathbf{X}_k) \\ &\text{subject to} \quad \sum_{k=1}^{K} \mathrm{tr}(\mathbf{A}_{k,l}\mathbf{X}_k) = b_l, \quad l = 1, \cdots, L \\ &\qquad\qquad \mathbf{X}_k = \mathbf{X}_k^H \succeq 0, \quad k = 1, \cdots, K, \end{aligned} \tag{2.52}$$

where $\mathbf{C}_k$, $\mathbf{A}_{k,l}$ and $\mathbf{X}_k$ are all $n \times n$ symmetric matrices, b_l is a scalar and the constraint $\mathbf{X}_k^H \succeq 0$ denotes that the matrix $\mathbf{X}_k$ is a Hermitian positive semidefinite. Even this is a highly nonlinear constraint, it is still convex because a set of positive semidefinite matrices form a convex cone. In practice, several program packages are available to efficiently find the solution of (2.52), for example the SeDuMi toolbox [91] (see Appendix 9.2). We say that an optimization problem is feasible when there is at least one point that satisfies all constraints.
Many convex optimization problems, e.g., LP and (convex) QCQPs, can be cast as SDP problems, so that SDP offers a unified way to study the properties and derive algorithms for a wide variety of convex optimization problems. SDP problems include LP and SOCP problems as special cases, but can also be used to solve many other nonlinear, nondifferentiable problems.

Chapter 3

Dynamic System Level Simulator for UMTS-FDD with Smart Antennas

A SAS employs a spatio-temporal processing technique such as beamforming to reduce the inter-cell as well as intra-cell interference in cellular wireless systems thereby increasing the system capacity significantly. As a result, SAS can be used in interference limited systems like UMTS for capacity improvement. However, much focus has been on the link level benefit of the SAS. The system implications have received less attention and are not immediately obvious due to the complex nature of the adaptive antenna array processing technique and its interaction with the system features such as multiple access technology, power control, receiver architecture. The only realistic approach for evaluating the system performance of SA techniques for UMTS is through means of simulation. There are a number of commercial UMTS system simulators available, but most of them do not model the spatial channel response required to evaluate SA techniques.

3.1 Introduction

In this chapter we develop a dynamic system level simulator for investigating the capacity improvement in a UMTS-FDD system employing SAs at BSs. The simulator can be used for the performance evaluation of beamforming algorithms for both uplink and downlink communications of a UMTS-FDD based wireless network. The uplink performance is measured by finding the average number of MSs that can be supported in uplink with a certain QoS. Similarly, the downlink performance is evaluated by finding the average number of MSs for which a specified QoS requirement is fulfilled in downlink. In 3G mobile communication systems like UMTS, the downlink traffic load is supposed to be

higher than the uplink traffic load. Because of this traffic asymmetry, the overall system capacity is limited by the downlink capacity. The use of SA technology is therefore more relevant for the downlink communications than compared to the uplink. As a result, we focus mainly on downlink capacity improvement that can be obtained from the use of SA technology. We present, analyses of the downlink capacity for different numbers of array elements, both with and without power control. Moreover, this chapter compares downlink beamforming with different diagonal loadings and shows the effect of spatial fading correlations on downlink capacity. When using SAs, the real amount of performance improvement can only be estimated by system level simulations. Hence, dynamic system level simulations for UMTS-FDD are carried out which take into account the statistical nature of almost all parameters, e.g. wave propagation, user motion and traffic scenarios.

The three major system aspects of SA technology in wireless communications, i.e., SA receiver, wireless network control, and planning are surveyed in [14]. A UMTS-FDD system level simulator is proposed in [79] for comparing the relative performance of different SA technologies like switched beams, phased arrays and adaptive arrays. The main task of this simulator [79], given the network layout with mobiles, BSs and channel propagation conditions, are to iteratively find the maximum number of users which can be supported with a given service within the system limitations. In our method we consider both Broadcast Channels (BCH) like the Common Pilot Channel (CPICH) and dedicated channels (DCH) like the Dedicated Physical Data Channel (DPDCH). Downlink beamforming is carried out for dedicated channels while the omnidirectionally transmitted CPICH channel is used for MS to BS assignment and soft handover. We use the closed-loop fast power control method as proposed in 3GPP release 4. We assume that in the downlink the users are separated by spreading codes under a single scrambling code. Thus, our method is well compatible with 3GPP specifications. We carry out dynamic system level simulations using simple mobility and traffic update models in order to determine the gain in overall system capacity.

The rest of the chapter is organized as follows: In section 3.2, the simulation concept is presented with the description of each module of the simulator. The simulation results are presented in section 3.3. The chapter concludes with a summary in section 3.4.

3.2 Simulation Concept

3.2.1 Simulation Flow

Figure 3.1 shows the simulation flow. The simulation is based upon snapshots. In each

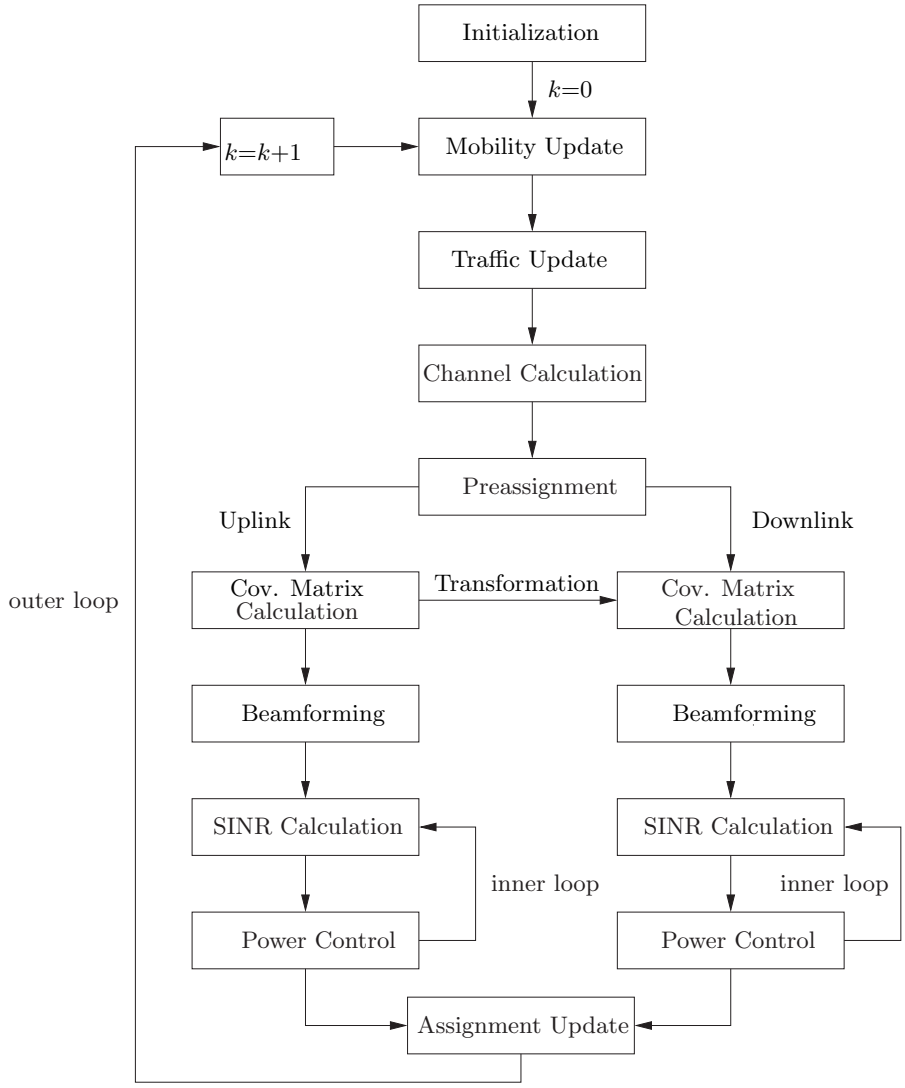

Figure 3.1: Block diagram of simulation flow

snapshot, the MSs move, the traffic situation changes and hence the uplink and downlink channels for all possible combinations of the MSs and BSs are either newly calculated or updated. MSs are assigned to BSs based upon the received pilot channel power. After a preliminary assignment of the MSs, uplink and downlink spatial covariance matrices can be either calculated or estimated. In general, the downlink spatial covariance matrix is estimated from the uplink one by frequency transformation. Uplink and downlink

beamforming are carried out for the DPDCH channels in the uplink and the downlink, respectively. For the uplink, SINR values for the DPDCH channel are calculated at each BS. For the downlink, SINR values for the DPDCH and CPICH channels are calculated at each MS. An iterative fast closed-loop power control method with a frequency of $f_{\mathrm{pc}} = 1.5$ kHz is used to adjust the powers of uplink and downlink DPDCH channels so that the MSs achieve the SINR target value for the DPDCH channel.
The MSs that cannot be provided with the target SINR for DPDCH at the end of power control loop are considered to be in outage. The assignment of MSs to BSs is updated after dropping the MSs that are out of coverage range or could not be provided with required quality of service. The outer loop starts the next iteration with a new snapshot. The inner loop or power control loop is assumed to be converged within the time difference T between two consecutive snapshots. The time duration of the outer loop T represents the sampling time used for simulation. In the following, we describe the modules of the simulation flow for the downlink communication.

3.2.2 Initialization

In the first part of the initialization procedure all the parameters that remain constant during the whole simulation are set. The parameters related with the cellular scenario like the total number of areas, total number of BSs per area, radius of the cells etc. can be changed by a user before starting a simulation run. The MS and BS related parameters are chosen according to 3GPP specifications [1]. A cellular configuration consisting of a main area and six surrounding areas is created as shown in Fig. 3.2.
The areas other than the main area represent the periodic continuation of the main area in all possible directions. They are used to simulate a wrap-around technique [43]. Each area consists of a central hexagonal cell surrounded by six other hexagonal cells. Each cell has a single BS at its centre.
This type of cellular structure is useful for simulating the effects of intra- and intercell interference in the cells that are located at the center as well as at the boundary of the main area. The wrap-around technique enhances the computational speed of the simulator. The MSs are distributed uniformly in the main area. Although the SINR evaluation is done only for MSs in the main area, because of the wrap-around technique the effect of equivalent mobile and BSs of all other areas has to be considered. Thus, it is clear that a BS of the main area and its equivalent BSs in all other areas have the same downlink beam patterns and same transmission powers.

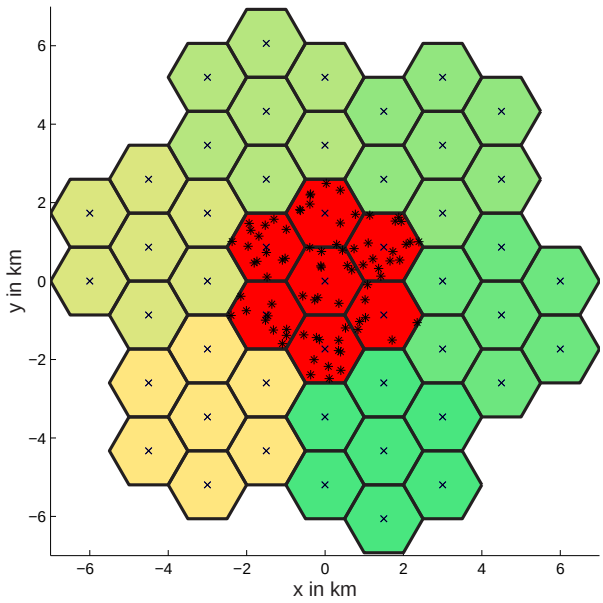

Figure 3.2: Locations of BSs and MSs

3.2.3 Mobility Model

The performance of a radio network is highly influenced by the mobility of the users in the cell [14]. The beamforming algorithm should be optimized according to the propagation scenario in which MSs move with different behaviours. In the mobility update procedure (see Fig. 3.3), the locations $\mathbf{r}(t)$ and directions of movement $\varphi(t)$ of the MSs are updated according to [43] as

$$\mathbf{r}(kT+T) = \mathbf{r}(kT) + \mathbf{v}(kT) \cdot T \tag{3.1}$$

$$\varphi(kT+T) = \varphi(kT) + A \cdot \Delta\varphi(kT)\,, \qquad \text{where} \tag{3.2}$$

$$\mathbf{v}(kT) = v(kT)\mathbf{e}_v(kT), \text{ and} \tag{3.3}$$

$$\mathbf{e}_v^T(kT) = (\cos(\varphi(kT)),\ \sin(\varphi(kT)))\,. \tag{3.4}$$

The MS speed $v(kT)$ at each snapshot is generated from a Gaussian distribution $f_v(v)$ with average speed $\overline{v}$ and standard deviation σ_v

$$f_v(v) = \frac{1}{\sqrt{2\pi}\sigma_v} \mathrm{e}^{-\frac{1}{2}\left(\frac{v-\overline{v}}{\sigma_v^2}\right)^2}. \tag{3.5}$$

The direction of movement $\varphi(t)$ of each MS at the $k+1$-th snapshot is obtained by updating its direction at the k-th snapshot. This is done by multiplying a uniformly distributed random variable $\Delta\varphi$ with another random variable A taking the values 0 and 1 according to the discrete probability density function $f_A(a)$

$$f_A(a) = p_{\mathrm{dc}}\delta(a-1) + (1-p_{\mathrm{dc}})\,\delta(a). \tag{3.6}$$

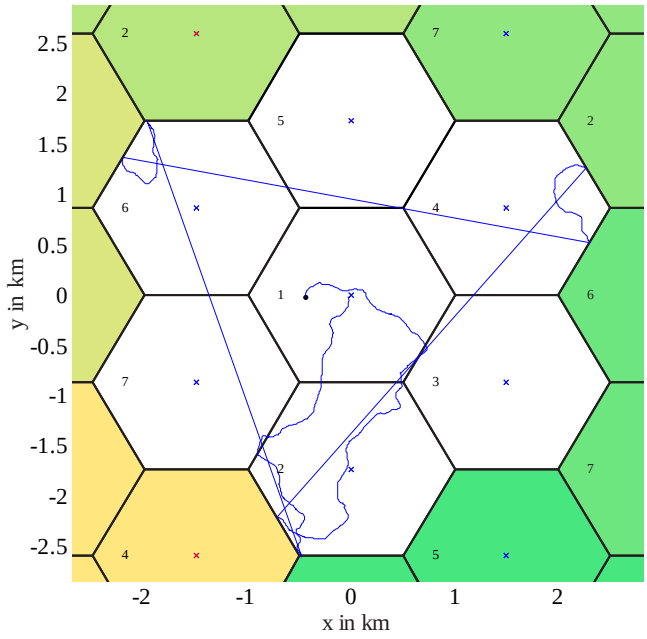

Figure 3.3: Random walk of a MS

The maximum change in direction, also called maximum swinging angle is limited to $\Delta\varphi_{\max}$. The probability density function of the swinging angle $\Delta\varphi$ is given by

$$f_{\Delta\varphi}(\Delta\varphi) \quad = \quad \frac{1}{\Delta\varphi_{\max}} \mathrm{rect}\left(\frac{\varphi}{\varphi_{\max}}\right) \ . \tag{3.7}$$

The maximum change in direction, also called maximum swinging angle is limited to $\Delta\varphi_{\max}$. The probability of direction change p_{dc} is used to make a decision whether or not a particular MS changes its direction. If the MS does not change its direction ($A = 0$), the direction calculated at the previous snapshot remains unchanged. A random walk model of a user in the cell is depicted in Fig. 3.3. The MS that is initially assigned to BS 1 of the main area (white background), gradually starts moving with a random speed and at some time moves away from the main area (like cell no. 2 of main area) to another area (cell no. 4 of the area at the bottom-left). At the same time another MS with the same specification enters the main area from the opposite direction (like from cell no. 2 of the area at the top-right to cell no. 4 of the main area). This ensures that the density of MSs in main area remains fixed.

3.2.4 Traffic Model

In this module, the traffic situation is updated according to a Poisson process. The probability of n new call arrivals within the sampling period T is given by

$$p_n(T) = \frac{(\lambda_\mathrm{r} T)^n}{n!} \mathrm{e}^{-\lambda T} \ , \tag{3.8}$$

where λ_r denotes the average arrival rate. For each new call, an exponentially distributed random variable describing the holding time t_H is generated from a pdf:

$$\begin{aligned} f_{t_H}(t_H) &= \tilde{\mu} \mathrm{e}^{-\tilde{\mu} t_\mathrm{H}}, \text{ for } t_\mathrm{H} \geq 0 \\ &= 0 \text{ else,} \end{aligned} \tag{3.9}$$

where $\tilde{\mu}$ is called the mean call duration or mean holding time.

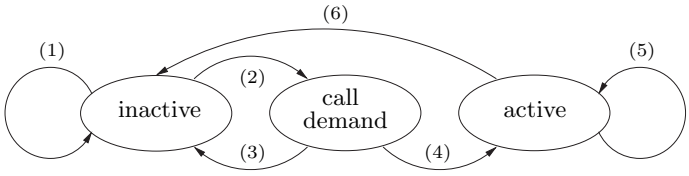

Figure 3.4: Traffic state diagram

During a simulation run, MSs can be *inactive*, *active* or in *call demand*. The corresponding state diagram is illustrated in Fig. 3.4. *Inactive* MSs may remain *inactive* (transition 1) or they can generate new calls according to (3.8) and enter into *call demand* state (transition 2). If a MS in the *call demand* state gets the reliable link, it enters into the *active* state (transition 4). Otherwise, it is blocked and set to *inactive* state (transition 3). An *active* MS may remain *active* (transition 5) or finish its call according to (3.9) and becomes *inactive* (transition 6). However, if the link quality gets degraded during the call, *active* MSs are dropped and set to the *inactive* state (transition 6).

3.2.5 Propagation Model

A completely probabilistic propagation model between each base and MS is used [26] [27]. Because of the high transmission bandwidth and significant multipath time dispersion, a frequency-selective fading channel has to be considered for UMTS-FDD. In this simulation, the number of paths between a MS and a BS is random and exhibits a binomial distribution. The path loss $L_l(k_0)$ (in dB) for path l at time instant $k_0 T$ is modeled as [26]

$$L_l(k_0) = L_\mathrm{d}(k_0) + c_\tau \tau_l(k_0) + L_\mathrm{sf}(k_0) + (c_\mathrm{r} + L_{\mathrm{pf},l}(k_0)) \ , \tag{3.10}$$

where $L_{\mathrm{d}}(k_0)$ denotes the distance attenuation according to the COST-Hata model and $c_\tau \cdot \tau_l(k_0)$ is an additional attenuation component which is proportional to the excess delay attenuation and is described by the average power decaying factor c_τ [dB/μs]. $L_{\mathrm{sf}}(k_0)$ is the log-normal fading of the received power at the MS and $L_{\mathrm{pf},l}(k_0)$ is the log-normal fading of reflected paths with respect to the direct path. c_{r} denotes the average attenuation of reflected paths. Both $L_{\mathrm{sf}}(k_0)$ and $L_{\mathrm{pf},l}(k_0)$ exhibit a Gaussian distribution with zero mean and standard deviation σ_{sf} and σ_{pf}, respectively. The excess delays $\tau_l(k_0)$ of reflected paths are exponentially distributed, so that the channel exhibits an exponential power delay profile. Finally, the DoAs are assumed to be Laplacian distributed. As the MSs move, the path loss does not remain constant over time. The time correlation of log-normal fading is not known in general. However, measured data [49] reveal that it can be modeled as a simple exponentially decreasing correlation function. This can be realized by filtering white Gaussian noise by a simple first order infinite impulse response (IIR) filter with a pole at

$$a = \varepsilon^{\frac{v(kT)T}{D}} \quad \Rightarrow \quad H(z) = \frac{z}{z-a}\,, \tag{3.11}$$

where ε is the spatial correlation between two points separated by a distance D, T denotes the sampling period, and $v(kT)$ is the velocity of the MS. The autocorrelation function is then given by

$$R_{\mathrm{f}}(k) = \mathrm{E}\left\{L_{\mathrm{sf}}(t)L_{\mathrm{sf}}(t+kT)\right\} = \sigma_{\mathrm{sf}}^2 a^{|k|}\,, \tag{3.12}$$

where σ_{sf}^2 is the variance of the log-normal fading. With the assumption that the number of scatterers around a MS does not change with time, the number of paths between a MS and a BS can be kept constant. The excess delays and all DoAs are updated according to the variations of the delay and DoA of direct path, respectively.

3.2.6 Handover - Preselection

We consider a soft handover process [54] where the radio links are added and abandoned in such a manner that the MS always keeps at least one radio link established. During the soft handover a MS has more than one active links at the same time. Based upon the path losses between a MS and all BSs, the active set AS_i for MS i is determined according to the received powers of the omnidirectionally transmitted CPICH channel. The active set AS_i is the set of all BSs from which the mobile user i receives the strongest CPICH channel within a margin known as hand-over margin (HO). Mathematically, the BSs of every active set should satisfy both the conditions: $P_{\mathrm{r}} > P_{\mathrm{th}}$ and $P_{\mathrm{r}} > (P_{\mathrm{r,max}} - \Delta P_{\mathrm{HO}})$, where P_{r} is the CPICH power received by MS, P_{th} is its threshold value, $P_{\mathrm{r,max}}$ is its

maximum received power and ΔP_{HO} is the handover margin. The maximum active set size in our simulation is set to 2.

In the downlink of the WCDMA system, users assigned to the same BS can only be separated by the spreading codes. The Orthogonal Variable Spreading Factor (OVSF) codes with spreading factors between 4 and 512 are available in WCDMA, depending on the data rate a MS requests for. Therefore, a simplified code administration method is incorporated which takes into account a limited number of different spreading codes in the downlink. According to this, MSs can only be assigned to BSs if a code is available. We assume that a BS uses a single scrambling code. In our dynamic simulator, the code administration method can be activated or deactivated according to parameters chosen by the user.

3.2.7 Downlink Beamforming

Because of limited terminal size, we consider the application of antenna arrays only at BSs. Investigations carried out in [26] for different array topologies show that a UCA is the best choice. Hence, in our simulation, we use UCAs. A spatial covariance matrix based beamforming method [27] is performed for the dedicated channels in UMTS.

Covariance Matrix Calculation

In a multipath-rich environment like the UMTS radio channel, the number of incoming wavefronts can be excessively high. However, in our method we use a simplified discrete DoA model which takes only the strongest Q_{ij} paths into account. Assuming all paths $l = 1 \ldots Q_{ij}$ are uncorrelated, the spatial covariance matrix (averaged over fast fading) [31, 98] between mobile i and BS j can be approximated by (2.27)

$$\mathbf{R}_{ij} = \sum_{l=1}^{Q_{ij}} \alpha_{ijl}^2 \mathbf{a}\left(\theta_{ijl}\right) \mathbf{a}^H\left(\theta_{ijl}\right), \tag{3.13}$$

where $\alpha_{ijl}^2 = 10^{-\frac{L_l}{10}}$ can be interpreted as an estimate of the medium-term expectation of the transmission factor $\alpha_{ijl}^2(t)$ corresponding to the wave of path l. $\mathbf{a}\left(\theta_{ijl}\right)$ denotes the array response vector of a wave incident at the BS with the angle θ_{ijl}. The steering vector $\mathbf{a}\left(\theta_{ijl}\right)$ for a UCA consisting of M elements is given by (2.30). For the simulation results presented in this chapter, we assume perfect knowledge of all DoAs and average path attenuations in the downlink. In practice, these parameters can be estimated by transmitting WCDMA downlink CPICH channel with antenna specific sequences that are mutually orthogonal to each other. In this case a BS has to rely upon feedback

information from a MS. Another way is to estimate the average spatial covariance matrix in the uplink and transform it to the downlink frequency which is described in **Chapter 4**. Training or (semi-)blind methods [67, 81] can be used for uplink covariance matrix estimation. However, estimation and transformation errors will reduce the performance of beamforming.

Beamforming Algorithm

The used algorithm maximizes the average signal power P_{S} received by the desired MS i assigned to BS $c(i)$ while keeping the sum of the total interference power P_{I} at all undesired MSs constant. This problem can be formulated as

$$\begin{aligned} \max_{\mathbf{w}_i} P_{\mathrm{S}} &= \max_{\mathbf{w}_i} P_i \mathbf{w}_i^H \mathbf{R}_{i,c(i)} \mathbf{w}_i \quad \text{subject to} \\ P_{\mathrm{I}} &= P_i \mathbf{w}_i^H \sum_{m \neq i} \mathbf{R}_{m,c(i)} \mathbf{w}_i = \text{const} , \end{aligned} \tag{3.14}$$

where P_i, $\mathbf{w}_i$ and $\mathbf{R}_{i,c(i)}$ denote the BS transmit power for MS i, the weight vector for MS i and the covariance matrix between the desired MS i and its corresponding BS $c(i)$, respectively. $\mathbf{R}_{m,c(i)}$ represents the covariance matrix between an undesired MS m and the same BS $c(i)$. The solution of (3.14) is the eigenvector associated with the largest eigenvalue (generalized eigenvalue problem) of the characteristic equation [72]

$$\mathbf{R}_{i,c(i)} \mathbf{w}_i = \lambda \left(\sum_{m \neq i} \mathbf{R}_{m,c(i)} \right) \mathbf{w}_i. \tag{3.15}$$

Examples for downlink beam patterns of an adaptive beamformer which uses a UCA with 4 and 8 antenna elements are shown in Fig. 3.5. The green line represents the average channel fading gain for the user of interest where as the red lines represent the average channel fading gains for interfering users. The longer the red lines, the stronger are the undesired MSs interfered. The blue curves represent the radiation patterns of the antenna arrays. We can observe that the number of interferers is much higher than the number of nulls the adaptive arrays of size M can produce. As a consequence, the beamformer attempts to provide nulls towards the strongest interferers, thereby reducing the interference level. As the number of antenna elements increases, the beamformer's capability to suppress the interference also increases.

We also carry out simulations using the same beamforming algorithm (3.15) incorporating different interference covariance matrices. Considering additional spatially white noise power P_N, the ideal interference covariance matrix $\mathbf{R}_{I,i}$ of user i from (3.14) can be

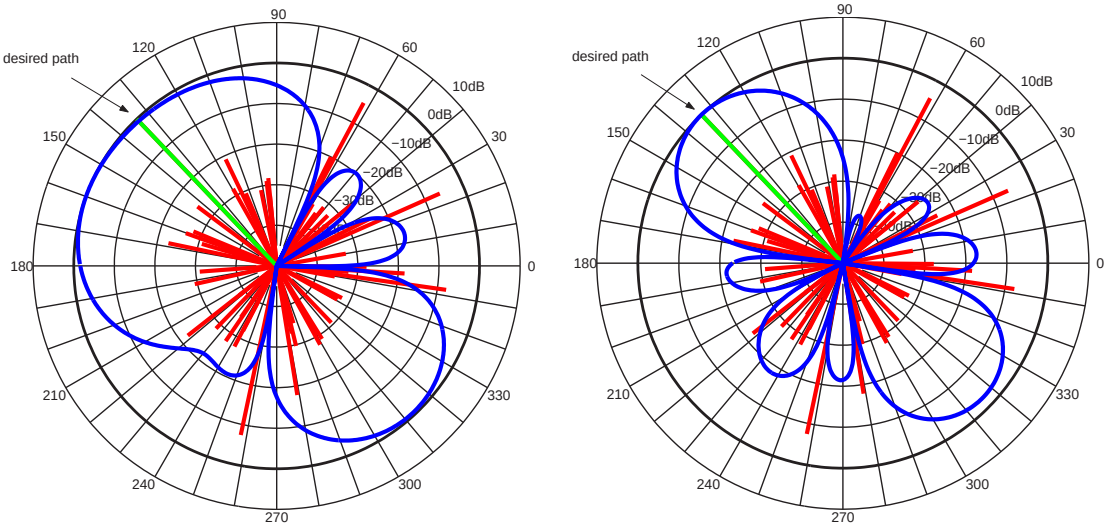

(a) Four array elements

(b) Eight array elements

Figure 3.5: Examples of beam patterns for different numbers of array elements

extended to [88] as

$$\mathbf{R}_{I,i} = \sum_{m \neq i} \mathbf{R}_{m,c(i)} + P_N \mathbf{I}_M. \tag{3.16}$$

Simulations have been carried out taking into account

- a) no noise power, i.e. $P_N = 0$
- b) only receiver thermal noise power, described by the white Gaussian noise of variance σ_{N}^2 i. e. $P_N = \sigma_{\mathrm{N}}^2$
- c) both thermal noise and received CPICH channel power (P_{CPICH} at the MSs i.e. $P_N = \sigma_{\mathrm{N}}^2 + P_{\mathrm{CPICH}} \cdot \sum_{m \neq i} \left(\mathbf{R}_{m,c(i)}\right)_{1,1}$, where $\left(\mathbf{R}_{m,c(i)}\right)_{1,1}$ represents the element of the first row and first column of the matrix $\mathbf{R}_{m,c(i)}$.

3.2.8 SINR Calculation

The SINR at MS i assigned to BS $c(i)$ is calculated by dividing the received desired signal power P_{S} by the interference and noise power, and multiplying by the processing gain G_{p}. Signal powers transmitted from the same BS $c(i)$ but dedicated to other users are also received by the desired MS i. This is seen as intracell interference power I_{intra} to the MS i. Intercell interference I_{inter} is interference power from other cells. Considering non-perfect orthogonality of the signals from the same BS due to multipaths and estimation errors,

intracell interference cannot be neglected and is taken into account by weighting with the Orthogonality Factor (OF) α. The effect of the downlink OF on WCDMA performance is investigated in [78]. It is found that the OF decreases as the MS moves closer to the BS and the OF is positively correlated with the shadow fading (also called lognormal fading) component of the radio channel. This shows that OF varies within the cells but for simplicity the downlink OF is assumed to be constant within a cell. Hence, the SINR at MS i can be calculated by [1]

$$\mathrm{SINR}_i = \frac{G_{\mathrm{p},i} \cdot P_{\mathrm{S},i}}{\sigma_{\mathrm{N}}^2 + P_{\mathrm{Intra},i} + P_{\mathrm{Inter},i}}, \tag{3.17}$$

where σ_{N}^2 is thermal noise power, the desired signal power $P_{\mathrm{S,i}}$ is given by

$$P_{\mathrm{S},i} = P_i \mathbf{w}_i^H \mathbf{R}_{i,c(i)} \mathbf{w}_i, \tag{3.18}$$

the intracell interference power $P_{\mathrm{Intra},i}$ equals

$$P_{\mathrm{Intra},i} = \alpha \sum_{m \neq i} P_m \mathbf{w}_m^H \mathbf{R}_{i,c(i)} \mathbf{w}_m + \alpha P_{\mathrm{CPICH}} \left(\mathbf{R}_{i,c(i)} \right)_{1,1}, \tag{3.19}$$

and, finally, the intercell interference power $P_{\mathrm{Inter},i}$ can be expressed as

$$P_{\mathrm{Inter},i} = \sum_{n \neq i} P_n \mathbf{w}_n^H \mathbf{R}_{i,c(n)} \mathbf{w}_n + P_{\mathrm{CPICH}} \sum_{c(n) \neq c(i)} \left(\mathbf{R}_{i,c(i)} \right)_{1,1}. \tag{3.20}$$

P_n and $\mathbf{w}_n$ denote the transmission power and weight vector for user n assigned to BS $c(n)$, respectively. P_{CPICH} is the constant transmission power of the omnidirectional broadcast channel, $\left(\mathbf{R}_{i,c(i)} \right)_{1,1}$ denotes the element of the first row and column of covariance matrix $\mathbf{R}_{i,c(i)}$. For $P_N = 0$ (negligible thermal noise power) and neglected interference from CPICH, the SINR for the ith mobile user can be written in a simplified form as

$$\mathrm{SINR}_i = \frac{G_{\mathrm{p},i} \cdot P_{\mathrm{S},i}}{\sigma_{\mathrm{N}}^2 + \alpha \underbrace{\sum_{m \neq i} P_m \mathbf{w}_m^H \mathbf{R}_{i,c(i)} \mathbf{w}_m}_{I_{\mathrm{intra}}} + \underbrace{\sum_{n \neq i} P_n \mathbf{w}_n^H \mathbf{R}_{i,c(n)} \mathbf{w}_n}_{I_{\mathrm{inter}}}}. \tag{3.21}$$

For large delay differences ($\geq$ chip period), paths of the desired signal can be resolved and path diversity gain can be obtained at the MSs. RAKE receivers with MRC can be used for exploiting this multipath diversity. In the present simulation, it is assumed that all paths Q_{ij} can be resolved. An exact expression of SINR after the rake receiver is given in [51]. If the number of rake fingers is equal to the number of resolvable paths,

the SINR at the output of rake receiver is given by

$$\begin{aligned}\mathrm{SINR}_i &= \sum_{l=1}^{Q_{ij}} \mathrm{SINR}_{il} \\ &= \sum_{l=1}^{Q_{ij}} \frac{G_{\mathrm{p},i} \cdot P_i \mathbf{w}_i^H (\alpha_{ijl}^2 \mathbf{a}(\theta_{ijl})^H \mathbf{a}(\theta_{ijl})) \mathbf{w}_i}{\sigma_N^2 + \alpha \sum_{l' \neq l} \sum_{m \neq i} P_m \mathbf{w}_m^H (\alpha_{ic(i)l'}^2 \mathbf{a}(\theta_{ic(i)l'})^H \mathbf{a}(\theta_{ic(i)l'})) \mathbf{w}_m + P_{\mathrm{Inter},i}},\end{aligned} \tag{3.22}$$

where $P_{\mathrm{Inter},i} = \sum_{n \neq i} P_n \mathbf{w}_n^H \mathbf{R}_{i,c(n)} \mathbf{w}_n$ represents the inter-cell interference. Here, we assume that the MS receives a large number of statistically independent interfering signals, and hence the interference powers are identical for all the desired paths. In other words, this assumption results in the same denominator of (3.22) for all the paths ($l = 1, \cdots, Q_{ij}$). Therefore, it can be easily observed that the SINR given by (3.22) can be approximated by (3.21) and can be regarded as the SINR after RAKE reception with MRC.

3.2.9 Power Control

Power control is applied to ensure the QoS constraints per user at the MSs. But power control in conjunction with the use of optimum downlink beamforming [12, 30, 46] leads to a coupled optimization problem, where the optimization has to be performed jointly with respect to powers and beamforming weights. Because all the beamformers of MSs assigned to a BS of interest are involved in the joint power control and beamforming solution, there is a clear indication that the optimum joint solution must be calculated centrally for the BS. Moreover, the mobile radio channel between every combination of BSs and the MSs has to be known. Therefore, in this section we restrict to suboptimum downlink power control methods which can be easily accomodated in system level simulators. In this regard, power control methods that can be implemented in a decentralised or distributed fashion i. e. per MS, have been found to be computationally efficient. As proposed by Foschini et. al. in [37], these algorithms control each power adjustment separately without requiring knowledge of power settings of all other users. This iterative approach of power control is the basis for UMTS-FDD fast power control. The power update procedure can be expressed mathematically in the form

$$\hat{P}_{\mathrm{S},i}(kT) = \frac{\gamma_{th} \hat{P}_{\mathrm{S},i}((k-1)T)}{\mathrm{SINR}_i}, \tag{3.23}$$

where $\hat{P}_{\mathrm{S},i}$ is the power transmitted to the ith MS, k denotes the iteration index, T is the sampling period, SINR_i is the instantaneous SINR measured after the RAKE

receiver and γ_{th} is the threshold value of SINR_i. A simple fast inner loop power control algorithm (3.23) according to 3GPP [1] is used for the DPDCH channel. Power control is not used for a common channel like the CPICH. Based upon the measured SINR_i of the dedicated channels, a predefined threshold value γ_{th} and maximum value $\gamma_{\max}$, the algorithm procedure is as follows:

1. $\mathrm{SINR}_i < \gamma_{th}$: MS issues power up command $\rightarrow P_{\mathrm{new,dB}} = P_{\mathrm{old,dB}}$ + step size
2. $\mathrm{SINR_i} > \gamma_{\max}$: MS issues power down command $\rightarrow P_{\mathrm{new,dB}} = P_{\mathrm{old,dB}}$ - step size
3. $\gamma_{\max} > \mathrm{SINR}_i > \gamma_{th}$: SINR is within predefined range $\rightarrow P_{\mathrm{new,dB}} = P_{\mathrm{old,dB}}$

As suggested in [1], the power control step size is 1 dB. We assume that the power control commands are perfectly received by the BS without any delay in order to simplify our method. Furthermore, the transmission power of each BS is bounded by its minimum and maximum values. Mobiles which are not able to fulfill the required threshold SINR value for the DPDCH channel after completion of the power control loop are considered to be in outage.

3.2.10 Assignment Update

If the SINR value measured at the MS for CPICH or DPDCH channel is below the threshold value, the mobile is dropped. When the SINR value for CPICH is below the threshold value, the MS is out of the coverage range of the corresponding BS. Similarly, when the SINR value for DPDCH is below the threshold value, the MS cannot be provided with acceptable link quality. However, a time window is considered during which a BS tries to hold the connection although the link quality is not sufficient. Therefore, a drop counter decides whether the MSs in outage are really dropped.

3.3 Simulation Results

The simulation results are the average of ten simulation runs. Each simulation run is carried out for a time interval of $2000T$ with the parameters listed in Table 3.1.
The number of MSs (in the main area) that can be supported in the downlink with a data rate of 384 kbit/s for different numbers of antenna elements with and without power control versus simulation time are shown in Fig. 3.6 and Fig. 3.7, respectively. After a transient, the number of MSs that can be supported in the downlink remains more or less constant. This indicates that even if new MSs are generating calls in each snapshot, the

Number of BSs	49	Cell radius	1 km
Average number of paths	3	Max. number of paths	6
STD of slow fading	10 dB	STD of path fading	6 dB
Correlation distance for slow fading	100 m	Spatial correlation	0.82
STD angular spread	20°	STD mobile speed	5 m/s
Mean mobile speed	0 m/s	Call arrival rate	5 s^{-1}
Mean call duration	1.5 min	Sampling period (T)	200 ms
Number of snapshots	2000	Max. TX power	43 dBm
Max. DPDCH power	30 dBm	CPICH power	30 dBm
Handover Margin	3 dB	Orthogonality factor	0.4
DPDCH threshold $SINR_{th}$	4.5 dB	DPDCH max. $SINR_{max}$	6.5 dB
Power control frequency	1.5 kHz	Power control range	25 dB
Power control step size	1 dB	Data rate	384 kbit/s
Spreading factor for CPICH	256	Spreading factor for DPDCH	8

Table 3.1: Simulation parameters

number of MSs that can be served is limited. Thus, the downlink capacity of the system reaches saturation. The fluctuations in the curves are because of the limited number of simulation runs that are averaged.

It can be easily seen that as the number of array elements increases, the downlink capacity also increases. Although the omnidirectionally transmitted CPICH channel causes severe interference to the directionally transmitted DPDCH channel, the improvement in capacity due to a higher number of antenna elements is significant. This improvement is even higher in case of a system with power control than compared to that without power control.

It can also be observed that power control plays a considerable role especially in case of antenna arrays with a higher number of elements. The downlink capacity for a single element antenna without power control is almost similar to that with power control. However, it is not true for antenna arrays with more elements. For example, a four element antenna array can support about 40 MSs without power control in contrast to about 60 with power control. Hence, it can be stated that the antenna arrays with a higher number of elements provide a greater degree of freedom to suppress the interference and

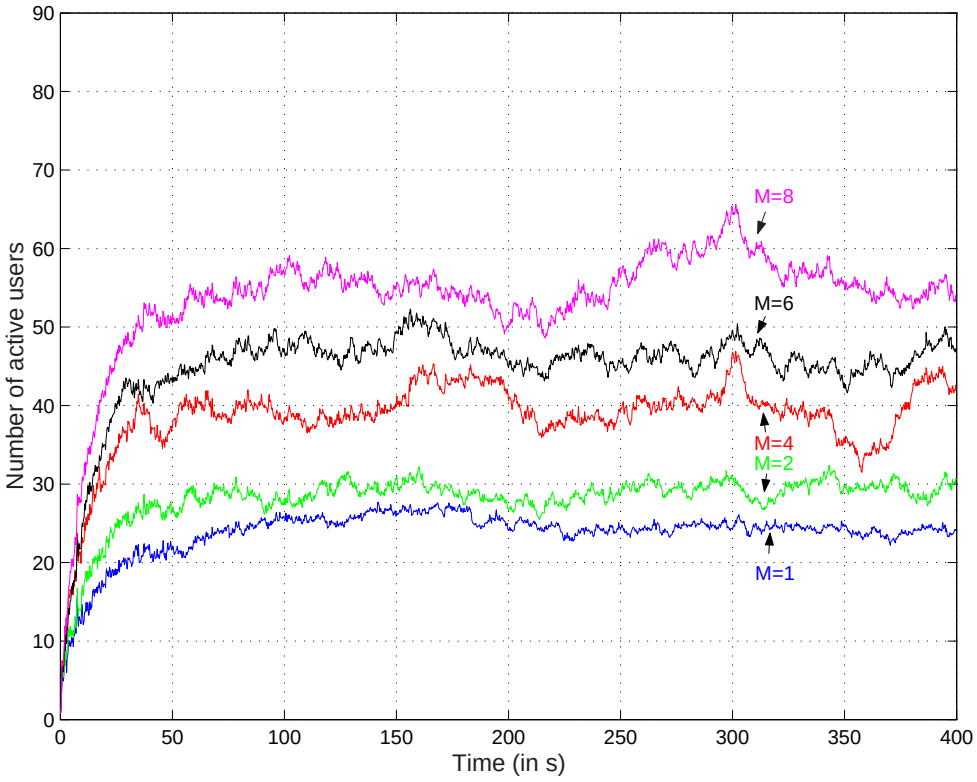

Figure 3.6: Number of active users in the main area versus time without power control

adjust the transmission powers of DPDCH channel such that more MSs can be supported with the required QoS. This fact is further illustrated with the histograms of the downlink DPDCH channel power for one and four element antenna arrays using power control as shown in Fig 3.8. In order to fulfill the SINR criterion for the DPDCH channel, the BSs with single omnidirectional antenna, require to provide most of the transmission links with powers close to the maximum power (see figure 3.8(a)). This is similar to the case without power control, where all BSs transmit with the highest possible power. Since beamforming allows to reduce DPDCH channel powers even more (see figure 3.8(b)), the effect of power control is vital. Figure 3.9 shows the number of active users that can be supported in downlink with the following beamforming methods;

- a) optimized beamforming after (3.15) where no thermal noise power is included in $\mathbf{R}_{I,i}$,
- b) optimized beamforming after (3.15) where only thermal noise power is taken into account in $\mathbf{R}_{I,i}$ and
- c) optimized beamforming after (3.15) where both thermal noise and received

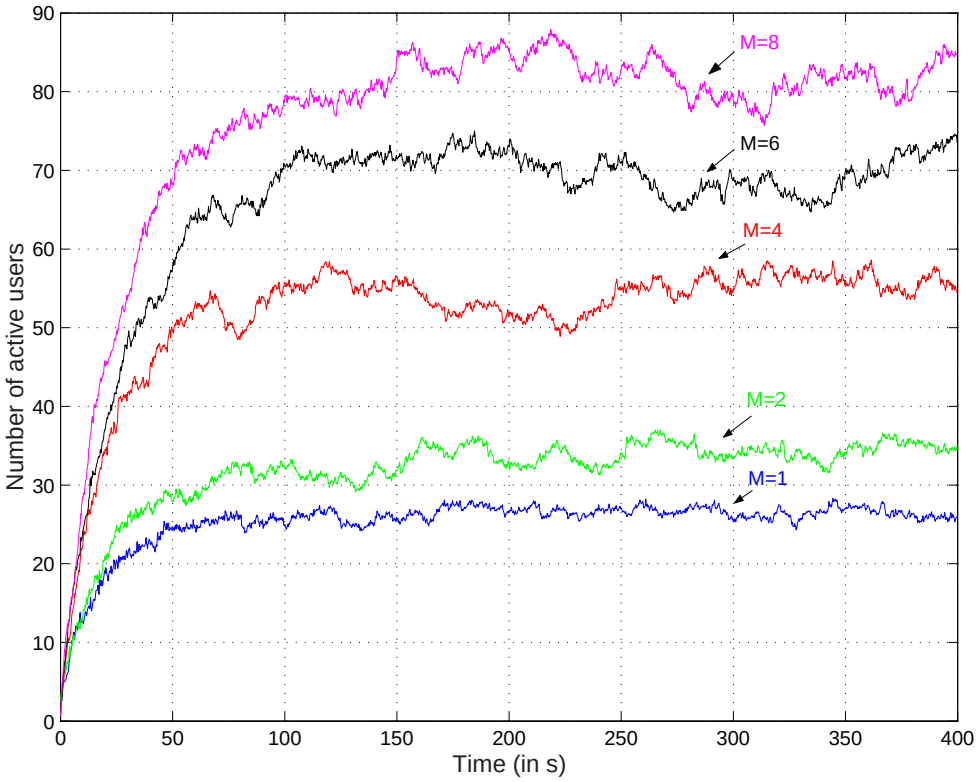

Figure 3.7: Number of active users in the main area versus time with power control

CPICH channel power at the MSs is included in $\mathbf{R}_{I,i}$.

It can be observed from Fig. 3.9 that for the considered numbers of array elements M and the chosen simulation parameters (see Table 3.1), the number of satisfied users increases almost linearly with respect to M. In this figure, we keep receiver thermal noise power to -99 dBm. Although the CPICH channel is transmitted with the highest allowed channel transmit power (30 dBm) and produces therefore considerable background interference for all users, beamforming has still got a significant impact on the system capacity.
Moreover, beamforming strategy (c) which takes noise and CPICH channel power into consideration outperforms other methods, independent of M. E.g., for eight array elements, the system can support in average about 13% more users with beamforming strategy (c) than with (b) and even about 16% more users than with (a). This indicates that a large fraction of the overall interference is caused by broadcast channels that cannot be suppressed by beamforming since they have to be transmittted omnidirectionally. Consequently, as P_N increases, the algorithm (3.15) turns to a beamforming approach based upon maximization of the SNR.
It can be observed from equation (3.13) that the average transmission factor α_{ijl}^2 corre-

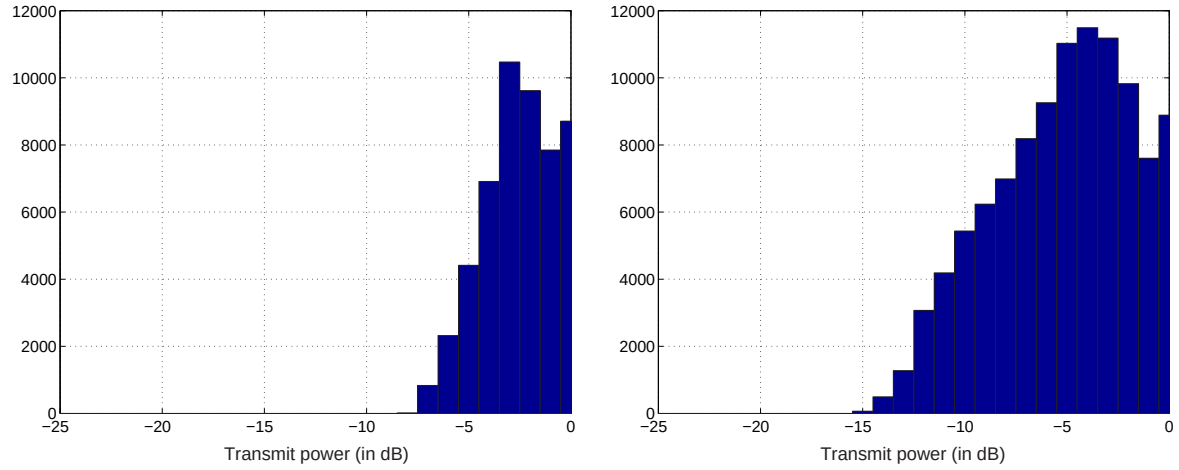

(a) Omnidirectional antennas

(b) Four element antenna arrays

Figure 3.8: Histograms of transmit powers for different number of array elements with power control

sponding to the wave of path l multiples all the elements of the steering vector $\mathbf{a}(\theta_{ijl})$. This means that the fading among the elements of the antenna array is perfectly correlated. This case is called perfect correlation. By the introduction of spatial fading correlation (2.34), the elements of the steering vector $\mathbf{a}(\theta_{ijl})$ are multiplied with the weighted average transmission factor α_{ijl}^2, where the weights for the transmission factors depend on the spatial correlation among the antenna elements. We call this case partial correlation. Note that in a dynamic system level simulator as the channel varies in each snapshot, the spatial correlation is updated in each snapshot. Fig. 3.10 shows the performance of the downlink beamforming algorithm (3.15) for perfectly (3.13) and partially (2.34) correlated spatial fading cases. The simulation is carried out for an OF of $\alpha = 0.6$ and $M = 4$ with the average and maximum number of paths (see Table 3.1) set to 2 and 4, respectively. It can be observed that as the spatial fading correlation between the antenna elements decreases, the downlink capacity decreases. The spatial fading correlation has been modeled and calculated according to (2.34). The capacity also decreases as the OF increases (compare the results with that of $\alpha = 0.4$ (Fig. 3.9)).

3.4 Summary

In this chapter, a new dynamic system level simulator for UMTS-FDD systems with SAs has been presented. Simulation results for different numbers of arrays elements have

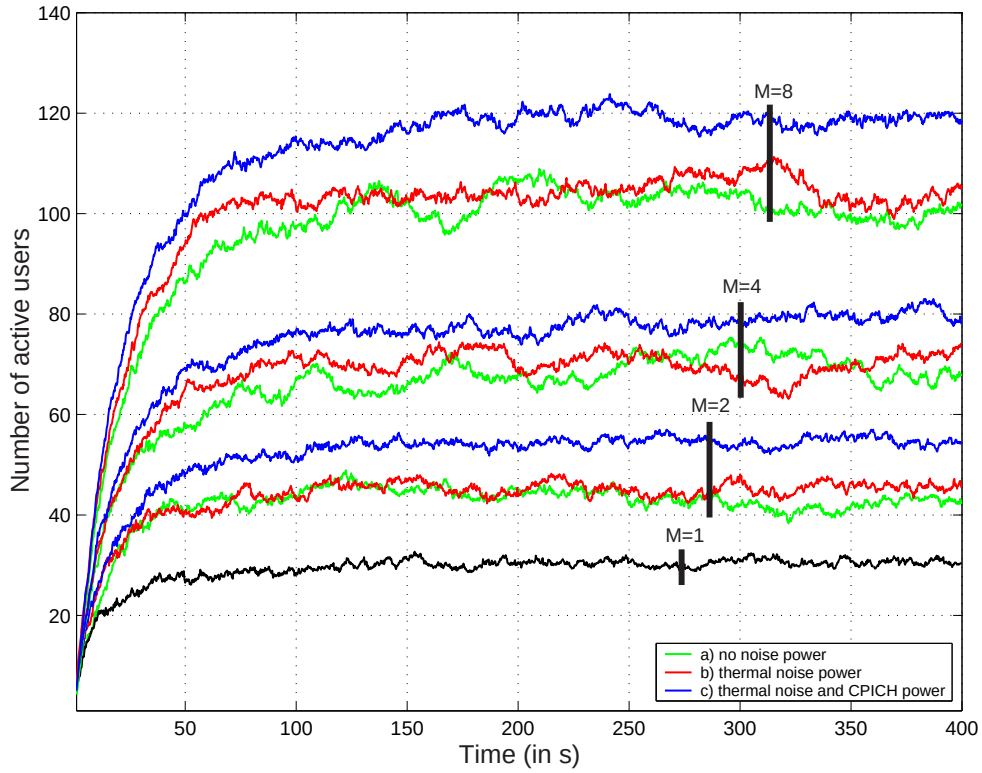

Figure 3.9: Number of active users in the main area versus time with different beamforming algorithms

shown a significant downlink capacity increase when beamforming is applied although omnidirectionally transmitted broadcast channels produce significantly high background interference. In a realistic radio environment, the use of power control provides significant improvement in the performance of beamforming. Among the compared beamforming concepts, the algorithm considering both noise and CPICH power turns out to be the best method of choice. The effect of spatial fading correlation and that of the OF on the system level performance of a UMTS-FDD system are also investigated. Simulation results show that the downlink capacity decreases if the fading correlation between the antenna elements decreases. Similarly, the higher the OF, the lower is the downlink capacity.

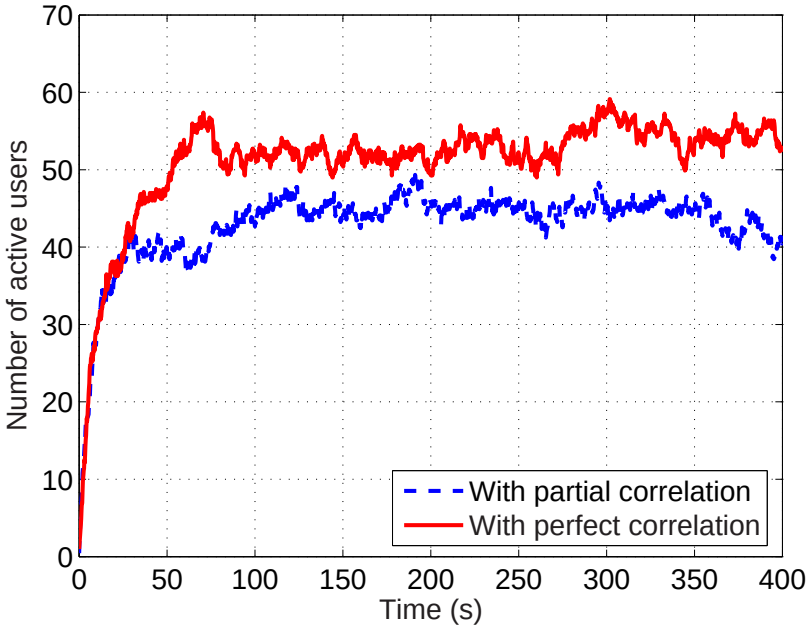

Figure 3.10: Number of active users in the main area versus time with different spatial fading correlation

Chapter 4

Uplink to Downlink Covariance Matrix Transformation Methods

Although the downlink capacity of 3G mobile communication systems like UMTS is limited by co-channel and inter-symbol interference, they are going to provide high data rate services such as video and internet. By exploiting the spatial domain like using adaptive antennas at the BSs, the downlink capacity can be increased significantly. The task of extracting downlink radio channel parameters from the uplink received signal is difficult in case of FDD systems because of the significant frequency separation between the uplink and downlink channels. However, measured data reveal that second order statistics like the Azimuthal Power Spectrum (APS) [55] and average fading gains for uplink and downlink channels show significant correlations. Therefore, it is possible to perform downlink beamforming with the transformed uplink spatial covariance matrix. This chapter deals with both non-robust and robust uplink to downlink spatial covariance matrix transformation methods. In non-robust methods the transformation is carried out based on the assumption that the uplink spatial signature is perfectly estimated at the BS where as robust methods are based on the assumption that only an estimate of the uplink spatial signature is known at the BS.

4.1 Introduction

In 3G mobile communication systems like UMTS with FDD transmission, the uplink and downlink channels are separated by a frequency difference of about 190 MHz. The uplink and downlink channels have different wavelengths, and therefore different responses, direct downlink adaptation based on channel estimates of the uplink is generally not fea-

sible. An array configuration that adapts the uplink channel to the downlink channel is proposed in [53]. This array employs $M+1$ antenna elements with log-periodic spacing, that comprises two overlapping subarrays, each with M elements, that are scaled versions of each other, with the scaling factor equal to the ratio of the uplink wavelength to downlink wavelength. The drawback of this approach is the requirement of complicated antenna structure with more elements. Downlink beamforming for WCDMA over Rayleigh fading channels based on prediction of the downlink channels is proposed in [29]. The BS predicts the downlink channel using a linear prediction based on an autoregressive model.

Uplink to downlink adaptation methods that require only second-order statistics of the uplink and downlink channels are proposed by [5, 34, 55]. In this regard, uplink to downlink covariance matrix transformation techniques like the MMSE and the MVDR filter for downlink beamforming have been presented in [5, 34] and [55], respectively. In our method we consider both broadcast channels like the Common Pilot Channel (CPICH) and dedicated channels like the Dedicated Physical Data Channel (DPDCH) of the UMTS-FDD system. Downlink beamforming based on transformation methods is carried out for dedicated channels while the omnidirectionally transmitted CPICH channel is used for MS to BS assignment and soft handover.

Another approach is to introduce robustness against the small errors in the esimated or assumed steering vectors. Hence in robust methods, we consider that the exact uplink steering vectors at the BS are different from the presumed one because of multipath and angular spreading effects. The exact uplink steering vector is modeled as a presumed steering vector with bounded uncertainty. A transformation is carried out in a least-squares sense from uplink to downlink frequency under the condition that the bounded uncertainty in uplink steering vector is maximized. In literature [15] such a method is also known as a constrained LS method or Robust Least Squares (RLS) method. Moreover, we use the closed-loop fast power control method as described in **Chapter 3**. We assume that in the downlink the users are separated by spreading codes under a single scrambling code. Thus, our method is well compatible with 3GPP specifications. We carry out dynamic system level simulations (**Chapter 3**) using simple mobility and traffic models in order to determine the gain in overall system capacity.

The chapter is organized as follows: In Section 4.2, the propagation model is described from a system level perspective. The uplink covariance matrix estimation and its trans-

formation to the downlink covariance matrix are presented in sections 4.3 and 4.4, respectively. Here, we describe the non-robust transformations based on the MVDR and MMSE methods. Moreover, the proposed robust transformation method is also presented in Section 4.4. Section 4.5 deals with downlink beamforming. Modifications of the simulator with respect to that of **Chapter 3** are described briefly in section 4.6 and simulation results are presented in section 4.7. In Section 4.8, a summary of the chapter is presented.

4.2 Propagation Model

The propagation model between each base and MS is based upon spatial as well as temporal characteristics of the radio channel as described in **Chapter 3**. The BS uses the same UCA for uplink and downlink. The complex uplink and downlink steering vectors depend upon the carrier wavelength. For M array elements, the uplink and downlink steering vectors are

$$\begin{aligned} \mathbf{a}\left(\theta, \lambda_{\text{up}}\right) &= \left[\mathrm{e}^{-\mathrm{j}2\pi \frac{r}{\lambda_{\text{up}}} \cos\theta}, \mathrm{e}^{-\mathrm{j}2\pi \frac{r}{\lambda_{\text{up}}} \cos\left(\theta - \frac{1}{M}2\pi\right)}, \ldots, \mathrm{e}^{-\mathrm{j}2\pi \frac{r}{\lambda_{\text{up}}} \cos\left(\theta - \frac{M-1}{M}2\pi\right)}\right]^T \\ \mathbf{a}\left(\theta, \lambda_{\text{dl}}\right) &= \left[\mathrm{e}^{-\mathrm{j}2\pi \frac{r}{\lambda_{\text{dl}}} \cos\theta}, \mathrm{e}^{-\mathrm{j}2\pi \frac{r}{\lambda_{\text{dl}}} \cos\left(\theta - \frac{1}{M}2\pi\right)}, \ldots, \mathrm{e}^{-\mathrm{j}2\pi \frac{r}{\lambda_{\text{dl}}} \cos\left(\theta - \frac{M-1}{M}2\pi\right)}\right]^T, \end{aligned} \tag{4.1}$$

where r, λ_{up} and λ_{dl} are the geometrical radius of the circular array, the uplink and downlink carrier wavelengths, respectively. A UCA of size $M = 4$ as shown in Fig. 4.1

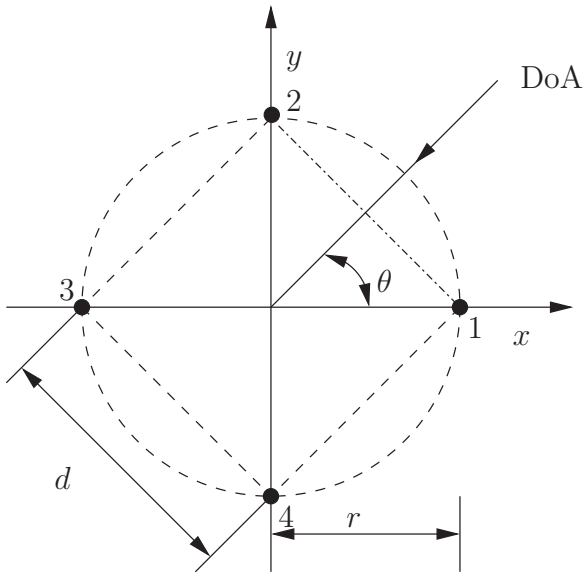

Figure 4.1: Uniform circular array for uplink and downlink transmissions

is used for uplink as well as downlink beamforming. A linear wavefront from a distant

source is incident on the array at an angle of incidence θ with respect to the reference array element 1. For a distance $d = \frac{\lambda_{\text{up}}}{2}$ between two consecutive array elements, the ratio of geometrical radius of the UCA to uplink and downlink carrier wavelengths can be defined as

$$\begin{aligned} \frac{r}{\lambda_{\text{up}}} &= \frac{1}{4\sin\left(\frac{\pi}{M}\right)} \\ \frac{r}{\lambda_{\text{dl}}} &= \frac{r f_{\text{dl}}}{\lambda_{\text{up}} f_{\text{up}}}, \end{aligned} \tag{4.2}$$

where f_{up} and f_{dl} are the uplink and downlink carrier frequencies, respectively.

4.3 Uplink Covariance Matrix Estimation

Assuming all paths $l = 1 \ldots Q_{ij}$ are uncorrelated, the estimated spatial covariance matrix (averaged over fast fading)[31, 98] between mobile i and BS j can be represented as (see eqn. 3.13)

$$\mathbf{R'}_{ij}(\lambda_{\text{up}}) = \sum_{l=1}^{Q_{ij}} \alpha_{ijl}^2 \mathbf{a'}\left(\theta_{ijl}, \lambda_{\text{up}}\right) \mathbf{a'}^H\left(\theta_{ijl}, \lambda_{\text{up}}\right). \tag{4.3}$$

In (4.3), the estimated uplink steering vector is $\mathbf{a'}\left(\theta_{ijl}, \lambda_{\text{up}}\right) = \mathbf{a}\left(\theta_{ijl}, \lambda_{\text{up}}\right) + \mathbf{e}_{ijl}$, where $\mathbf{e}_{ijl}$ is an arbitrary complex vector that describes the effect of the mismatches [100] between the assumed and the actual steering vectors. It is assumed that $\mathbf{a}\left(\theta_{ijl}, \lambda_{\text{up}}\right)$ is the steering vector for a wave incident at the BS with an angle θ_{ijl} . We assume perfect knowledge of average path attenuations in the uplink.

4.4 Uplink to Downlink Transformation

The exact downlink spatial covariance matrix

$$\mathbf{R}_{ij}(\lambda_{\text{dl}}) = \sum_{l=1}^{Q_{ij}} \alpha_{ijl}^2 \mathbf{a}\left(\theta_{ijl}, \lambda_{\text{dl}}\right) \mathbf{a}^H\left(\theta_{ijl}, \lambda_{\text{dl}}\right) \tag{4.4}$$

is not known in practice [5, 34]. In an FDD system, the MS of interest has to send the estimates of the downlink channel to its home BS, so that it can optimize the transmission power and the beamforming vector to maintain the required link quality. This indicates that some feedback information regarding the downlink channel is required before the BS carries out beamforming. However, because of the fast varying mobile channels, a lot of information has to be transmitted as a feedback from the MS to the BS very frequently. This will significantly reduce the capacity of the system. Therefore, methods which do

not require feedback information are very important from a cellular commmunication's perspective.

It can be noted from (4.3) and (4.4) that because of the frequency-dependent array response, the uplink weight vectors calculated from the uplink covariance matrix cannot be used directly for downlink beamforming. We need methods to transform the spatial covariance matrix from uplink to downlink frequency. In that case the resulting downlink covariance matrix is an estimate of (4.4). Techniques to obtain an estimate $\hat{\mathbf{R}}_{ij}(\lambda_{\mathrm{dl}})$ of the downlink covariance matrix $\mathbf{R}_{ij}(\lambda_{\mathrm{dl}})$ have been proposed in [5, 34] and [55] for known uplink steering vectors i.e., if the error vectors $\mathbf{e}_{ijl} = 0$.

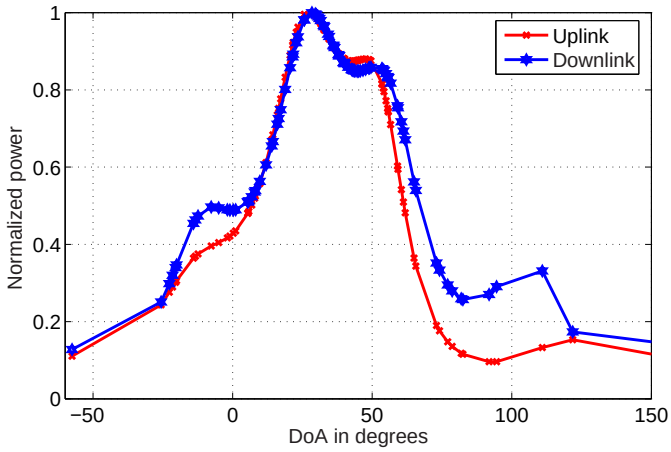

Figure 4.2: Normalized APS for uplink and downlink channels

First, we investigate the performance of the MMSE and MVDR based transformation methods in a cellular system that incorporates mobility, traffic scenarios, soft handover and power control methods. Then, we propose a robust technique to obtain $\hat{\mathbf{R}}_{ij}(\lambda_{\mathrm{dl}})$ from (4.3). It is important to note that the validity of transformation method depends on the correlation between the second-order statistics of the uplink and downlink channels, which in this case is shown in Fig. 4.2 as an APS. The uplink and downlink fast fadings are independent and Rayleigh distributed where as the angular spreading follows a Laplacian distribution with the same average DoA in uplink and downlink.

4.4.1 Non-robust Methods

In case of non-robust methods it is assumed that the BS has an exact knowledge of the uplink steering vector and hence the uplink spatial covariance matrix is given by

$$\mathbf{R}_{ij}(\lambda_{\text{up}}) = \sum_{l=1}^{Q_{ij}} \alpha_{ijl}^2 \mathbf{a}\left(\theta_{ijl}, \lambda_{\text{up}}\right) \mathbf{a}^H\left(\theta_{ijl}, \lambda_{\text{up}}\right), \tag{4.5}$$

which is obtained from (4.3) for $\mathbf{e}_{ijl} = \mathbf{0}$ i. e. when there is no uncertainty in uplink steering vector. The average fading in the uplink can be estimated using semi-blind algorithms or algorithms utilizing training sequences.

Minimum Mean Square Error (MMSE) Method

A suboptimum linear transformation as proposed in [5, 34], can be used to transform the uplink steering vector onto downlink steering vector. For this purpose, a transformation matrix $\mathbf{T} \in \mathcal{C}^{M \times M}$ is used as

$$\hat{\mathbf{a}}\left(\theta_{ijl}, \lambda_{\text{dl}}\right) = \mathbf{T}\mathbf{a}\left(\theta_{ijl}, \lambda_{\text{up}}\right), \tag{4.6}$$

where $\mathbf{a}\left(\theta_{ijl}, \lambda_{\text{up}}\right) \in \mathcal{C}^{M \times 1}$ is the uplink steering vector for the DoA θ_{ijl} corresponding to lth path. The mean square error between the estimated and true downlink steering vectors is

$$\begin{aligned} e =& ||\hat{\mathbf{A}}_{\text{DL}} - \mathbf{A}_{\text{DL}}||_{\text{F}}^2 \\ =& \text{tr}\left(\left(\mathbf{T}\mathbf{A}_{\text{UP}} - \mathbf{A}_{\text{DL}}\right)^H \left(\mathbf{T}\mathbf{A}_{\text{UP}} - \mathbf{A}_{\text{DL}}\right) \right) \\ =& \text{tr}\left(\mathbf{A}_{\text{UP}}^H \mathbf{T}^H \mathbf{T} \mathbf{A}_{\text{UP}}\right) - \text{tr}\left(\mathbf{A}_{\text{UP}}^H \mathbf{T}^H \mathbf{A}_{\text{DL}}\right) - \text{tr}\left(\mathbf{A}_{\text{DL}}^H \mathbf{T} \mathbf{A}_{\text{UP}}\right) + \text{tr}\left(\mathbf{A}_{\text{DL}}^H \mathbf{A}_{\text{DL}}\right), \end{aligned} \tag{4.7}$$

where

$$\begin{aligned} \mathbf{A}_{\text{UP}} =& \left[\mathbf{a}\left(\theta_{ij1}, \lambda_{\text{up}}\right), \mathbf{a}\left(\theta_{ij2}, \lambda_{\text{up}}\right), \ldots, \mathbf{a}\left(\theta_{ijP}, \lambda_{\text{up}}\right)\right] \in \mathcal{C}^{M \times P} \\ \mathbf{A}_{\text{DL}} =& \left[\mathbf{a}\left(\theta_{ij1}, \lambda_{\text{dl}}\right), \mathbf{a}\left(\theta_{ij2}, \lambda_{\text{dl}}\right), \ldots, \mathbf{a}\left(\theta_{ijP}, \lambda_{\text{dl}}\right)\right] \in \mathcal{C}^{M \times P} \end{aligned} \tag{4.8}$$

are the matrices of true steering vectors for uplink and downlink, respectively. In practice, an uplink and downlink calibration table of the antenna array for a particular set of DoAs is used to construct the matrices $\mathbf{A}_{\text{UP}}$ and $\mathbf{A}_{\text{DL}}$. These matrices can also be obtained by sampling the array manifolds at uplink and downlink frequencies [98]. Differentiating e w.r.t $\mathbf{T}$ and setting to zero, we get the transformation matrix

$$\begin{aligned} \frac{\text{d}e}{\text{d}\mathbf{T}} &= 2\mathbf{T}\mathbf{A}_{\text{UP}}\mathbf{A}_{\text{UP}}^H - 2\mathbf{A}_{\text{DL}}\mathbf{A}_{\text{UP}}^H = 0 \\ \mathbf{T} &= \mathbf{A}_{\text{DL}}\mathbf{A}_{\text{UP}}^H \left(\mathbf{A}_{\text{UP}}\mathbf{A}_{\text{UP}}^H\right)^{-1}. \end{aligned} \tag{4.9}$$

It is assumed that the uplink and downlink channels have same average fading gains and same average number of paths. Substituting the estimate of the downlink steering vector (4.6) in (4.4) and combining with (4.5), the estimated downlink covariance matrix can be written as

$$\begin{aligned}
\hat{\mathbf{R}}_{ij}(\lambda_{\mathrm{dl}}) &= \sum_{l=1}^{Q_{ij}} \alpha_{ijl}^2 \hat{\mathbf{a}}\left(\theta_{ijl}, \lambda_{\mathrm{dl}}\right) \hat{\mathbf{a}}^H\left(\theta_{ijl}, \lambda_{\mathrm{dl}}\right) \\
&= \sum_{l=1}^{Q_{ij}} \alpha_{ijl}^2 \mathbf{T}\mathbf{a}\left(\theta_{ijl}, \lambda_{\mathrm{up}}\right) \mathbf{a}^H\left(\theta_{ijl}, \lambda_{\mathrm{up}}\right) \mathbf{T}^H \\
&= \mathbf{T} \cdot \sum_{l=1}^{Q_{ij}} \alpha_{ijl}^2 \mathbf{a}\left(\theta_{ijl}, \lambda_{\mathrm{up}}\right) \mathbf{a}^H\left(\theta_{ijl}, \lambda_{\mathrm{up}}\right) \cdot \mathbf{T}^H \\
&= \mathbf{T}\mathbf{R}_{ij}(\lambda_{\mathrm{up}})\mathbf{T}^H. \qquad (4.10)
\end{aligned}$$

Replacing $\mathbf{R}_{i,c(i)}$ and $\mathbf{R}_{m,c(i)}$ by $\mathbf{R}_{i,c(i)}(\lambda_{\mathrm{dl}})$ and $\mathbf{R}_{m,c(i)}(\lambda_{\mathrm{dl}})$, respectively in the downlink beamforming method (3.14) and using the relation (4.10), the transformation matrix $\mathbf{T}$ can also be used to transform the antenna weights from uplink to downlink as

$$\hat{\mathbf{w}}_{\mathrm{DL}} = \mathbf{T}^H \mathbf{w}_{\mathrm{UP}}. \qquad (4.11)$$

Minimum Variance Distortionless Response (MVDR) Method

The objective of an MVDR beamformer is to maintain a distortionless response to a desired direction by minimizing the output power contributed by interfering signals from other directions. The consequence is that it maximizes the SINR [39] at the output of the beamformer. In our method, we estimate the uplink APS $P\left(\theta_{ij}\right)$ corresponding to a channel between a MS i and a BS j using the MVDR filter. The APS respresents the distribution of power among each individual path l with certain DoA value. As there are $l = 1 \ldots Q_{ij}$ paths between the MS i and the BS j, the optimum uplink weight vector is calculated by minimizing the power of the MVDR filter output under the condition that the gain towards a desired direction θ_{ijl} is constant. The problem can be formulated as

$$\begin{aligned}
&\min_{\mathbf{w}_i} \left(P = \mathbf{w}_i^H \mathbf{R}_{ij}\left(\lambda_{\mathrm{up}}\right) \mathbf{w}_i\right) \\
&\quad \text{subject to } \mathbf{w}_i^H \mathbf{a}\left(\theta_{ijl}, \lambda_{\mathrm{up}}\right) = 1. \qquad (4.12)
\end{aligned}$$

It is important to note that (4.12) considers all possible links between the active (see **Chapter 3**) MSs and BSs where each link described by $\mathbf{R}_{ij}\left(\lambda_{\mathrm{up}}\right)$ is taken into account independently. By the method of Lagrange multipliers, the optimum weight vector that

minimizes the objective and satisfies the constraint of (4.12) is given by [72]

$$\mathbf{w}_{i,\text{opt}} = \frac{\mathbf{R}_{ij}^{-1}(\lambda_{\text{up}})\,\mathbf{a}(\theta_{ijl},\lambda_{\text{up}})}{\mathbf{a}^{H}(\theta_{ijl},\lambda_{\text{up}})\,\mathbf{R}_{ij}^{-1}(\lambda_{\text{up}})\,\mathbf{a}(\theta_{ijl},\lambda_{\text{up}})}. \tag{4.13}$$

Combining (4.12) and (4.13), the scalar output power for a single steering direction (also a path) can be obtained as

$$P(\theta_{ijl}) = \frac{1}{\mathbf{a}^{H}(\theta_{ijl},\lambda_{\text{up}})\,\mathbf{R}_{ij}^{-1}(\lambda_{\text{up}})\,\mathbf{a}(\theta_{ijl},\lambda_{\text{up}})}, \tag{4.14}$$

which as an example is also shown in Fig. 4.2 for uplink and downlink channels separated by a frequency of 190 MHz. As proposed in [55], the spatial covariance matrix at the downlink frequency is constructed by replacing the average downlink fading gains α_{ijl}^2 with the average power $P(\theta_{ijl})$ per path and hence the estimated downlink covariance matrix is

$$\hat{\mathbf{R}}_{ij}(\lambda_{\text{dl}}) = \sum_{l=1}^{Q_{ij}} P(\theta_{ijl})\,\mathbf{a}(\theta_{ijl},\lambda_{\text{dl}})\,\mathbf{a}^{H}(\theta_{ijl},\lambda_{\text{dl}}). \tag{4.15}$$

4.4.2 Robust Methods

Robust transformation methods provide robustness to uplink steering vector estimation errors in a frequency selective fading environment. In this section, we propose two robust methods; the matrix RLS and the regularization method known as Tikhonov regularization [19, 42]. The matrix RLS problem can be formulated in a convex form as a SOC program and solved efficiently using the well-established interior point methods. The regularization method provides diagonal loading for the MMSE solution of (4.9). The performance of the proposed robust methods are compared with that of MVDR [55] and MMSE [5, 34] using a dynamic system level simulator (see **Chapter 3**) developed for investigating the capacity improvement of the UMTS-FDD system with SAs at the BS. As before, downlink capacity is used as a measure of system performance by finding the number of users for which a certain QoS requirement can be fulfilled. System level simulations carried out for 4-element UCA show that our method outperforms both the MVDR [55] and the MMSE [5, 34] methods without any significant degradation in performance when compared to the MMSE [34] with known uplink spatial signature.

Problem Formulation

Using a linear transformation [34], the downlink steering vectors can also be estimated from the erroneous uplink steering vectors as

$$\begin{aligned}\hat{\mathbf{a}}\left(\theta_{ijl},\lambda_{\mathrm{dl}}\right) &= \mathbf{T}_R\mathbf{a}'\left(\theta_{ijl},\lambda_{\mathrm{up}}\right)\\ &= \mathbf{T}_R(\mathbf{a}\left(\theta_{ijl},\lambda_{\mathrm{up}}\right)+\mathbf{e}_{ijl}),\end{aligned} \tag{4.16}$$

where $\mathbf{T}_R \in \mathcal{C}^{M\times M}$ is the transformation matrix for the robust method and has a rank between 1 and M. From (4.8), the matrices of the true steering vectors for uplink and downlink are $\mathbf{A}_{\mathrm{UP}} \in \mathcal{C}^{M\times P}$ and $\mathbf{A}_{\mathrm{DL}} \in \mathcal{C}^{M\times P}$, respectively. The perturbation matrix $\mathbf{E} \in \mathcal{C}^{M\times P}$ for the uplink steering matrix is defined as

$$\mathbf{E}=\left[\mathbf{e}\left(\theta_{ij1}\right),\mathbf{e}\left(\theta_{ij2}\right),\ldots,\mathbf{e}\left(\theta_{ijP}\right)\right]. \tag{4.17}$$

Now the objective is to find the optimum $\mathbf{T}_R$ that minimizes the Frobenius norm of the difference between the matrices $\mathbf{T}_R(\mathbf{A}_{\mathrm{UP}}+\mathbf{E})$ and $\mathbf{A}_{\mathrm{DL}}$ for the maximum possible uncertainty $\mathbf{E}$, where the Frobenius norm of $\mathbf{E}$ is bounded by some positive constant $\delta > 0$. Thus our approach is based upon optimization of the worst-case performance [100]. Mathematically, the problem can be formulated as

$$\begin{aligned}&\min_{\mathbf{T}_R}\underbrace{\max_{\mathbf{E}}\ \ ||\mathbf{T}_R(\mathbf{A}_{\mathrm{UP}}+\mathbf{E})-\mathbf{A}_{\mathrm{DL}}||}\\ &\text{subject to}\ \ ||\mathbf{E}||\leq\delta.\end{aligned} \tag{4.18}$$

Lagrange Multiplier Method

In this section, we try to solve the optimization problem (4.18) using Lagrange multiplier method. The mini-max problem can be separated into constrained maximization and minimization. We first consider the problem of maximization of braced term of (4.18) over $\mathbf{E}$. The equivalent problem can be formulated as

$$\begin{aligned}&\max_{\mathbf{E}}\ \ ||\mathbf{T}_R(\mathbf{A}_{\mathrm{UP}}+\mathbf{E})-\mathbf{A}_{\mathrm{DL}}||^2\\ &\text{subject to}\ \ ||\mathbf{E}||^2\leq\delta^2.\end{aligned} \tag{4.19}$$

The Lagrange multiplier function can be written as

$$\begin{aligned} L\left(\mathbf{E},\mu\right) = & \operatorname{tr}\left(\left(\mathbf{T}_R\left(\mathbf{A}_{\mathrm{UP}}+\mathbf{E}\right)-\mathbf{A}_{\mathrm{DL}}\right)^H\left(\mathbf{T}_R\left(\mathbf{A}_{\mathrm{UP}}+\mathbf{E}\right)-\mathbf{A}_{\mathrm{DL}}\right)\right)+\mu\left(\delta^2-||\mathbf{E}||^2\right) \\ = & \operatorname{tr}\left(\left(\mathbf{A}_{\mathrm{UP}}+\mathbf{E}\right)^H\mathbf{T}_R^H\mathbf{T}_R\left(\mathbf{A}_{\mathrm{UP}}+\mathbf{E}\right)\right)-2\operatorname{tr}\left(\left(\mathbf{A}_{\mathrm{UP}}+\mathbf{E}\right)^H\mathbf{T}_R^H\mathbf{A}_{\mathrm{DL}}\right)+ \\ & \operatorname{tr}\left(\mathbf{A}_{\mathrm{DL}}^H\mathbf{A}_{\mathrm{DL}}\right)+\mu\left(\delta^2-\operatorname{tr}\left(\mathbf{E}^H\mathbf{E}\right)\right) \\ = & \operatorname{tr}\left(\mathbf{A}_{\mathrm{UP}}^H\mathbf{T}_R^H\mathbf{T}_R\mathbf{A}_{\mathrm{UP}}\right)+\operatorname{tr}\left(\mathbf{A}_{\mathrm{UP}}^H\mathbf{T}_R^H\mathbf{T}_R\mathbf{E}\right)+\operatorname{tr}\left(\mathbf{E}^H\mathbf{T}_R^H\mathbf{T}_R\mathbf{A}_{\mathrm{UP}}\right)+ \\ & \operatorname{tr}\left(\mathbf{E}^H\mathbf{T}_R^H\mathbf{T}_R\mathbf{E}\right)-2\operatorname{tr}\left(\mathbf{A}_{\mathrm{UP}}^H\mathbf{T}_R^H\mathbf{A}_{\mathrm{DL}}\right)-2\operatorname{tr}\left(\mathbf{E}^H\mathbf{T}_R^H\mathbf{A}_{\mathrm{DL}}\right)+ \\ & \operatorname{tr}\left(\mathbf{A}_{\mathrm{DL}}^H\mathbf{A}_{\mathrm{DL}}\right)+\mu\left(\delta^2-\operatorname{tr}\left(\mathbf{E}^H\mathbf{E}\right)\right). \end{aligned} \tag{4.20}$$

Simplifying (4.20), differentiating $L\left(\mathbf{E},\mu\right)$ with respect to $\mathbf{E}$ and equating to zero, we get $\mathbf{E}$ in terms of Lagrange multiplier parameter μ

$$\begin{aligned} \frac{\delta\{L(\mathbf{E},\mu)\}}{\delta\mathbf{E}} &= 2\mathbf{A}_{\mathrm{UP}}^H\mathbf{T}_R^H\mathbf{T}_R+2\mathbf{E}^H\mathbf{T}_R^H\mathbf{T}_R-2\mathbf{A}_{\mathrm{DL}}^H\mathbf{T}_R-2\mu\mathbf{E}^H=0 \\ \mathbf{E} &= \left(\mu\mathbf{I}-\mathbf{T}_R^H\mathbf{T}_R\right)^{-1}\mathbf{T}_R^H\left(\mathbf{T}_R\mathbf{A}_{\mathrm{UP}}-\mathbf{A}_{\mathrm{DL}}\right). \end{aligned} \tag{4.21}$$

Similarly differentiation of $L\left(\mathbf{E},\mu\right)$ with respect to μ gives

$$\delta^2=\operatorname{tr}\left(\mathbf{E}^H\mathbf{E}\right). \tag{4.22}$$

Generally, it is possible to solve for the unknowns $\mathbf{E}$ and μ with the help of (4.21) and (4.22). However, as the transformation matrix $\mathbf{T}_R$ is a general $M\times M$ matrix, the matrix inversion operation of (4.21) makes the task difficult. Therefore we solve the problem using the triangle inequality property of the matrix norms.

Triangle Inequality

A geometric interpretation of the min-max optimization problem (4.18) when the matrices $\mathbf{A}_{\mathrm{UP}}$, $\mathbf{E}$ and $\mathbf{A}_{\mathrm{DL}}$ are represented in the form of vectors is provided in [19, 20]. Similarly, the connection of such a min-max optimization problem to a Total Least Squares (TLS) [48] is discussed in [19, 20, 42]. In this section, we also first consider the constrained maximization problem (braced term of (4.18)). Using triangle inequality property of matrix norms [19], we can write

$$\begin{aligned} ||\mathbf{T}_R\left(\mathbf{A}_{\mathrm{UP}}+\mathbf{E}\right)-\mathbf{A}_{\mathrm{DL}}|| &\leq ||\mathbf{T}_R\mathbf{A}_{\mathrm{UP}}-\mathbf{A}_{\mathrm{DL}}||+||\mathbf{T}_R\mathbf{E}|| \\ &\leq ||\mathbf{T}_R\mathbf{A}_{\mathrm{UP}}-\mathbf{A}_{\mathrm{DL}}||+\delta||\mathbf{T}_R||. \end{aligned} \tag{4.23}$$

The right hand side of (4.23) is an upper-bound for its left hand side. Thus the maximum of left hand side with respect to $\mathbf{E}$ becomes upper-bound when the inequality (4.23)

becomes equality. An equivalent representation of (4.23) can be written as

$$||\text{vec}\left(\mathbf{T}_R\left(\mathbf{A}_{\text{UP}}+\mathbf{E}\right)\right)-\text{vec}\left(\mathbf{A}_{\text{DL}}\right)|| \;\leq\; ||\text{vec}\left(\mathbf{T}_R\mathbf{A}_{\text{UP}}\right)-\text{vec}\left(\mathbf{A}_{\text{DL}}\right)||+ \delta||\text{vec}\left(\mathbf{T}_R\right)||, \tag{4.24}$$

where vec($\mathbf{A}$) represents the long vector formed by stacking the columns of the matrix $\mathbf{A}$. If the vectors $\text{vec}\left(\mathbf{T}_R\mathbf{E}\right) \in \mathcal{C}^{MP\times 1}$ and $\left(\text{vec}\left(\mathbf{T}_R\mathbf{A}_{\text{UP}}\right)-\text{vec}\left(\mathbf{A}_{\text{DL}}\right)\right) \in \mathcal{C}^{MP\times 1}$ point to the same direction, their sum results in an additive effect. This means that $||\mathbf{T}_R\mathbf{A}_{\text{UP}}-\mathbf{A}_{\text{DL}}+\mathbf{T}_R\mathbf{E}||$ will be greater than both of the individual norms $||\mathbf{T}_R\mathbf{A}_{\text{UP}}-\mathbf{A}_{\text{DL}}||$ and $||\mathbf{T}_R\mathbf{E}||$. Mathematically, this condition can be expressed as

$$\mathbf{T}_R\mathbf{E} = ||\mathbf{T}_R\mathbf{E}||\frac{\mathbf{T}_R\mathbf{A}_{\text{UP}}-\mathbf{A}_{\text{DL}}}{||\mathbf{T}_R\mathbf{A}_{\text{UP}}-\mathbf{A}_{\text{DL}}||}. \tag{4.25}$$

In order to have a maximum value of $||\mathbf{T}_R\mathbf{A}_{\text{UP}}-\mathbf{A}_{\text{DL}}+\mathbf{T}_R\mathbf{E}||$, (4.25) has also to be evaluated for the maximum norm of $||\mathbf{T}_R\mathbf{E}||$ for the known $\mathbf{T}_R$, which is given by

$$\max_{\mathbf{E}}||\mathbf{T}_R\mathbf{E}|| = \delta||\mathbf{T}_R||. \tag{4.26}$$

With the help of (4.26), (4.25) can be written as

$$\mathbf{T}_R\mathbf{E} = \delta||\mathbf{T}_R||\frac{\mathbf{T}_R\mathbf{A}_{\text{UP}}-\mathbf{A}_{\text{DL}}}{||\mathbf{T}_R\mathbf{A}_{\text{UP}}-\mathbf{A}_{\text{DL}}||}. \tag{4.27}$$

If $\mathbf{T}_R$ is a full rank matrix, the error matrix $\mathbf{E}$ can be expressed as

$$\mathbf{E} = \delta\frac{\mathbf{T}_R^{-1}(\mathbf{T}_R\mathbf{A}_{\text{UP}}-\mathbf{A}_{\text{DL}})||\mathbf{T}_R||}{||\mathbf{T}_R\mathbf{A}_{\text{UP}}-\mathbf{A}_{\text{DL}}||}. \tag{4.28}$$

For this choice of $\mathbf{E}$ ($\mathbf{T}_R$ is a full rank matrix) or $\mathbf{T}_R\mathbf{E}$ ($\mathbf{T}_R$ is not a full rank matrix)

$$||\mathbf{T}_R(\mathbf{A}_{\text{UP}}+\mathbf{E})-\mathbf{A}_{\text{DL}}|| = ||\mathbf{T}_R\mathbf{A}_{\text{UP}}-\mathbf{A}_{\text{DL}}||+\delta||\mathbf{T}_R||, \tag{4.29}$$

which is the desired upper-bound. Hence the constrained mini-max problem can be reduced to the following minimization problem

$$\min_{\mathbf{T}_R}\left\{||\mathbf{T}_R\mathbf{A}_{\text{UP}}-\mathbf{A}_{\text{DL}}||+\delta||\mathbf{T}_R||\right\}, \tag{4.30}$$

which can be rewritten as

$$\begin{aligned} \text{minimize} \quad & z_1+\delta z_2 \\ \text{subject to} \quad & ||\mathbf{T}_R\mathbf{A}_{\text{UP}}-\mathbf{A}_{\text{DL}}|| \leq z_1 \\ & ||\mathbf{T}_R|| \leq z_2. \end{aligned} \tag{4.31}$$

The objective function as well as the constraints of (4.31) are convex [15] and hence it is a convex optimization problem.

Second-Order Cone Implementation

In order to make the convex optimization problem (4.31) suitable for SOC implementation [91], we change the complex matrices $\mathbf{T}_R$, $\mathbf{A}_{\mathrm{UP}}$ and $\mathbf{A}_{\mathrm{DL}}$ into real matrices and then into vectors. We introduce a real matrix $\mathbf{U} = [\mathbf{u}_{i,j}] \in \mathcal{R}^{2P \times 2M}$ with 2×2 sub-matrices

$$\mathbf{u}_{i,j} = \begin{pmatrix} \mathrm{Re}\{\mathbf{A}_{\mathrm{UP}}(i,j)\} & -\mathrm{Im}\{\mathbf{A}_{\mathrm{UP}}(i,j)\} \\ \mathrm{Im}\{\mathbf{A}_{\mathrm{UP}}(i,j)\} & \mathrm{Re}\{\mathbf{A}_{\mathrm{UP}}(i,j)\} \end{pmatrix} \quad \text{for} \quad i = 1 \cdots P,\ j = 1 \cdots M, \tag{4.32}$$

and the real vectors $\hat{\mathbf{t}} = [\mathbf{t}_i] \in \mathcal{R}^{2MM \times 1}$ and $\hat{\mathbf{a}} = [\mathbf{a}_i] \in \mathcal{R}^{2MP \times 1}$ with 2×1 sub-vectors

$$\mathbf{t}_i = \begin{pmatrix} \mathrm{Re}\{(\mathbf{vec}\,(\mathbf{T}_R))_i\} \\ \mathrm{Im}\{(\mathbf{vec}\,(\mathbf{T}_R))_i\} \end{pmatrix} \quad \text{for} \quad i = 1 \cdots M \times M, \tag{4.33}$$

and

$$\mathbf{a}_i = \begin{pmatrix} \mathrm{Re}\{(\mathbf{vec}\,(\mathbf{A}_{\mathrm{DL}}))_i\} \\ \mathrm{Im}\{(\mathbf{vec}\,(\mathbf{A}_{\mathrm{DL}}))_i\} \end{pmatrix} \quad \text{for} \quad i = 1 \cdots M \times P \tag{4.34}$$

respectively, where **vec**(.) is the column vector formed by stacking the transpose of each row of the corresponding matrix. Rewriting (4.31) in an equivalent form

$$\begin{aligned} \text{minimize} \quad & z_1 + \delta z_2 \\ \text{subject to} \quad & ||\mathbf{V}\hat{\mathbf{t}} - \hat{\mathbf{a}}|| \leq z_1 \\ & ||\hat{\mathbf{t}}|| \leq z_2, \end{aligned} \tag{4.35}$$

where

$$\mathbf{V} = \begin{pmatrix} \mathbf{U_1} & \mathbf{0} & \cdots & \mathbf{0} \\ \mathbf{0} & \mathbf{U_2} & \cdots & \mathbf{0} \\ \cdot & \cdot & \cdot & \cdot \\ \cdot & \cdot & \cdot & \cdot \\ \mathbf{0} & \mathbf{0} & \cdots & \mathbf{U_M} \end{pmatrix}, \tag{4.36}$$

is a block diagonal matrix of size $(2PM) \times (2MM)$, $(\mathbf{U_1}, \mathbf{U_2} \cdots, \mathbf{U_M}, \mathbf{0}) \in \mathcal{R}^{2P \times 2M}$ and $\hat{\mathbf{t}} \in \mathcal{R}^{2MM \times 1}$ is the optimization variable. Using convex optimization toolbox SeDuMi 1.02 (see Appendix 9.2), the optimum $\hat{\mathbf{t}}$ can be computed. Let us define

$$\begin{aligned} \mathbf{b} &= [-1, -\delta, \mathbf{0}]^T \in \mathcal{R}^{(2MM+2)\times 1} \\ \mathbf{c} &= \left[0, -\hat{\mathbf{a}}^T, 0, \mathbf{0}\right]^T \in \mathcal{R}^{(2MP+2MM+2)\times 1} \\ \mathbf{y} &= \left[z_1, z_2, \hat{\mathbf{t}}^T\right]^T \in \mathcal{R}^{(2MM+2)\times 1}, \end{aligned} \tag{4.37}$$

where $\mathbf{0} \in \mathcal{R}^{1\times 2MM}$ is a vector of zeros. Define a matrix $\mathbf{A}^T$

$$\begin{pmatrix} -1 & 0 & \mathbf{0} \in \mathcal{R}^{(1\times 2MM)} \\ \mathbf{0} \in \mathcal{R}^{(2MP\times 1)} & \mathbf{0} \in \mathcal{R}^{(2MP\times 1)} & -\mathbf{V} \\ 0 & -1 & \mathbf{0} \in \mathcal{R}^{(1\times 2MM)} \\ \mathbf{0} \in \mathcal{R}^{(2MM\times 1)} & \mathbf{0} \in \mathcal{R}^{(2MM\times 1)} & -\mathbf{I} \in \mathcal{R}^{(2MM\times 2MM)} \end{pmatrix}.$$

With these definitions, the SOC optimization problem (4.35) can be transformed into a standard dual form SeDuMi [91] optimization problem as

$$\begin{aligned} &\max_{\mathbf{y}} \quad \mathbf{b}^T\mathbf{y} \\ &\text{subject to} \quad \mathbf{c} - \mathbf{A}^T\mathbf{y} \in \mathrm{SOC}_1{}^{(2MP+1)} \times \mathrm{SOC}_2{}^{(2MM+1)}, \end{aligned} \tag{4.38}$$

where $\mathbf{y}$ is the vector of variables, SOC_1 and SOC_2 are the SOCs of the dimensions $(2MP+1)$ and $(2MM+1)$, repectively which correspond to the inequality constraints in (4.35). The optimum solution $\mathbf{y}$ contains both real and imaginary parts of all the elements of the transformation matrix $\mathbf{T}_R$.

Regularisation Method

It can be observed from (4.30) that the optimium $\mathbf{T}_R$ is the one which minimizes both $||\mathbf{T}_R\mathbf{A}_{\mathrm{UP}} - \mathbf{A}_{\mathrm{DL}}||$ and $||\mathbf{T}_R||$. Hence, (4.30) can also be expressed as

$$\min_{\mathbf{T}_R} \left\{ ||\mathbf{T}_R\mathbf{A}_{\mathrm{UP}} - \mathbf{A}_{\mathrm{DL}}||, ||\mathbf{T}_R|| \right\}, \tag{4.39}$$

which is a multi-objective unconstrained optimization problem [15, 85]. By introducing a regularisation parameter [15] $\gamma > 0$, the function that has to be minimised with respect to $\mathbf{T}_R$ is given by

$$e = ||\mathbf{T}_R\mathbf{A}_{\mathrm{UP}} - \mathbf{A}_{\mathrm{DL}}||^2 + \gamma^2||\mathbf{T}_R||^2. \tag{4.40}$$

Differentiating e of (4.40) with respect to $\mathbf{T}_R$ and equating to zero, we get the optimum transformation matrix

$$\mathbf{T}_R = \mathbf{A}_{\mathrm{DL}}\mathbf{A}_{\mathrm{UP}}^H \left(\mathbf{A}_{\mathrm{UP}}\mathbf{A}_{\mathrm{UP}}^H + \gamma^2 I\right)^{-1}, \tag{4.41}$$

which is the MMSE solution [34] with a positive diagonal loading.

After determining the optimum $\mathbf{T}_R$ from (4.38) and (4.41), we can estimate the downlink covariance matrix. Like in the case of non-robust methods, since the uplink and downlink have same paths with same average fading gains, combining (4.3) and (4.4) with the help of (4.16), the estimated downlink covariance matrix can be written as

$$\hat{\mathbf{R}}_{ij}(\lambda_{\mathrm{dl}}) = \mathbf{T}_R\mathbf{R'}_{ij}(\lambda_{\mathrm{up}})\mathbf{T}_R^H. \tag{4.42}$$

4.5 Downlink Beamforming

In cellular wireless communications, downlink beamforming can be carried out once the downlink spatial covariance matrices that contain all the information about downlink channels in average are known. With the help of an estimated downlink spatial covariance matrix (4.10) or (4.15)(for non-robust methods) and (4.42) (for robust methods), we use the max-SINR (maximization of SINR) algorithm for downlink beamforming (see **Chapter 3**). The solution of this algorithm is the eigenvector associated with the largest eigenvalue (generalized eigenvalue problem) of the characteristic equation (3.15). Note that many optimum transmit beamforming algorithms [8, 30, 99] which optimize BS transmit power, subject to satisfying QoS requirements at the MSs are also found to achieve good results. However, the major disadvantage of all these optimum methods is that the BS has to know downlink channels of the MSs that are power controlled by other BSs. This means that there should be some exchange of parameters among the BSs, the consequence is that a centralised unit is necessary for downlink beamforming.

The beam patterns of the 4-element UCA are shown in Fig. 4.3 for downlink beamforming (3.15) based on the non-robust methods MMSE (4.10) and MVDR (4.15), respectively. As the estimated downlink covariance matrix from the two methods are not exactly same, the beam patterns also differ. In case of non-robust methods, simulations have been carried out for the following cases:

a) uplink covariance matrix is directly used for downlink beamforming,

b) uplink to downlink covariance matrix transformation with the MMSE method,

c) transformation with the MVDR method.

The dynamic system level simulations have been also carried out for the proposed robust method namely the SOC optimization method (4.38).

4.6 Simulator

We use a dynamic system level simulator (see **Chapter 3**) for analyzing the downlink capacity of the UMTS-FDD cellular system for different numbers of antenna elements with uplink to downlink covariance transformation methods. The simulator uses mobility and traffic models based upon a random walk model [43] and Poisson processes [52],

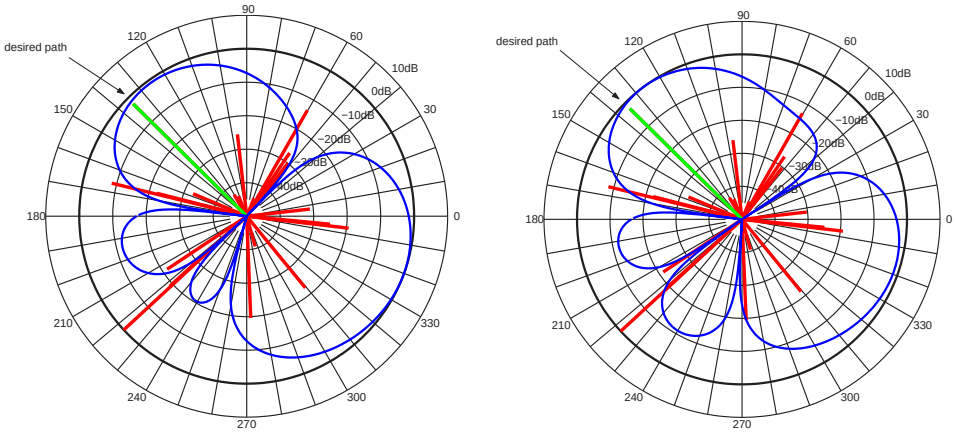

(a) With MVDR (b) With MMSE

Figure 4.3: Examples of beam patterns with transformation methods for $M = 4$ element arrays

(also described in **Chapter 3**) respectively. Soft handover, power control and downlink SINR calculation etc. are implemented as proposed in [1].

4.6.1 Simulation flow

Fig. 4.4 shows the simulation flow for the downlink. The simulation flow was described in **Chapter 3**. Moreover, the description of each module of the simulator was also given in **Chapter 3**. The uplink spatial covariance matrix is calculated for all the possible combinations of channels between the BSs and active [52] MSs. The non-robust methods like MMSE and MVDR, and the proposed robust methods are used to estimate the downlink covariance matrix.

4.7 Simulation Results

The simulation results are the average of ten simulation runs. Each simulation is carried out for a time interval of $2000T$ with the parameters listed in Table 3.1. The number of active users versus time that can be supported in the downlink with a data rate of 384 kbits/s with and without transformation techniques is shown in Fig. 4.5 for different numbers of antenna elements. After a transient, the average number of MSs that can be supported in the downlink remains relatively constant. This indicates that even if new MSs generate calls in each snapshot, the number of MSs that can be served with

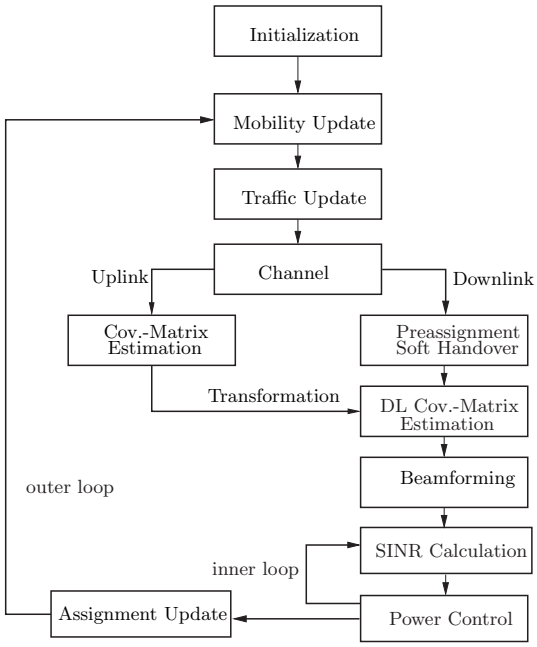

Figure 4.4: Block diagram of simulation flow

the required link quality is limited. Thus the downlink capacity of the system reaches saturation. The fluctuations in the curves are because of the limited number of simulation runs that are averaged. As discussed before, we compare the capacity improvement with three different approaches

a) no transformation of covariance matrix (using the uplink spatial covariance matrix directly for the downlink),

b) transformation of covariance matrices based upon the MMSE method,

c) transformation of covariance matrices based upon the MVDR method.

It can be observed that for $M = 2$ array elements and chosen simulation parameters, the difference between the average number of satisfied users with transformation (b & c) and without transformation (a) is within the range of $1 - 2$, which is not significant from a system level perspective. For $M = 4$ array elements, (b) and (c) outperform (a) by supporting in average about 32% and about 36% more users than (a), respectively. Similarly, with $M = 8$ array elements, the MVDR method (c) supports 21% and 5% more users in average than method (a) and method (b), respectively. Thus in all the cases the MVDR method performs better than the MMSE method. For a higher number of antenna elements ($M = 4$ & $M = 8$), downlink beamforming based upon the direct use

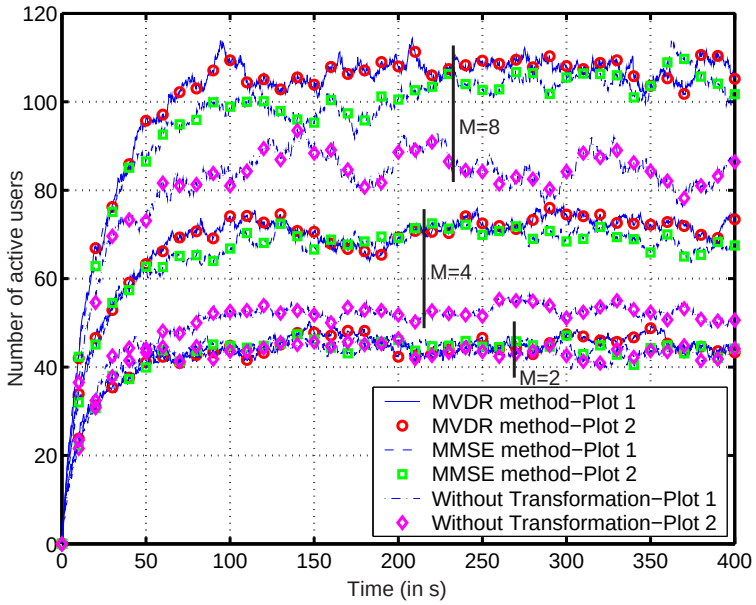

Figure 4.5: Number of active users in the main area versus time for different number of antenna arrays

of the uplink covariance matrix (a) decreases the number of satisfied users significantly. This is due to the fact that as the number of antenna elements increases, the effect of the difference between the uplink and downlink steering vectors becomes more significant.
It is important to again note that the CPICH channel that is transmitted omnidirectionally with the highest allowed power (30 dBm) produces considerable background interference for all users. Simulation results indicate that even in the presence of the strong interference caused by the CPICH channel, downlink beamforming based upon the transformation method improves the system performance significantly (mainly with higher values of M). The higher the number of antenna arrays ($M = 4$ & $M = 8$), the greater is the neccessity of suitable covariance matrix transformation method.

The number of active users versus time that can be supported in the downlink with a data rate of 384 kbits/s with the proposed transformation technique (RLS) is compared with MMSE and MVDR methods as shown in Fig. 4.6 for $M = 4$. Here, we take the simulation parameters as listed in Table 3.1, except that the average and maximum number of paths are set to 2 and 4, respectively. Moreover, we fix δ to 2. Note that for illustrative convenience, only 10 out of 2000 sampling periods have been shown with the marks joined by straight lines. We also compare the performance of the RLS method with that of the MMSE method for the known uplink steering vector case. It can be observed that

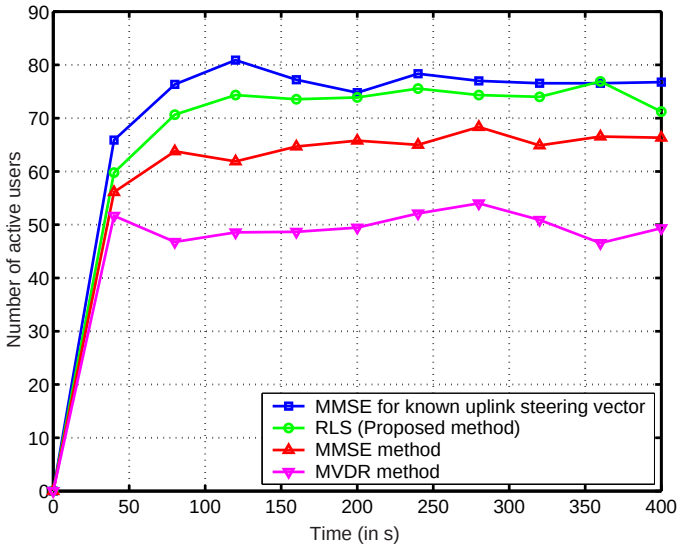

Figure 4.6: Number of active users in the main area versus time for different transformation methods ($M = 4$)

for $M = 4$ antennas the proposed RLS method supports in average about 48% more users than the MVDR method [55] which is a significant improvement. When compared to the MMSE method [5, 34], the RLS method still supports in average about 15% more users than the MMSE method. Therefore, the robust method outperforms both the MVDR and MMSE methods in terms of downlink capacity improvement when the BS does not know exactly the uplink steering vector. The performance of the RLS method is very much similar to that of the MMSE method with exactly known uplink steering vectors. Hence it can be seen that RLS method outperfoms the other two methods without creating degradation in performance of the system. The same result can be shown for a higher number of antennas. The major shortcoming of MVDR and MMSE algorithms is that they do not provide enough robustness against the mismatches between the presumed and the actual uplink steering vectors.

4.8 Summary

A dynamic system level simulator for UMTS-FDD systems with SAs has been used to evaluate the performance of uplink to downlink covariance transformation techniques. It has been found that for higher number of antenna elements ($M = 4$ & $M = 8$) the downlink capacity decreases significantly if the covariance matrix calculated in the uplink frequency is directly used for downlink beamforming. The transformation methods are

necessary to avoid this degradation. Since this degradation is significant, the use of higher number of antenna arrays ($M = 4$ & $M = 8$) without transformation is not sufficient for downlink capacity enhancement.

A new robust method based upon uplink to downlink covariance matrix transformation for downlink beamforming has also been proposed. The performance of the proposed technique is compared with the MVDR and MMSE methods using a dynamic system level simulator for UMTS-FDD systems with SAs. It has been found that the uncertainty of uplink steering vectors cause significant degradation in downlink capacity. Using the proposed transformation technique that is more robust against such mismatches, the problem can be solved without causing any degradation in system level performance.

Chapter 5

Robust Uplink Beamforming based on Minimization of the Outage Probability

In this chapter, we propose a new uplink beamforming algorithm that provides robustness against the uncertainty of the spatial covariance matrix estimated at the BS. Sources of this uncertainty include imprecise knowledge of the DoAs, differences between the presumed and the actual array response as well as estimation errors of the fading coefficients. In our method, we exploit the assumed statistical distribution of the uncertainty to minimize the outage probability of each MS in the uplink. Our approach leads to a semidefinite relaxation problem that can be solved efficiently using the well-established interior point methods. Simulation results show that our method slightly outperforms the robust adaptive beamforming based upon worst-case performance optimization [86]. Moreover, the proposed technique avoids the necessity of the knowledge of norm bounds of the uncertainty of uplink spatial covariance matrix.

5.1 Introduction

The capacity of a wireless cellular system is limited by the mutual interference among simultaneous users. Receive beamforming is an effective way to overcome this problem and increase the uplink capacity of the system. However, the performance of the beamformer degrades significantly in case of unknown channel perturbations. Wireless communication channels may exhibit rich scattering properties with multipath and angular spreading effects. Therefore, beamforming based upon the spatial covariance matrix of rank higher

than one is proposed in [31, 98] and [55].
Robust adaptive beamforming methods have been a subject of tremendous interest during recent years because they provide robustness against channel perturbations. An extension of the classical minimum variance beamforming [69] that is robust to uncertainties in the array response, explicitly models the uncertainty via an uncertainty ellipsoid which gives the possible values of the array response for a given look direction. The robust adaptive beamformer proposed in [86] and [100] is based on explicit modeling of uncertainties in the desired signal array response and data covariance matrix as well as worst-case optimization. In most of these robust beamforming methods, the perturbation is arbitrarily modeled with bounded norm. In wireless systems, it is not practical to find the upper bound of the norm of this perturbation. As the channel varies randomly, it is logical to use the statistical distribution of the perturbation. In communication systems errors in channel parameters are caused by a mismatch in modelling of the random noise, fading and delay effects. Physical layer processing is a part of a communication system. As higher layers deal with the worst-case of the physical layer a useful notion of "worst case" at the physical layer becomes unclear. Moreover, the design goal of the physical layer signal processing is to provide good performance in average (like average BER). Thus average robustness appears as a consistent notion of the robustness.

This chapter is organized as follows. Some necessary background on robust uplink beamforming based upon the spatial covariance matrix is presented in Section 5.2. In Section 5.3, we develop our formulation of the robust beamforming based upon minimization of the outage probability. The semidefinite optimization problem formulated in 5.3 is changed to a convex quadratic problem in Section 5.4 that results to a solution of robust eigenvalue beamforming. Section 5.5 presents numerical simulation results where the performance of the proposed method is compared with robust max-SINR based upon worst-case optimization as well as with a non-robust max-SINR method. Simulation results are shown both for probabilistic (randomly varying channels with moving users) and deterministic models of the propagation environment. The chapter is concluded with a summary in Section 5.6.

5.2 Background

The average information regarding actual uplink channels like the spatial covariance matrix may not be exactly known at the BS. Assume that the channel has an actual

covariance matrix $\mathbf{R}_i^a = \mathbf{R}_i + \mathbf{E}_i$, where $\mathbf{R}_i \in \mathcal{C}^{M\times M}$ is the assumed spatial covariance matrix for the ith desired MS. $\mathbf{E}_i \in \mathcal{C}^{M\times M}$ is the error matrix that corresponds to the estimation errors of the actual covariance matrix $\mathbf{R}_i^a$. In robust methods, a design strategy is introduced to provide robustness against small errors in $\mathbf{R}_i$. We consider a cellular system with a single cell having a BS with M antenna elements. The BS serves K MSs each having a single antenna element. With the receive beamforming at the BS, the SINR for the i-th MS (desired MS) can be expressed as [86]

$$\gamma_i = \frac{\mathbf{w}_i^H \left(\mathbf{R}_i + \mathbf{E}_i\right) \mathbf{w}_i}{\sum\limits_{k\neq i, k=1}^{K} \mathbf{w}_i^H \left(\mathbf{R}_k + \mathbf{E}_k\right) \mathbf{w}_i + \sigma_n^2 \mathbf{w}_i^H \mathbf{w}_i}, \tag{5.1}$$

where $\mathbf{R}_k \in \mathcal{C}^{M\times M},\ k \neq i,\ k = 1, \cdots, K$ are the assumed spatial covariance matrices for the kth undesired MSs. $\mathbf{E}_k,\ k \neq i,\ k = 1, \cdots, K$ are error matrices that correspond to the estimation errors of the actual spatial covariance matrices $\mathbf{R}_k^a = \mathbf{R}_k + \mathbf{E}_k$. We note that $\mathbf{R}_i + \mathbf{E}_i$ and $\mathbf{R}_k + \mathbf{E}_k, k \neq i, k = 1, \cdots, K$ are positive semidefinite matrices. The beamforming vector for i th desired MS is $\mathbf{w}_i \in \mathcal{C}^{M\times 1}$ and the BS receiver noise is represented by σ_n^2. The BS is surrounded by a number of scatterers corresponding to an angular spread of σ_θ, as seen from the MS. For a linear receiving antenna array with half wavelength spacing, the spatial covariance matrix is thus approximated as [8]

$$[\mathbf{R}(\theta, \sigma_\theta)]_{kl} = \alpha_{kl} \mathrm{e}^{(\mathrm{j}\pi(k-l)\sin\theta)} \mathrm{e}^{\left(-\frac{(\pi(k-l)\sigma_\theta\cos\theta)^2}{2}\right)}, \tag{5.2}$$

where $\alpha_{kl} = 1$ is the scaling factor, θ is the DoA of the MS and the indices k and l represent the elements of the $M \times M$ covariance matrix $\mathbf{R}(\theta, \sigma_\theta)$. Note that the spatial covariance matrix (5.2) is normalized. A robust beamforming method based upon maximization of the SINR (5.1) under the condition that the Frobenius norms of the error matrices $\mathbf{E}_i$ and $\mathbf{E}_k$ are bounded with known constants, has been proposed in [86]. We repeat the problem formulation of the robust max-SINR method [86] for the case of spatial covariance matrices as

$$\begin{aligned} &\min_{\mathbf{w}_i} \max_{||\mathbf{E}_I|| \leq \Delta_1} \mathbf{w}_i^H \left(\mathbf{R}_I + \mathbf{E}_I\right) \mathbf{w}_i \\ &\text{subject to } \ \mathbf{w}_i^H \left(\mathbf{R}_i + \mathbf{E_i}\right) \mathbf{w}_i \geq 1, \ \text{ for all } \ ||\mathbf{E}_i|| \leq \Delta_2, \end{aligned} \tag{5.3}$$

which can be rewritten in a much simpler equivalent form

$$\begin{aligned} &\min_{\mathbf{w}_i} \mathbf{w}_i^H \left(\mathbf{R}_I + \Delta_1 \mathbf{I}\right) \mathbf{w}_i \\ &\text{subject to } \ \mathbf{w}_i^H \left(\mathbf{R}_i - \Delta_2 \mathbf{I}\right) \mathbf{w}_i = 1, \end{aligned} \tag{5.4}$$

where

$$\begin{aligned}\mathbf{R}_I &= \sum_{k\neq i,k=1}^{K} \mathbf{R}_k \\ \mathbf{E}_I &= \sum_{k\neq i,k=1}^{K} ||\mathbf{E}_k|| \leq \Delta_1 \\ ||\mathbf{E}_i|| &\leq \Delta_2. \end{aligned} \tag{5.5}$$

In (5.5), $||\cdot||$ represents the Frobenius norm and the constants $\Delta_1 > 0$ and $\Delta_2 > 0$ are the bounds of the uncertainties of the undesired and desired covariance matrices, respectively. The solution of (5.4) is the eigenvector of $(\mathbf{R}_I + \Delta_1\mathbf{I})^{-1}(\mathbf{R}_i - \Delta_2\mathbf{I})$ corresponding to the largest eigenvalue. The major disadvantage of this approach is that it is necessary to know the bounds of the error matrices which are difficult to obtain in a practical scenario. Moreover, this approach provides robustness based upon a worst-case scenario which is a pessimistic approach. In the following section, we formulate a technique for robust beamforming based upon minimization of the outage probability of the considered MS in the uplink. We exploit the assumed statistical distribution of the error matrices for analytical simplicity.

5.3 Minimum Outage Probability (MOP)

The outage probability for the ith MS is defined as the probability that the actual SINR at the BS is less than a threshold SINR (γ_{th}) and is expressed as

$$\begin{aligned} P^i_{\text{out}}(\gamma_{th}) &= \text{pr}\left(\gamma_i \leq \gamma_{th}\right) \\ &= \text{pr}\left(\frac{\mathbf{w}_i^H\left(\mathbf{R}_i + \mathbf{E}_i\right)\mathbf{w}_i}{\sum_{k\neq i,k=1}^{K}\mathbf{w}_i^H\left(\mathbf{R}_k + \mathbf{E}_k\right)\mathbf{w}_i + \sigma_n^2||\mathbf{w}_i||^2} \leq \gamma_{th}\right). \end{aligned} \tag{5.6}$$

We introduce the following relations

$$\begin{aligned} \mathbf{w}_i^H\mathbf{R}_i\mathbf{w}_i &= \text{tr}\left(\mathbf{w}_i^H\mathbf{R}_i\mathbf{w}_i\right) \\ &= \text{tr}\left(\mathbf{R}_i\mathbf{w}_i\mathbf{w}_i^H\right) \\ &= \text{tr}\left(\mathbf{R}_i\mathbf{W}_i\right), \end{aligned} \tag{5.7}$$

where $\mathbf{W}_i = \mathbf{w}_i\mathbf{w}_i^H$ is a rank 1 beamforming matrix and tr (.) is the trace of the matrix. Using (5.7), we can rewrite (5.6) as

$$P^i_{\text{out}}(\gamma_{th}) = \text{pr}\left\{\text{tr}\left(\left(\mathbf{R}_i + \mathbf{E}_i\right)\mathbf{W}_i\right) \leq \gamma_{th}\sum_{k\neq i,k=1}^{K}\text{tr}\left(\left(\mathbf{R}_k + \mathbf{E}_k\right)\mathbf{W}_i\right) + \sigma_n^2\gamma_{th}\text{tr}(\mathbf{W}_i)\right\}, \tag{5.8}$$

where

$$||\mathbf{w}_i||^2 = \mathbf{w}_i^H \mathbf{w}_i = \mathrm{tr}(\mathbf{w}_i \mathbf{w}_i^H) = \mathrm{tr}(\mathbf{W}_i). \tag{5.9}$$

By introducing the following matrices

$$\begin{aligned} \widetilde{\mathbf{R}}_i &= \left(\mathbf{R}_i - \gamma_{th} \sum_{k \neq i, k=1}^{K} \mathbf{R}_k \right) \\ \widetilde{\mathbf{E}}_i &= \left(\mathbf{E}_i - \gamma_{th} \sum_{k \neq i, k=1}^{K} \mathbf{E}_k \right), \end{aligned} \tag{5.10}$$

we can express (5.8) as

$$P_{\mathrm{out}}^i(\gamma_{th}) = \mathrm{pr}\left\{ \mathrm{tr}\left(\left(\widetilde{\mathbf{R}}_i + \widetilde{\mathbf{E}}_i \right) \mathbf{W}_i \right) \leq \gamma_{th} \sigma_n^2 \mathrm{tr}(\mathbf{W}_i) \right\}. \tag{5.11}$$

$\mathbf{R}_i$ and $\mathbf{R}_k$ are deterministic positive semidefinite Hermitian matrices and hence $\mathbf{E}_i$ and $\mathbf{E}_k$ are also Hermitian. For simplicity of analysis, we assume that the elements of Hermitian matrices $\mathbf{E}_i$ and $\mathbf{E}_k$ are independent, Zero Mean Circularly Symmetric Complex Gaussian (ZMCSCG) distributed with the variances σ_i^2 and σ_k^2, respectively. For a large number of users in the system ($K \to \infty$), the elements of $\widetilde{\mathbf{E}}_i$ approach Gaussain distribution even if the elements of $\mathbf{E}_i$ and $\mathbf{E}_k$ ($i \neq k,\ k = 1, \cdots, K$) are non-Gaussian according to Central Limit Theorem. Therefore, the assumption of ZMCSCG for the elements of $\mathbf{E}_i$ and $\mathbf{E}_k$ is not strict. Let us define a random variable

$$y = \mathrm{tr}\left(\left(\widetilde{\mathbf{R}}_i + \widetilde{\mathbf{E}}_i \right) \mathbf{W}_i \right), \tag{5.12}$$

which is real because $\widetilde{\mathbf{R}}_i + \widetilde{\mathbf{E}}_i$ and $\mathbf{W}_i$ are both Hermitian matrices. The probability distribution of y can be found by using the following lemma.

Lemma 1:

If $\mathbf{X}$ is a random Hermitian matrix with independent and circularly symmetric complex Gaussian random elements with zero mean and variance σ_x^2, then for an arbitrary deterministic matrix $\mathbf{A}$, the following relation can be found

$$\mathrm{tr}(\mathbf{AX}) \sim \mathrm{N_c}(0, \sigma_x^2 \mathrm{tr}(\mathbf{A}\mathbf{A}^H)), \tag{5.13}$$

where $\mathrm{N_c}(0, \sigma_x^2 \mathrm{tr}(\mathbf{A}\mathbf{A}^H))$ represents the ZMCSCG distribution with a variance of $\sigma_x^2 \mathrm{tr}(\mathbf{A}\mathbf{A}^H)$. The notation $\sim$ in (5.13) tells that $\mathrm{tr}(\mathbf{AX})$ follows a distribution described by $\mathrm{N_c}(0, \sigma_x^2 \mathrm{tr}(\mathbf{A}\mathbf{A}^H))$.

Proof:

Consider $\mathbf{A} \in \mathcal{C}^{M\times N}$ and $\mathbf{X} \in \mathcal{C}^{N\times M}$ general matrices. Then $\mathrm{tr}(\mathbf{AX})$ is the sum of the weighted elements of the random matrix $\mathbf{X}$ and is given by

$$\begin{aligned}\mathrm{tr}(\mathbf{AX}) &= \left(\mathrm{vec}(\mathbf{A}^H)\right)^H \mathrm{vec}(\mathbf{X}) \\ &= \sum_{i=1}^{M}\sum_{j=1}^{N} a_{ij}x_{ji}. \end{aligned} \tag{5.14}$$

As the elements of $\mathbf{X}$ are independent ZMCSCG, (5.14) is also complex circular Gaussian distributed with zero mean. Even if the elements of $\mathbf{X}$ are non-Gaussian random variables, their weighted sum will be at least close to a Gaussian distribution due to the Central Limit Theorem. The variance of (5.14) is given by

$$\begin{aligned}&\mathrm{E}\left(\mathrm{vec}(\mathbf{A}^H)^H\mathrm{vec}(\mathbf{X})\mathrm{vec}(\mathbf{X})^H\mathrm{vec}(\mathbf{A}^H)\right) \\ &= \mathrm{vec}(\mathbf{A}^H)^H E\left(\mathrm{vec}(\mathbf{X})\mathrm{vec}(\mathbf{X})^H\right)\mathrm{vec}(\mathbf{A}^H) \\ &= \mathrm{vec}(\mathbf{A}^H)^H\sigma_x^2\mathbf{I}\mathrm{vec}(\mathbf{A}^H) \\ &= \sigma_x^2\mathrm{tr}\left(\mathbf{A}^H\mathbf{A}\right). \end{aligned} \tag{5.15}$$

This completes the proof. □

Using the result of **Lemma 1**, we can write $y \sim \mathrm{N}(\mathbf{tr}(\widetilde{\mathbf{R}}_i\mathbf{W}_i), \sigma_e^2\mathrm{tr}(\mathbf{W}_i\mathbf{W}_i^H))$ i. e. y is a Gaussian distributed random variable with mean $\mathbf{tr}(\widetilde{\mathbf{R}}_i\mathbf{W}_i)$ and variance $\sigma_e^2\mathrm{tr}(\mathbf{W}_i\mathbf{W}_i^H)$. σ_e^2 is the variance of the elements of matrix $\widetilde{\mathbf{E}}_i$ and is given by

$$\sigma_e^2 = \sigma_i^2 + \gamma_{th}^2\sum_{k\neq i,k=1}^{K}\sigma_k^2, \tag{5.16}$$

where K is the total number of MSs in the system. For $\sigma_1^2 = \sigma_2^2 = \cdots = \sigma_K^2 = \sigma^2$, eqn. (5.16) can be written as

$$\sigma_e^2 = \sigma^2(1 + \gamma_{th}^2(K-1)). \tag{5.17}$$

The outage probability $P_{\mathrm{out}}^i(\gamma_{th}) = Pr\left(y \leq \gamma_{th}\sigma_n^2\mathrm{tr}(\mathbf{W}_i)\right)$ can be expressed as

$$P_{\mathrm{out}}^i(\gamma_{th}) = \int_{-\infty}^{\gamma_{th}\sigma_n^2\mathrm{tr}(\mathbf{W}_i)} \frac{1}{\sqrt{2\pi}\sigma_e||\mathbf{W}_i||}\exp\left(-\frac{(y-\mu)^2}{2\sigma_e^2||\mathbf{W}_i||^2}\right)dy, \tag{5.18}$$

where $\mu = \mathrm{tr}\left(\widetilde{\mathbf{R}}_i\mathbf{W}_i\right) \geq 0$ and $\mathrm{tr}(\mathbf{W}_i\mathbf{W}_i^H) = ||\mathbf{W}_i||^2$. With the help of the error function

$$\mathrm{erf}(z) = \frac{2}{\sqrt{\pi}}\int_0^z \exp\left(-u^2\right)du, \tag{5.19}$$

the outage probability for the condition $\mu \leq \gamma_{th}\sigma_n^2 \mathrm{tr}(\mathbf{W}_i)$ can be expressed as

$$P_{\mathrm{out}}^i(\gamma_{th}) = \frac{1}{2} + \frac{1}{2}\mathrm{erf}\left(\frac{\gamma_{th}\sigma_n^2 \mathrm{tr}(\mathbf{W}_i) - \mu}{\sqrt{2}\sigma_e ||\mathbf{W}_i||}\right). \tag{5.20}$$

Note that $\mathbf{W}_i = \mathbf{w}_i\mathbf{w}_i^H$ is a rank one matrix and thus $||\mathbf{W}_i|| = \mathrm{tr}\,(\mathbf{W}_i)$. Here, we emphasize that the problem of the minimization of the outage probability remains the same even if $\mu \geq \gamma_{th}\sigma_n^2 \mathrm{tr}(\mathbf{W}_i)$, although the expression of the outage probability (5.20) in this case is given by

$$P_{\mathrm{out}}^i(\gamma_{th}) = \frac{1}{2} - \frac{1}{2}\mathrm{erf}\left(\frac{\mu - \gamma_{th}\sigma_n^2 \mathrm{tr}(\mathbf{W}_i)}{\sqrt{2}\sigma_e ||\mathbf{W}_i||}\right). \tag{5.21}$$

The objective is now to find out the matrix $\mathbf{W}_i$ that minimizes the outage probability (5.20) for the ith MS. It can be observed that $P_{\mathrm{out}}^i(\gamma_{th})$ with respect to $\mathbf{W}_i$ approaches its minimum value of zero, when erf( ) of (5.20) takes the value -1. This means the argument of error function erf( ) must tend to minus infinity which is possible by minimizing its numerator and keeping its denominator to a constant value. The minimization problem is then expressed as

$$\begin{aligned} &\min_{\mathbf{W}_i} \left(\gamma_{th}\sigma_n^2 \mathrm{tr}(\mathbf{W}_i) - \mathrm{tr}\left(\widetilde{\mathbf{R}}_i \mathbf{W}_i\right)\right) \\ &\text{subject to } \sqrt{2}\sigma_e \mathrm{tr}\,(\mathbf{W}_i) = 1, \end{aligned} \tag{5.22}$$

which with additional constraints on beamforming matrix $\mathbf{W}_i$ is equivalent to

$$\begin{aligned} \max_{\mathbf{W}_i} &\left(\mathrm{tr}\left(\left(\mathbf{R}_i - \gamma_{th}\sum_{k\neq i, k=1}^{K}\mathbf{R}_k\right)\mathbf{W}_i\right) - \gamma_{th}\sigma_n^2 \mathrm{tr}(\mathbf{W}_i)\right) \\ \text{subject to} \quad &\mathrm{tr}\,(\mathbf{W}_i) = \frac{1}{\sqrt{2}\sigma_e} \\ &\mathbf{W}_i \succeq 0 \\ &\mathrm{rank}(\mathbf{W}_i) = 1, \end{aligned} \tag{5.23}$$

where $\mathbf{W}_i \succeq 0$ means that $\mathbf{W}_i$ is a positive semidefinite matrix. We transform this problem into a more tractable convex optimization problem, the rank constraint is simply removed as described in [8]. Moreover, the optimization problem is independent of the variance σ_e^2 of the error matrix $\widetilde{\mathbf{E}}_\mathbf{i}$ because it is just a scaling factor for the trace of the beamforming matrix $\mathbf{W}_i$. Note that the objective of (5.23) is non-convex because of maximization of the objective function with respect to $\mathbf{W}_i$. The maximization problem can be changed to minimization simply by reversing the sign of the objective function

and hence the resulting convex optimization problem is written as

$$\begin{aligned} \min_{\mathbf{W}_i} & \left(\gamma_{th}\sigma_n^2 \mathrm{tr}(\mathbf{W}_i) + \mathrm{tr}\left(\left(\gamma_{th} \sum_{k\neq i, k=1}^{K} \mathbf{R}_k - \mathbf{R}_i \right) \mathbf{W}_i \right) \right) \\ \text{subject to} \quad & \mathrm{tr}\left(\mathbf{W}_i\right) = p \\ & \mathbf{W}_i \succeq 0, \end{aligned} \tag{5.24}$$

where we keep $\mathrm{tr}(\mathbf{W}_i)$ to a value of p. The SINR and hence the outage probability remains independent of this scaling factor. This is a SDP problem which has a linear objective, linear constraint and semidefinite constraints [15]. Relaxing the restriction of the rank of $\mathbf{W}_i$ gives a semidefinite optimization problem with a solution that is always a lower bound for the original problem [9].

Lemma 2: There exists a rank 1 solution of $\mathbf{W}_i$ for the semidefinite relaxed problem of (5.24).

Proof: It can be observed from (5.2) that the rank of the spatial covariance matrix reduces to one when the angular spreading tends to zero. We provide a similar proof as that of [102]. We assume that the rank of the spatial covariance matrices is one. The Lagrangian for the primal problem (5.24) is given by

$$\begin{aligned} L(\mathbf{W}_i, \lambda_i, \mathbf{V}_i) &= \gamma_{th} \sum_{k\neq i, k=1}^{K} \mathrm{tr}\left(\mathbf{R}_k \mathbf{W}_i\right) - \mathrm{tr}\left(\mathbf{R}_i \mathbf{W}_i\right) + \gamma_{th}\sigma_n^2 \mathrm{tr}(\mathbf{W}_i) \\ &\quad + \lambda_i \left(\mathrm{tr}\left(\mathbf{W}_i\right) - p\right) - \underbrace{\mathrm{tr}\left(\mathbf{V}_i \mathbf{W}_i\right)}. \end{aligned} \tag{5.25}$$

Note that the underbraced term of (5.25) arises because of the positive semidefinite constraint on the beamforming matrix $\mathbf{W}_i$. Assuming that the Slater condition [15] holds for the convex primal problem (5.24), the Karush-Kuhn-Tucker (KKT) conditions [15] for optimality are:

- Stationarity condition: the gradient of Lagrangian $L(\mathbf{W}_i, \lambda_i, \mathbf{V}_i)$ with respect to $\mathbf{W}_i$ vanishes

$$\gamma_{th} \sum_{k\neq i, k=1}^{K} \mathbf{R}_k - \mathbf{R}_i + (\lambda_i + \gamma_{th}\sigma_n^2)\mathbf{I} - \mathbf{V}_i = 0. \tag{5.26}$$

- Complementary slackness: the condition that two non-negative vectors are orthogonal. Here, this condition arises for the matrices.

$$\begin{aligned} \mathrm{tr}\left(\mathbf{V}_i \mathbf{W}_i\right) &= 0 \\ \Longrightarrow \mathbf{V}_i \mathbf{W}_i &= 0. \end{aligned} \tag{5.27}$$

- Condition on $\mathbf{V}_i$

$$\mathbf{V}_i \succeq 0. \tag{5.28}$$

Note that $\mathbf{R}_i$ has one non-zero eigenvalue and $M-1$ zero eigenvalues. Let the non-zero eigenvalue be t_i and its corresponding eigenvector to be $\mathbf{x}_i$. Assume $\mathbf{y}_i$ lies in the null space of $\mathbf{R}_i$. Now, multiplying (5.26) with $\mathbf{x}_i$ we have

$$\begin{aligned}
\gamma_{th}\sum_{k\neq i,k=1}^{K}\mathbf{R}_k\mathbf{x}_i - t_i\mathbf{x}_i + (\lambda_i+\gamma_{th}\sigma_n^2)\mathbf{x}_i - \mathbf{V}_i\mathbf{x}_i &= 0 \\
\left(\mathbf{V}_i - \gamma_{th}\sum_{k\neq i,k=1}^{K}\mathbf{R}_k\right)\mathbf{x}_i &= \left(\lambda_i+\gamma_{th}\sigma_n^2 - t_i\right)\mathbf{x}_i.
\end{aligned} \tag{5.29}$$

Similarly multiplying (5.26) with $\mathbf{y}_i$ we get

$$\begin{aligned}
\gamma_{th}\sum_{k\neq i,k=1}^{K}\mathbf{R}_k\mathbf{y}_i + (\lambda_i+\gamma_{th}\sigma_n^2)\mathbf{y}_i - \mathbf{V}_i\mathbf{y}_i &= 0 \\
\left(\mathbf{V}_i - \gamma_{th}\sum_{k\neq i,k=1}^{K}\mathbf{R}_k\right)\mathbf{y}_i &= (\lambda_i+\gamma_{th}\sigma_n^2)\mathbf{y}_i.
\end{aligned} \tag{5.30}$$

Let $\mathbf{C}_i = \left(\mathbf{V}_i - \gamma_{th}\sum_{k\neq i,k=1}^{K}\mathbf{R}_k\right)$. We can select $\lambda_i > 0$ in such a way that the equations (5.26), (5.29) and (5.30) are all satisfied. If we choose $\lambda_i = t_i - \gamma_{th}\sigma_n^2$, then from (5.29) and (5.30) we can see that $\mathbf{C}_i$ has one zero eigenvalue and $M-1$ eigenvalues equal to t_i. Note that the dimension of the null space of $\mathbf{R}_i$ is $M-1$. Furthermore, we note that $\mathbf{V}_i$ and $\gamma_{th}\sum_{k\neq i,k=1}^{K}\mathbf{R}_k$ are positive semidefinite matrices and hence we use the relation; $\text{rank}(\mathbf{A}+\mathbf{B}) \geq \max(\text{rank}(\mathbf{A}), \text{rank}(\mathbf{B}))$ to get the following expression

$$\begin{aligned}
\text{rank}(\mathbf{V}_i) &\geq \text{rank}(\mathbf{C}_i) \\
\text{rank}(\mathbf{V}_i) &\geq M-1.
\end{aligned} \tag{5.31}$$

As $\mathbf{W}_i \neq 0$, it has at least one non-zero eigenvalue. Let $\mathbf{u}$ be the eigen vector of $\mathbf{W}_i$ corresponding to this non-zero eigenvalue. Then from equation (5.27), we can write $\mathbf{V}_i(\mathbf{W}_i\mathbf{u}) = 0$. Since, $\mathbf{W}_i\mathbf{u} \neq 0$, $\mathbf{V}_i$ is a rank deficient matrix. Using (5.31), we can write $\text{rank}(\mathbf{V}_i) = M-1$. Finally with the help

of Sylvester's identity we have

$$\begin{aligned} \text{rank}(\mathbf{V}_i\mathbf{W}_i) &\geq \text{rank}(\mathbf{V}_i) + \text{rank}(\mathbf{W}_i) - M \\ 0 &\geq \text{rank}(\mathbf{W}_i) - 1 \\ \text{rank}(\mathbf{W}_i) &= 1. \end{aligned} \tag{5.32}$$

Thus for rank 1 spatial covariance matrices, we can prove that the rank 1 solutions of $\mathbf{W}_i$ exist for the primal problem (5.24). For higher values of the angular spreading σ_θ or the higher ranks of spatial covariance matrices, we have found numerically that the optimum matrix $\mathbf{W}_i$ remains rank 1. This has been confirmed in all of our simulation scenarios.

5.4 Robust Eigenvalue Beamforming

We can also present the optimization problem (5.24) based upon minimization of the outage probability as a robust generalized eigenvalue beamforming. This can be done by re-writing (5.24) as

$$\begin{aligned} &\min_{\mathbf{w}_i} \left\{ \gamma_{th}\sigma_n^2 \mathbf{w}_i^H \mathbf{w}_i + \gamma_{th} \mathbf{w}_i^H \sum_{k=1,k\neq i}^{K} \mathbf{R}_k \mathbf{w}_i - \mathbf{w}_i^H \mathbf{R}_i \mathbf{w}_i \right\} \\ &\text{subject to } \mathbf{w}_i^H \mathbf{w}_i = p. \end{aligned} \tag{5.33}$$

Using the Lagrange multiplier method, the objective function as well as the constraint of the optimization problem (5.33) can be written as

$$L(\mathbf{w}_i, \lambda) = \gamma_{th}\sigma_n^2 \mathbf{w}_i^H \mathbf{w}_i + \gamma_{th} \mathbf{w}_i^H \sum_{k=1,k\neq i}^{K} \mathbf{R}_k \mathbf{w}_i - \mathbf{w}_i^H \mathbf{R}_i \mathbf{w}_i + \lambda \left(\mathbf{w}_i^H \mathbf{w}_i - p \right). \tag{5.34}$$

Differentiating $L(\mathbf{w}_i, \lambda)$ with respect to $\mathbf{w}_i$ and equating it to zero, we get the following relation

$$\left(\gamma_{th}\sigma_n^2 \mathbf{I} + \gamma_{th} \sum_{k=1,k\neq i}^{K} \mathbf{R}_k - \mathbf{R}_i \right) \mathbf{w}_i = -\lambda \mathbf{w}_i, \tag{5.35}$$

where $\mathbf{I}$ is the identity matrix of size $M \times M$. Thus the optimum beamforming vector is the eigenvector corresponding to maximum eigenvalue of the matrix $\left(\mathbf{R}_i - \gamma_{th} \sum_{k=1,k\neq i}^{K} \mathbf{R}_k - \gamma_{th}\sigma_n^2 \mathbf{I} \right)$.

5.5 Simulation Results

The performance of the proposed robust uplink beamforming algorithm is evaluated first in a simulation environment where the number of MSs in the cellular system remains constant and the effect of inter-cell interference is not taken into consideration. We call this as a deterministic scenario. In a second step we use the dynamic system level simulator described in **Chapter 3** to observe the performance of the proposed algorithm where a more realistic cellular propagation environment is considered with mobility and traffic models.

5.5.1 Deterministic Scenario

We illustrate the performance of the proposed uplink beamforming algorithm in a simulated scenario as given in [8]. We consider that three MSs are served by a single BS. One MS is located at $\theta_1 = 10^\circ$ relative to the array broadside and the two others at directions $\theta_{2,3} = 10^\circ \pm \delta$ where δ is varied from 1° to 50°. Thus the DoA of two MSs is varied keeping that of the first MS fixed for all the simulations. We consider a uniform linear array with $M = 8$ elements spaced at a distance of half a wavelength. For each DoA of the MSs, the outage probability is calculated using the results of 10,000 simulation runs. The threshold SINR for all MSs is taken as 5 dB, which is also a usual value for UMTS. The BS receiver noise power σ_n^2 is 1. The diagonal elements of the spatial covariance matrix (5.2) are equal to 1 whereas the absolute values of the non-diagonal elements are less than 1. We use the standard primal form of SeDuMi 1.02 [91] (see Appendix 9.2) to solve the optimization problem of (5.24). The vectors $\mathbf{b}$, c and the matrix $\mathbf{A}^T$ of the primal form for this case are

$$\begin{aligned} \mathbf{b} &= 1 \\ \mathbf{c} &= \begin{bmatrix} \gamma_{th}\sigma_n^2 \mathrm{vec}(\mathbf{I}) \\ \mathrm{vec}\left(-\mathbf{R}_i + \gamma_{th}\sum_{k=1,k\neq i}^{K} \mathbf{R}_k\right) \end{bmatrix} \\ \mathbf{A}^T &= \left(\mathrm{vec}(\mathbf{I})\right)^T, \end{aligned} \tag{5.36}$$

where $\mathbf{I}$ is the identity matrix of size $M \times M$ and vec(.) is the vectorised form of a matrix obtained by stacking its columns. Note that for this special case the vector $\mathbf{b}$ takes a scalar value and the matrix $\mathbf{A}^T$ becomes a row vector.

Figure 5.1 shows the simulated outage probability curves of the second MS versus the angular separation δ for different values of the variance of the elements of the uncertainty matrices $\mathbf{E}_i$ and $\mathbf{E}_k$. We consider that the variances of the elements of the error matrices

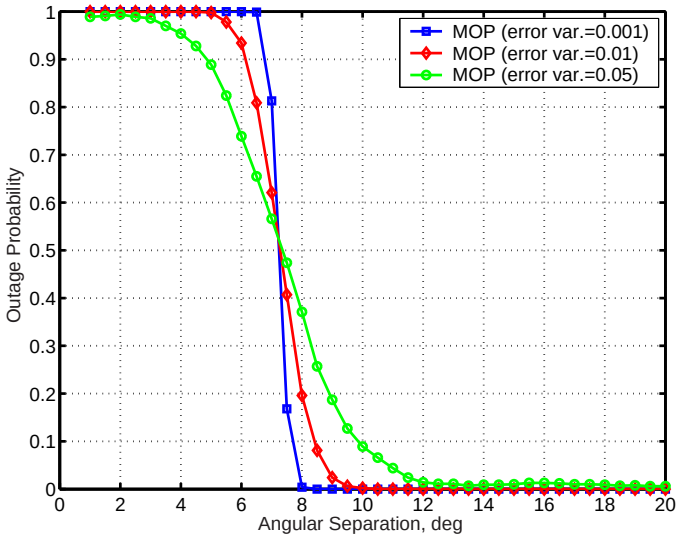

Figure 5.1: Outage probability for the MOP based beamforming method for different error variances σ^2

$\mathbf{E}_i$ and $\mathbf{E}_k$ are equal: $\sigma_1^2 = \sigma_2^2 = \sigma_3^2 = \sigma^2$ and take an angular spreading of 2°. The outage probability drops to 0.1 for an angular separation of 7.8° when the variance is 0.001. In order to achieve the same outage probability for variance of 0.01, the second MS has to be separated by more than 8.2° from first MS. It is important to note that the simulated outage probability for the second MS takes into account the third MS in the system. Similarly, as the error variance increases to 0.05, the outage probability decreases to 0.1 with an angular separation of 10°.

The performance of the beamforming based upon proposed MOP is compared with that of the robust Max-SINR beamforming method. The simulated outage probability of the second MS for both of the methods is shown in Fig. 5.2 versus the increasing angular separation. In order to make a fair comparison between the two methods, we choose the values of Δ_1 and Δ_2 in such a way that these values reflect the maximum Frobenius norms of the uncertainty matrices with $\sigma^2 = 0.001$. Therefore for the case of MOP, we use $\sigma^2 = 0.001$ for all values of angular spreadings. For the robust Max-SINR method, $\Delta_1 = 0.7$ and $\Delta_2 = 1.4$ are taken numerically as the norm bounds of the uncertainties of the desired and undesired spatial covariance matrices. For all the angular spreadings, the proposed MOP performs better than the robust Max-SINR method although the improvement is very small. However, the advantage of our method is that it does not need to know the norm bounds of the uncertainty matrices. The threshold SINR value (γ_{th}) is a system parameter and can be chosen depending upon the QoS needed for the MSs in the system.

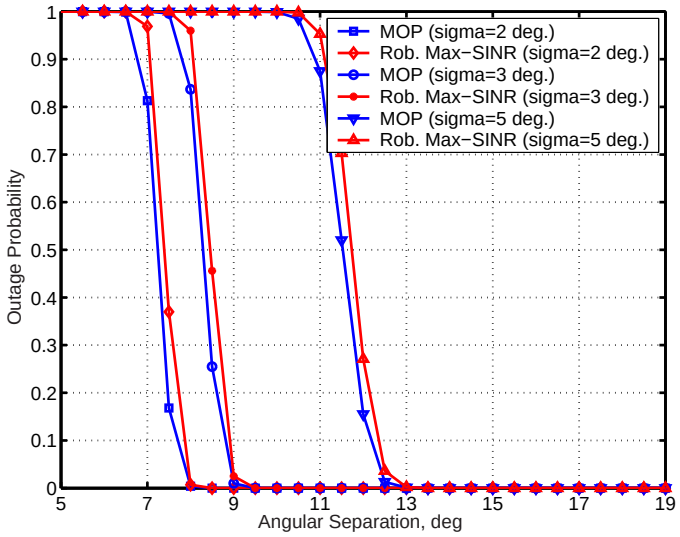

Figure 5.2: Comparison of MOP and robust max-SINR beamforming methods for different angular spreadings σ_θ

The outage probability curves using the max-SINR (non-robust) method are shown in Fig. 5.3 for different angular spreadings. In order to achieve an outage probability of 0.1, the proposed robust beamforming method based upon the MOP criterion needs an angular separation of about 7.8° whereas the non robust max-SINR method needs 36° of separation for the same angular spreading of 2°. Similar results can be observed for other values of angular spreading. This confirms that our approach provides robustness against the uncertainty of spatial covariance matrices. However, the MOP method needs the knowledge of the statistical distribution of the elements of the error matrices. In case of cellular systems with a large number of inter- and intra-cell users, the assumption of Gaussian distribution for the elements of uncertainty matrices is reasonable.

5.5.2 Probabilistic Scenario

We perform dynamic system level simulations (**Chapter 3**) in order to evaluate the uplink capacity of the UMTS-FDD system based upon the proposed robust beamforming algorithm (MOP method). The maximum number of MSs that can be supported in the uplink with the target SINR value provides the measure of the uplink capacity. Simulations have been carried out for the following beamforming methods with $M = 4$ antenna elements.

- a) Non-robust method based upon maximum SINR

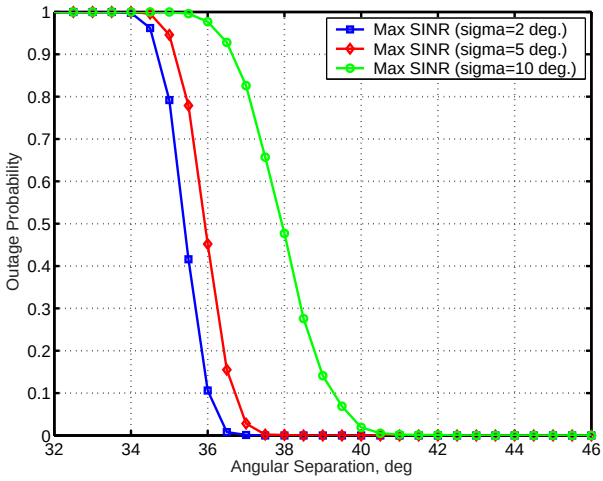

Figure 5.3: Outage probability for the maximum SINR based beamforming method for different angular spreadings σ_θ

- b) Robust method based upon MOP.

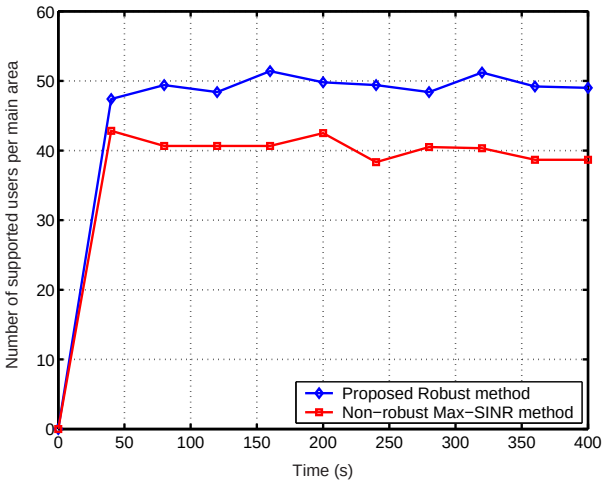

Figure 5.4: Number of average MSs supported in uplink versus time

As seen from Fig. 5.4, the proposed robust uplink beamforming method outperforms the non-robust method based upon max-SINR by supporting in average 25% more MSs than in case of max-SINR. Most of the chosen simulation parameters are the same as in **Chapter 3**, except that we introduce a uncertainty matrix $\mathbf{E}_i$ with i.i.d. complex Gaussian elements of variance σ_i^2 and the OF of 1. Moreover, we set the threshold and maximum values of the SINR of the uplink DPDCH channels to 6 dB and 8 dB, respectively. The average and maximum number of paths are set to 2 and 4, respectively. Here, the spatial covariance matrices are not normalized and modeled according to (3.13). Note that the

OF (see 3.2.8) of 0 represents the case when the codes exhibit the perfect orthogonality where as the OF of 1 represents that the codes are no more orthogonal to each other. In case of the downlink, a BS can synchronize its transmission to different users and therefore, the orthogonality is only affected by the multipath propagation. However, in the uplink of the UMTS-FDD system, users are transmitting to the BS independently and hence the codes used for the data transmission do not maintain the orthogonality property at all. This is the motivation behind the selection of an OF of 1 for the simulation results shown in Fig. 5.4. The receiver at the BS uses a rake receiver. Multiuser detection algorithms are not used in order to avoid huge computational tasks necessary for system level simulations. As in other cases, power control, soft handover along with mobility and traffic models (**Chapter 3**) were used while evaluating the performance of the proposed beamforming algorithm. Similar results can be shown for a higher number of antenna elements. The max-SINR algorithm does not provide enough robustness against the mismatches between the presumed and the actual spatial covariance matrices of the desired and undesired users, respectively.

5.6 Summary

This chapter proposed a new robust beamforming algorithm based upon minimization of the outage probability of a MS in the uplink. Our approach leads to a relaxation of a semidefinite optimization problem that can be solved efficiently using an optimization toolbox like SeDuMi 1.02. Simulation results show that our method is robust against uncertainties of the spatial covariance matrices and performs slightly better than the robust max-SINR method based upon worst-case performance optimization. The computational complexity of our approach is similar to that of the robust max-SINR method.

Chapter 6

Robust Downlink Beamforming based upon an Outage Probability Criterion

In this chapter, we propose a new downlink beamforming method that provides robustness against the uncertainty of the downlink spatial covariance matrix estimated at the BS that uses antenna arrays. This uncertainty arises due to the difference between the presumed and the actual array response as well as the estimation errors of the fading coefficients. In our method, we exploit the assumed statistical distribution of the uncertainty to minimize the total downlink transmit power under the condition that the outage probability of each MS in the downlink is less than a certain threshold value. Our approach leads to a convex optimization problem that can be solved efficiently using the well-established interior point methods. Computer simulations are used to compare the performance of our method with that of the robust transmit beamforming based upon worst-case performance optimization [8]. Moreover, the proposed technique avoids the necessity of the knowledge of the norm bounds of the uncertainty of the downlink spatial covariance matrices.

6.1 Introduction

In recent years, adaptive beamforming has found numerous applications in wireless communications [44, 83]. Downlink beamforming is an effective way to reduce the interference and increase the downlink capacity of the system. However, the major obstacle for the implementation of downlink beamforming is the uncertainty of the downlink channel.

The estimates of the downlink channel are available at the BS through a feedback channel from the MS. The drawbacks of this approach are the reduction of system capacity because of the frequent channel uses required for the transmission of the feedback information from MS to BS and the inherent time delays associated with the feedback. Another approach for downlink beamforming is to directly use the average channel information obtained from uplink for downlink transmission i. e. applying uplink weight vectors for downlink beamforming. Although this method works well for TDD systems with slowly varying channels, its performance degrades significantly (see **Chapter 4**) for FDD systems like UMTS where the frequency separation between uplink and downlink is significant. Therefore, uplink to downlink adaptation methods (like spatial covariance transformation methods) that require only second order statistics of the uplink and downlink channels were dealt in **Chapter 4**.

In all of the downlink beamforming methods overviewed above, the performance of the beamformer degrades if any of the assumptions on the propagation environment, sources, or sensor array becomes violated. For example the performance of MVDR based transformation method for downlink beamforming **Chapter 4** degrades significantly if the assumption of same APS for uplink and downlink does not hold true. Moreover, if the number of paths, their DoA and the time delays etc. do not hold reciprocity property [56] for uplink and downlink channels, then performance of other downlink beamforming methods [5] also fail to produce desired result. Therefore, robust approaches to downlink beamforming appear to be of primary importance in these cases.

There are several efficient approaches to the design of robust adaptive beamformers like linearly constrained minimum variance (LCMV) beamformer [72], signal blocking based algorithms [24, 45] and Bayesian beamformer [7] etc., which are mainly developed for providing robustness against signal look direction mismatch. The algorithms that use the diagonal loading of the sample covariance matrix [17, 25], the eigenspace-based beamformer [21, 33], and the covariance matrix taper (CMT) [50, 84] approach are known to provide an improved robustness against more general types of mismatches. The major drawback of diagonal loading technique is that there is no reliable way to choose the diagonal loading factor. Recently, another promising approach has been proposed in [100] that explicitly models an arbitrary mismatch bounded in norm in the desired signal array response and uses worst-case performance optimization to improve the robustness of the MVDR beamformer. However, a major shortcoming of these robust approaches is

that they have been originally developed for the point sources and most of them cannot be extended in a direct way to the case of spatially distributed (incoherently scattered) sources. The scenarios with randomly distorted wavefronts are very much typical in case of wireless communications where the radio channels exhibit rich scattering properties with multipath and angular spreading effects. For example, in rural and suburban environments with a high BS, one of the major problems is the fast fading due to local scattering in the vicinity of the MS [10, 78, 106].

A robust approach to adaptive beamforming for the case of general rank signal models (result of distributed signal sources like multipath phenomena) is proposed in [86] where the desired signal array response is characterised by the signal covariance matrix rather than the signal steering vector, and therefore, the robustness of adaptive beamformers against mismatches between the presumed and actual signal covariance matrices is considered. This method was developed for uplink beamforming and the importance of robust methods for uplink is not vital when compared to the downlink because in uplink there are several methods [32, 67] which can effectively estimate the spatial signatures and consequently the signal covariance matrices. The optimum downlink beamforming methods that provide robustness against channel uncertainties have been discussed in [8] and [102], where the mismatches between the presumed and actual spatial covariance matrices are taken into account. Robust downlink beamforming based on uplink to downlink spatial covariance transformation is proposed in **Chapter 4**. A downlink power adjustment method proposed in [11] provides a substantially improved robustness against imperfect knowledge of the wireless channel by means of maintaining the required quality of service for the worst-case channel uncertainty. In all of these robust beamforming methods, the perturbation is arbitrarily modeled whose norm is bounded. In real time wireless systems, it is difficult to find the upper bound of the norm of this perturbation. As the channel varies randomly, it is logical to use the stochastic approach for describing the perturbation.

In this chapter, we propose a new approach to robust downlink beamforming where the transmit power of the BS is optimized with outage probability constraints. The outage probability is one of the important parameters used to characterise the performance of the system and is defined as the probability that the SINR measured at the MS is higher than the specified threshold value of SINR. The mismatches between the presumed and actual downlink spatial covariance matrices are modeled with a matrix whose elements

are i.i.d Gaussian. The transmit power optimization problem formulated with outage probability constraints is changed into a convex optimization problem with second order cone and semidefinite constraints. We provide both robust optimum as well as computationally efficient robust suboptimum solutions of the resulting optimization problem. Unlike other robust designs, we use a probabilistic approach, where the mismatches are modeled as i.i.d Gaussian and hence measure of quality of service in terms of SINR becomes random.

This chapter is organized as follows. Some necessary background on robust downlink beamforming based upon the spatial covariance matrix is presented in Section 6.2. In Section 6.3, we develop our formulation of robust downlink beamforming based upon minimization of BS transmit power with constraints for the outage probability of a MS in the downlink. Here, both the optimum as well as suboptimum solutions of the constrained convex optimization problems are presented. Section 6.4 presents the numerical simulation results where the performance of the proposed method is compared with the robust method based upon worst-case optimization [8] as well as with the non-robust max-SINR method. The summary of the chapter is given in Section 6.5.

6.2 Background

We consider a cellular system with a single cell having a BS with M antenna elements. The BS serves K MSs each having a single antenna element. With the transmit beamforming at the BS, the SINR for the ith MS (desired MS) can be expressed as [11]

$$\gamma_i = \frac{\mathbf{w}_i^H \left(\mathbf{R}_i + \mathbf{E}_i\right) \mathbf{w}_i}{\sum\limits_{k \neq i, k=1}^{K} \mathbf{w}_k^H \left(\mathbf{R}_i + \mathbf{E}_i\right) \mathbf{w}_k + \sigma_i^2}, \tag{6.1}$$

where $\mathbf{R}_i \in \mathcal{C}^{M \times M}$ is the assumed spatial covariance matrix for the ith desired MS. $\mathbf{E}_i \in \mathcal{C}^{M \times M}$ is the error matrix that corresponds to the estimation errors of the actual spatial covariance matrix $\mathbf{R}_i^a = \mathbf{R}_i + \mathbf{E}_i$. We note that $\mathbf{R}_i + \mathbf{E}_i$ is a positive semidefinite matrix. $\mathbf{w}_i \in \mathcal{C}^{M \times 1}$ and $\mathbf{w}_k \in \mathcal{C}^{M \times 1}$ are the beamforming vectors for ith desired MS and kth undesired MS, respectively. The receiver noise is represented by σ_i^2. Each MS is surrounded by a large number of local scatterers corresponding to an angular spreading of σ_θ, as seen from the BS. For a linear transmitting antenna array with a half wavelength spacing, the spatial covariance matrix is thus approximated as [8] and is given by eqn. (5.2). Note that for $\sigma_\theta \neq 0$, the rank of the spatial covariance matrix (5.2) is greater

than 1 which is also the case for the approximation (3.13). The outage probability based optimum robust downlink beamforming algorithm to be proposed in this chapter is independent of the modeling of the spatial covariance matrix (see eqns. 5.2, 3.13).

Robust optimum transmit beamforming proposed in [8] is based upon the condition that the spectral norm of the error matrix $\mathbf{E}_i$ is upper bounded with a known constant. We repeat the problem formulation of [8] for the case of a cellular system with a single cell and a BS ($\mathbf{R}_{i,c(n)} = \mathbf{R}_i$, where index $c(n)$ represents the nth MS assigned to the $c(n)$th BS and $n \neq i$) as

$$\begin{aligned} &\min_{\mathbf{W}_i} \sum_{i=1}^{K} \mathrm{tr}(\mathbf{W}_i) \\ &\text{subject to} \quad \mathrm{tr}\left((\mathbf{R}_i - \epsilon_i \mathbf{I})\,\mathbf{W}_i\right) - \gamma_{th} \sum_{k \neq i, k=1}^{K} \mathrm{tr}\left((\mathbf{R}_i + \epsilon_i \mathbf{I})\,\mathbf{W}_k\right) \geq \gamma_{th}\sigma_i^2 \\ &\qquad\qquad \mathbf{W}_i \succeq 0 \\ &\qquad\qquad \mathbf{W}_i = \mathbf{W}_i^H, \quad \text{for} \quad i = 1,\ 2,\ \cdots,\ K, \end{aligned} \tag{6.2}$$

where

$$\begin{aligned} \mathbf{W}_i &= \mathbf{w}_i \mathbf{w}_i^H \\ \epsilon_i &\geq ||\mathbf{E}_i||, \quad \epsilon_i \geq 0. \end{aligned} \tag{6.3}$$

In (6.3), $||\cdot||$ represents the Frobenius norm and the constant $\epsilon_i > 0$ is the upper bound of the uncertainty of the spatial covariance matrix $\mathbf{R}_i$ for the desired MS. Since (6.2) is a semidefinite optimization problem, the solution for the global optimum exists. The major disadvantage of this approach is that it is necessary to know the upper bound of the Frobenius norm of the error matrix $\mathbf{E}_i$ which is difficult to determine in a practical scenario. Moreover, this approach provides robustness based upon a worst-case scenario which is a pessimistic approach. In the following section, we formulate a technique for robust downlink beamforming based upon minimization of the total BS transmit power by maintaining the non-outage probability of all MSs in the downlink above a certain threshold value. We exploit the assumed statistical distribution of the error matrix.

For the cases without spatial covariance matrix uncertainty, the optimum transmit beam-

forming algorithm can be expressed by substituting $\epsilon_i = 0$ in (6.2) as

$$\begin{aligned} &\min_{\mathbf{W}_i} \sum_{i=1}^{K} \mathrm{tr}(\mathbf{W}_i) \\ &\text{subject to} \quad \mathrm{tr}\left(\mathbf{R}_i\mathbf{W}_i\right) - \gamma_{th}\sum_{k\neq i,k=1}^{K}\mathrm{tr}\left(\mathbf{R}_i\mathbf{W}_k\right) \geq \gamma_{th}\sigma_i^2 \\ &\qquad\qquad \mathbf{W}_i \succeq 0, \\ &\qquad\qquad \mathbf{W}_i = \mathbf{W}_i^H, \quad \text{for } i = 1,\ 2,\ \cdots,\ K. \end{aligned} \tag{6.4}$$

For multiple BSs, the disadvantage of the optimum robust as well as non-robust transmit beamforming is that the BSs need to exchange information about the channels of the MSs that are in the neigbouring cells. This leads to a necessity of centralized signal processing whose complexity is very high for large cellular networks. To remedy this problem, a decentralised downlink beamforming algorithm is presented in [8]. The approach is to determine each beamformer separately, keeping the received SNR at the MS of interest above the threshold μ_i and the total transmitted power to the interfered users below the threshold ξ_i, which according to [8] results in the following optimization problem

$$\begin{aligned} &\min_{\mathbf{W}_i} \sum_{i=1}^{K} \mathrm{tr}(\mathbf{W}_i) \\ &\text{subject to} \quad \mathrm{tr}\left(\mathbf{R}_i\mathbf{W}_i\right) \geq \mu_i\sigma_i^2 \\ &\qquad\qquad \sum_{k\neq i,k=1}^{K}\mathrm{tr}\left(\mathbf{R}_i\mathbf{W}_k\right) \leq \xi_i \\ &\qquad\qquad \mathbf{W}_i \succeq 0 \\ &\qquad\qquad \mathbf{W}_i = \mathbf{W}_i^H, \quad \text{for } i = 1,\ 2,\ \cdots,\ K, \end{aligned} \tag{6.5}$$

which is again a semidefinite problem with rank one relaxation and provides a suboptimum solution. Figure 6.1 shows the transmit power of the BS using the optimum transmit beamforming algorithm (6.4) and the decentralised beamforming method (6.5). As can be observed, in terms of transmit power the optimum transmit beamforming outperforms the decentralised beamforming method.

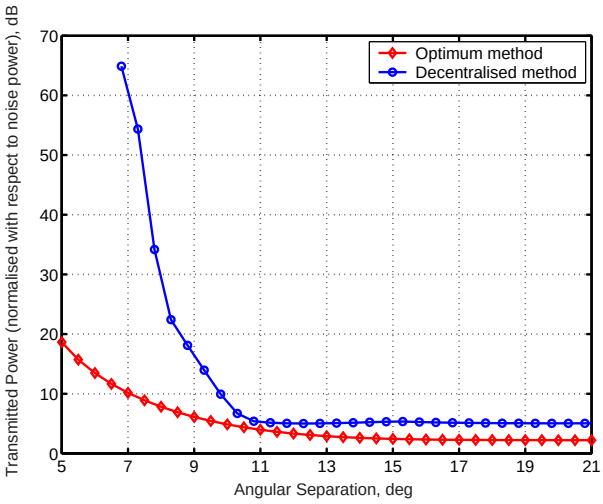

Figure 6.1: Comparison of the normalized BS transmit power with two non-robust beamforming methods

6.3 Robust Downlink Beamforming

In this section, we present the proposed robust downlink beamforming based on the outage probability criterion. The problem can be mathematically formulated as

$$\min_{\mathbf{w}_i} \sum_{i=1}^{K} ||\mathbf{w}_i||^2$$
$$\text{subject to } \tilde{P}^i_{\text{out}}(\gamma_{th}) \geq p_i, \text{ for } i = 1,\ 2,\ \cdots,\ K. \tag{6.6}$$

where $\tilde{P}^i_{\text{out}}(\gamma_{th})$ defines the probability that a user is not in outage. The non-outage probability for the ith MS is defined as the probability that the SINR provided by the BS is greater than a threshold SINR (γ_{th}) and is expressed as

$$\begin{aligned}\tilde{P}^i_{\text{out}}(\gamma_{th}) &= \text{pr}\left(\gamma_i \geq \gamma_{th}\right) \\ &= \text{pr}\left(\frac{\mathbf{w}_i^H\left(\mathbf{R}_i + \mathbf{E}_i\right)\mathbf{w}_i}{\sum_{k\neq i,k=1}^{K}\mathbf{w}_k^H\left(\mathbf{R}_i + \mathbf{E}_i\right)\mathbf{w}_k + \sigma_i^2} \geq \gamma_{th}\right).\end{aligned} \tag{6.7}$$

As seen from (5.7), we introduce the following relation

$$\mathbf{w}_i^H\mathbf{R}_i\mathbf{w}_i \;=\; \text{tr}\left(\mathbf{R}_i\mathbf{W}_i\right), \tag{6.8}$$

where $\mathbf{W}_i = \mathbf{w}_i\mathbf{w}_i^H$ is a rank 1 beamforming matrix and tr( ) is the trace of the matrix. Using (6.8), we can rewrite (6.7) as

$$\tilde{P}^i_{\text{out}}(\gamma_{th}) = \text{pr}\left\{\text{tr}\left(\left(\mathbf{R}_i + \mathbf{E}_i\right)\mathbf{W}_i\right) \geq \gamma_{th}\sum_{k\neq i,k=1}^{K}\text{tr}\left(\left(\mathbf{R}_i + \mathbf{E}_i\right)\mathbf{W}_k\right) + \gamma_{th}\sigma_i^2\right\}. \tag{6.9}$$

By introducing the following deterministic matrix

$$\mathbf{Z}_i \;=\; \mathbf{W}_i - \gamma_{th}\sum_{k\neq i,k=1}^{K}\mathbf{W}_k, \tag{6.10}$$

we can express (6.9) as

$$\tilde{P}^i_{\text{out}}(\gamma_{th}) \;=\; \text{pr}\Big\{\text{tr}\left(\left(\mathbf{R}_i+\mathbf{E}_i\right)\mathbf{Z}_i\right) \geq \gamma_{th}\sigma_i^2\Big\}. \tag{6.11}$$

Note that the matrix $\mathbf{E}_i$ is Hermitian, because it is the difference between the actual and estimated spatial covariance matrices which are both Hermitian. For simplicity of analysis, we assume that the elements of the Hermitian matrix $\mathbf{E}_i$ are independent, ZMCSCG with a variance σ_e^2. In **Lemma 1** (**Chapter 5**), we emphasize that this assumption is not strict. Let us define a random variable

$$y = \text{tr}\left(\left(\mathbf{R}_i+\mathbf{E}_i\right)\mathbf{Z}_i\right), \tag{6.12}$$

which is real because $\mathbf{R}_i+\mathbf{E}_i$ and $\mathbf{Z}_i$ are both Hermitian matrices. The probability distribution of y can be found by using the **Lemma 1** of Chapter 5. Therefore, we can write $y \sim \text{N}(\text{tr}(\mathbf{R}_i\mathbf{Z}_i), \sigma_e^2\text{tr}(\mathbf{Z}_i\mathbf{Z}_i^H))$ i. e. y is a Gaussian distributed random variable with mean $\mathbf{R}_i\mathbf{Z}_i$ and variance $\sigma_e^2\text{tr}(\mathbf{Z}_i\mathbf{Z}_i^H)$. The non-outage probability $\tilde{P}^i_{\text{out}}(\gamma_{th}) = Pr\left(y \geq \gamma_{th}\sigma_i^2\right)$ can be expressed as

$$\tilde{P}^i_{\text{out}}(\gamma_{th}) = \int_{\gamma_{th}\sigma_i^2}^{\infty}\frac{1}{\sqrt{2\pi}\sigma_e||\mathbf{Z}_i||}\exp\left(-\frac{(y-\mu)^2}{2\sigma_e^2||\mathbf{Z}_i||^2}\right)\,dy, \tag{6.13}$$

where $\mu = \text{tr}\left(\mathbf{R}_i\mathbf{Z}_i\right) \geq 0$. With the help of error function

$$\text{erf}(z) = \frac{2}{\sqrt{\pi}}\int_0^z \exp\left(-u^2\right)\,du, \tag{6.14}$$

the non-outage probability can be expressed as

$$\tilde{P}^i_{\text{out}}(\gamma_{th}) \;=\; \begin{cases} \frac{1}{2}+\frac{1}{2}\text{erf}\left(\frac{\mu-\gamma_{th}\sigma_i^2}{\sqrt{2}\sigma_e||\mathbf{Z}_i||}\right), & \text{for } \gamma_{th}\sigma_i^2 \leq \mu, \\ \frac{1}{2}-\frac{1}{2}\text{erf}\left(\frac{\gamma_{th}\sigma_i^2-\mu}{\sqrt{2}\sigma_e||\mathbf{Z}_i||}\right), & \text{for } \gamma_{th}\sigma_i^2 \geq \mu. \end{cases} \tag{6.15}$$

Note that for a reliable wireless communication link, the non-outage probability $\tilde{P}^i_{\text{out}}(\gamma_{th})$ must be close to 1 (with the ideal case $\tilde{P}^i_{\text{out}}(\gamma_{th}) = 1$). As the argument of the error function is positive for both equations in (6.15), the upper equation corresponds to $\tilde{P}^i_{\text{out}}(\gamma_{th}) \geq \frac{1}{2}$ whereas the lower equation corresponds to $\tilde{P}^i_{\text{out}}(\gamma_{th}) \leq \frac{1}{2}$. Therefore, the upper equation of (6.15) has to be considered. Using this equation, the non-outage

probability constraint in (6.6) can be expressed as

$$\begin{aligned} \tilde{P}^{i}_{\text{out}}(\gamma_{th}) &\geq p_i \\ \text{erf}\left(\frac{\mu-\gamma_{th}\sigma_i^2}{\sqrt{2}\sigma_e||\mathbf{Z}_i||}\right) &\geq 2p_i-1 \\ \left(\frac{\mu-\gamma_{th}\sigma_i^2}{\sqrt{2}\sigma_e||\mathbf{Z}_i||}\right) &\geq \text{erf}^{-1}(2p_i-1) \\ \text{tr}\left(\mathbf{R}_i\mathbf{Z}_i\right)-\gamma_{th}\sigma_i^2 &\geq c_i||\mathbf{Z}_i||, \end{aligned} \tag{6.16}$$

where $c_i = \sqrt{2}\sigma_e\text{erf}^{-1}(2p_i-1)$. Note that for $p_i < \frac{1}{2}$, c_i is negative and the constraint of (6.16) becomes non-convex. In order to maintain convexity of (6.16), it is required to have $p_i \geq \frac{1}{2}$, which is obviously a proper choice for the threshold value of the non-outage probability $\tilde{P}^{i}_{\text{out}}(\gamma_{th})$ which corresponds to the upper equation of (6.15). Thus, the optimization problem (6.6) can be written as

$$\begin{aligned} \min_{\mathbf{W}_i} \sum_{i=1}^{K} \text{tr}(\mathbf{W}_i) & \\ \text{subject to} \quad & ||\mathbf{Z}_i|| \leq \frac{1}{c_i}\left(\text{tr}\left(\mathbf{R}_i\mathbf{Z}_i\right)-\gamma_{th}\sigma_i^2\right) \\ & \mathbf{W}_i = \mathbf{W}_i^H \\ & \text{rank}(\mathbf{W}_i) = 1, \quad \text{for } i = 1,\ 2,\ \cdots,\ K, \end{aligned} \tag{6.17}$$

where $\mathbf{Z}_i$ is not a rank one matrix and given by (6.10). Now we provide robust optimum as well as suboptimum solutions for (6.17). The optimum solution gives better performance in terms of BS transmit power than that of suboptimum solution with a cost of increased computational complexity.

6.3.1 Robust Optimum Solution

The constraint on the rank of $\mathbf{W}_i$ makes the optimization problem (6.17) non-convex. We transform this problem into a more tractable convex optimization problem by replacing the rank-one constraint by the SDP constraint. Then the relaxed optimization problem (6.17) can be written as

$$\begin{aligned} \min_{\mathbf{W}_i} \sum_{i=1}^{K} \text{tr}(\mathbf{W}_i) & \\ \text{subject to} \quad & ||\mathbf{Z}_i|| \leq t_i \\ & t_i = \frac{1}{c_i}\left(\text{tr}\left(\mathbf{R}_i\mathbf{Z}_i\right)-\gamma_{th}\sigma_i^2\right) \\ & \mathbf{W}_i \succeq 0 \\ & \mathbf{W}_i = \mathbf{W}_i^H, \quad \text{for } i = 1,\ 2,\ \cdots,\ K, \end{aligned} \tag{6.18}$$

which has a linear convex objective function and linear, SOC as well as semidefinite constraints. Since all the constraints are convex, the optimization problem is a convex one and can be solved using the standard primal form of SeDuMi 1.02 [91] (see Appendix 9.2). It is important to note that there is a set of such linear, SOC and SDP constraints which increases with increasing K. Although the global optimum can be found for this problem, its computational complexity is very high. Therefore with some conservative approach, the convex optimization problem (6.18) can be reduced to a computationally efficient form i. e. the optimization problem which includes only linear and semidefinite constraints. In the following section, such a suboptimum method will be discussed.

6.3.2 Robust Suboptimum Solution

Since $||\mathbf{Z}_i||^2 = \mathrm{tr}(\mathbf{Z}_i\mathbf{Z}_i^H)$, the constraint in $\mathbf{Z}_i$ or $\mathbf{W}_i$ of problem (6.17) is nonlinear, although the objective is linear and the problem consists of semidefinite constraints. Substituting $\mathbf{Z}_i$ from (6.10) into the quadratic constraint of (6.17), we have

$$c_i||\mathbf{W}_i - \gamma_{th}\sum_{k\neq i,k=1}^{K}\mathbf{W}_k|| \leq \mathrm{tr}\left(\mathbf{R}_i\left(\mathbf{W}_i - \gamma_{th}\sum_{k\neq i,k=1}^{K}\mathbf{W}_k\right)\right) - \gamma_{th}\sigma_i^2. \tag{6.19}$$

Let us now approximate the left-hand side of (6.19) using the inequality $||\mathbf{A} - \alpha\mathbf{B}|| \leq ||\mathbf{A}|| + |\alpha| \cdot ||\mathbf{B}||$, where α is any real number. Although tightness of this inequality cannot be guaranteed for arbitrary $\mathbf{A}$, $\mathbf{B}$ and α, it will be shown via simulations that the proposed approximation is proper in terms of closeness of the original problem (6.18) and its simplified version. With this approximation, the constraint in (6.19) can be changed into the following two possible constraints

$$c_i||\mathbf{W}_i|| + c_i\gamma_{th}\sum_{k\neq i,k=1}^{K}||\mathbf{W}_k|| \leq \mathrm{tr}\left(\mathbf{R}_i\mathbf{W}_i\right) - \gamma_{th}\sigma_i^2 - \gamma_{th}\sum_{k\neq i,k=1}^{K}\mathrm{tr}\left(\mathbf{R}_i\mathbf{W}_k\right) \tag{6.20}$$

$$c_i||\mathbf{W}_i|| + c_i\gamma_{th}\sum_{k\neq i,k=1}^{K}||\mathbf{W}_k|| \geq \mathrm{tr}\left(\mathbf{R}_i\mathbf{W}_i\right) - \gamma_{th}\sigma_i^2 - \gamma_{th}\sum_{k\neq i,k=1}^{K}\mathrm{tr}\left(\mathbf{R}_i\mathbf{W}_k\right). \tag{6.21}$$

In Appendix 9.3, we show that the constraint (6.21) contradicts to the objective of (6.6) and, therefore, (6.20) has to be used. Hence, in the following we replace the constraint (6.19) by (6.20). Since $\mathbf{W}_i$ are rank-one matrices, $||\mathbf{W}_i|| = \mathrm{tr}\left(\mathbf{W}_i\right)$.
Thus, the constraint (6.20) can be further expressed as

$$\mathrm{tr}\left(\left(\mathbf{R}_i - c_i\mathbf{I}\right)\mathbf{W}_i\right) - \gamma_{th}\sum_{k\neq i,k=1}^{K}\mathrm{tr}\left(\left(\mathbf{R}_i + c_i\mathbf{I}\right)\mathbf{W}_k\right) \geq \gamma_{th}\sigma_i^2. \tag{6.22}$$

Using (6.22), and replacing rank-one constraint by an SDP constraint, we obtain the following optimization problem which is an approximation of (6.17):

$$\begin{aligned} &\min_{\mathbf{W}_i} \sum_{i=1}^{K} \mathrm{tr}(\mathbf{W}_i) \\ &\text{subject to} \quad \mathrm{tr}\left(\left(\mathbf{R}_i - c_i\mathbf{I}\right)\mathbf{W}_i\right) - \gamma_{th}\sum_{k\neq i,k=1}^{K}\mathrm{tr}\left(\left(\mathbf{R}_i + c_i\mathbf{I}\right)\mathbf{W}_k\right) \geq \gamma_{th}\sigma_i^2 \qquad (6.23) \\ &\qquad\qquad \mathbf{W}_i \succeq 0 \\ &\qquad\qquad \mathbf{W}_i = \mathbf{W}_i^H, \quad \text{for } i = 1,\ 2,\ \cdots,\ K. \end{aligned}$$

Note that the optimization problem (6.23) is similar to the robust problem (6.2) except that the negative and positive diagonal loading factor c_i for $\mathbf{R}_i$ is determined from the statistical distribution of the elements of $\mathbf{E}_i$. When compared to the non-robust problem (6.4), (6.23) is different because of the positive and negative diagonal loadings of $\mathbf{R}_i$. This is an SDP problem which has linear objective, and linear and semidefinite constraints.

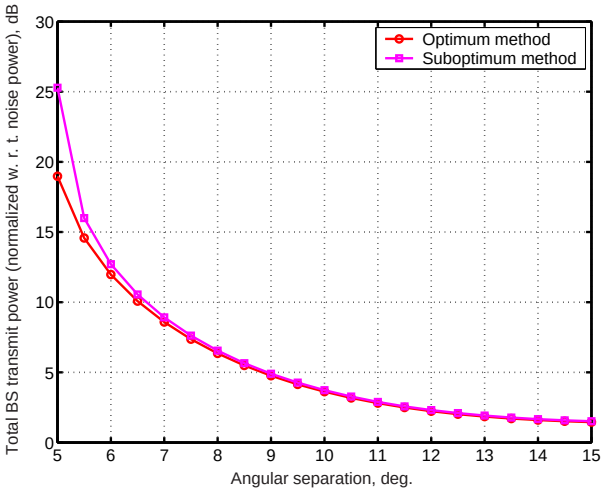

Figure 6.2: BS transmit power with the proposed suboptimum (6.23) and optimum (6.18) robust methods

As shown in Fig. 6.2, the proposed robust optimum method (6.18) performs better than the proposed suboptimum method (6.23) in terms of total BS transmission power. Fig. 6.3 displays the achieved non-outage probability versus the angular separation for the proposed optimum and suboptimum robust methods. Although both of the proposed methods achieve the target value of non-outage probability (which is set to 0.8) at the price of increase in the BS transmit power (see also Fig. 6.2), the suboptimum method achieves the non-outage probability that is higher than its target value. The computational cost of optimum method is much higher than that of the suboptimum method.

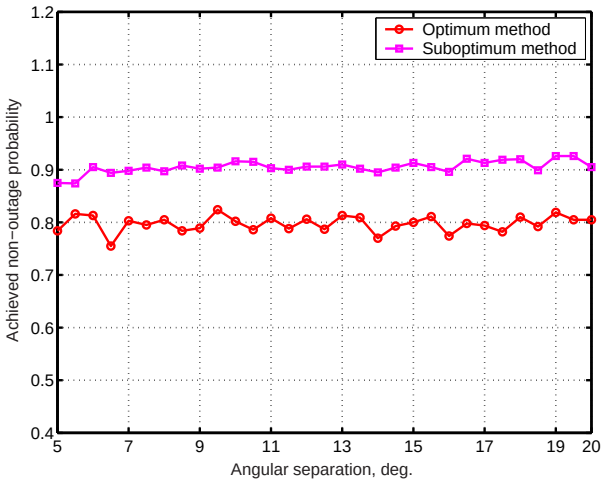

Figure 6.3: Achieved non-outage probability with the proposed suboptimum (6.23) and optimum (6.18) robust methods

While running MATLAB 6.01 in Pentium IV 1.8 GHz computer, the simulation time required for optimum method is almost three times that of the suboptimum method.

Lemma 2: There exists a rank 1 solution of $\mathbf{W}_i$ for the semidefinite relaxed problem of (6.23).

Proof: The proof of this lemma is given in **Lemma 2** of Chapter 5 for the special case of rank 1 spatial covariance matrices. Another type of proof for the case of general rank spatial covariance matrices can be found in [8] and [9]. We have found numerically that the optimum matrix $\mathbf{W}_i$ remains rank 1. This has been confirmed in all of our simulation scenarios.

6.4 Simulation Results

We illustrate the performance of the proposed downlink beamforming algorithm in a simulated scenario [8] as described in deterministic propagation of **Chapter 5**. We consider that three MSs are served by a single BS. One MS is located at $\theta_1 = 10^\circ$ relative array broadside and the two others at directions $\theta_{2,3} = 10^\circ \pm \delta$ where δ is varied from 1° to 50°. Thus the DoAs of two MSs is varied keeping that of the first MS fixed for all the simulations. We consider a ULA with $M = 8$ elements spaced at a distance of half a wavelength. For each DoA of the MSs, the non-outage probability is calculated using the results of 10,000 simulation runs. The threshold SINR for all MSs in the downlink is taken as 5 dB. The receiver noise power is $\sigma_i^2 = 1$ for all MSs. We use SeDuMi 1.02 [91] to solve the robust optimization problem of (6.18). Note that the spatial covariance matrix

$\mathbf{R}_i$ (see eqn. 5.2) is normalized. The target non-outage probability p_i, $(i = 1, \cdots, K)$ for all MSs is same, i.e. $p_1 = p_2 = \cdots, = p_K = p$.

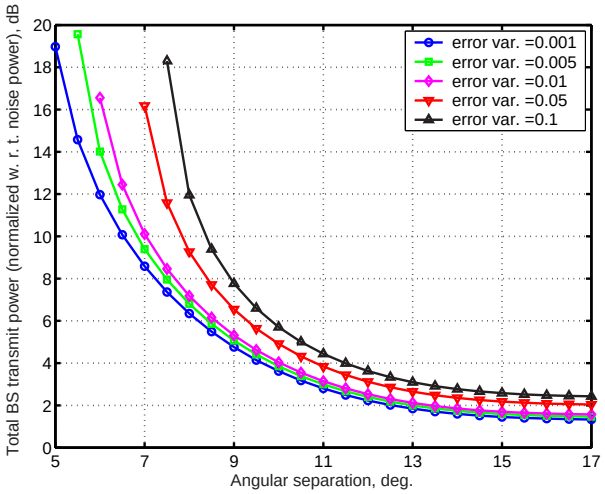

Figure 6.4: Total BS transmit power for the proposed robust optimum beamforming method (6.18)

Figure 6.4 shows the total BS transmit power versus angular separation δ for different values of the variance σ_e^2 of the elements of the uncertainty matrix $\mathbf{E}_i$. We take an angular spreading of 2° and keep the target non-outage probability to 0.8. For $\sigma_e^2 = 0.001$, the optimal solution (6.18) exists with $\delta \geq 5°$. It can be observed that as the variance σ_e^2 increases, the optimal solution exists only for increased values of δ. For example, for $\sigma_e^2 = 0.005$ and $\sigma_e^2 = 0.01$, the optimal solutions exist only for $\delta \geq 5.5°$ and $\delta \geq 6°$, respectively. For smaller values of δ, we can find that the BS transmit power increases with increasing σ_e^2. As an example, for $\sigma_e^2 = 0.001$, the BS needs about 8.6 dB of transmit power at an angular separation of $\delta = 7°$ in order to achieve target non-outage probability p of 0.8. With same $\delta = 7°$, for the case of $\sigma_e^2 = 0.05$, the BS needs transmit power of about 16.2 dB in order to keep the non-outage probability at 0.8. As δ increases, the transmit power curves for different values of σ_e^2 meet one another.

The total BS transmit power versus the angular separation δ for different target values of the non-outage probability p is shown in Fig. 6.5. We take $\sigma_e^2 = 0.001$. For a target non-outage probability $p = 0.51$, we can see that the optimum solution exists for $\delta \geq 3.5°$ with a BS transmit power of about 30 dB. As p increases, the angular separation δ needs to be increased in order to get the optimum solution. For $p = 0.9$, the optimum solution exists for $\delta \geq 5°$ with BS transmit power of about 25 dB. Again we can see that for a particular δ (especially smaller ones), as the target non-outage probability increases, the BS has to spend more transmit power.

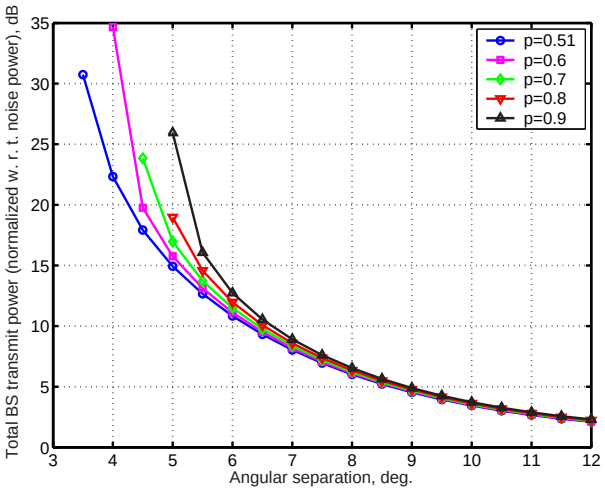

Figure 6.5: Total BS transmit power for the proposed beamforming method (6.18) with different p

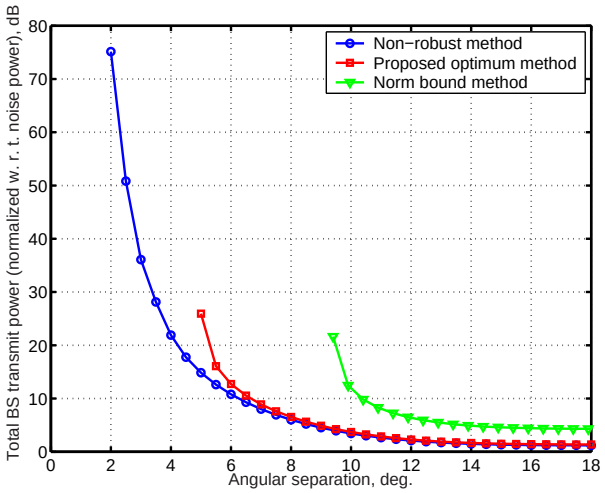

Figure 6.6: Comparison of BS transmit power with different beamforming methods

The BS transmit power versus the angular separation δ using different beamforming methods is shown in Fig. 6.6. The non-robust method (6.4) uses less transmit power than the other two methods and provides an optimal solution for $\delta \geq 2°$. The proposed optimum robust method (6.18) with $p = 0.9$ and $\sigma_e^2 = 0.001$ spends more transmit power than the non-robust method and the optimal solution exists only for $\delta \geq 5°$. The norm bound method (6.2) for which the maximum Frobenius norm of $\mathbf{E}_i$ with $\sigma_e^2 = 0.001$ is experimentally chosen as 0.5 needs more transmit power than the other two methods. As an example for $\delta = 10°$, the non-robust and the proposed method need less than 4 dB of transmit power whereas the norm bound method uses about 12 dB. The optimal solution for the norm bound method exists only for $\delta \geq 9.4°$.

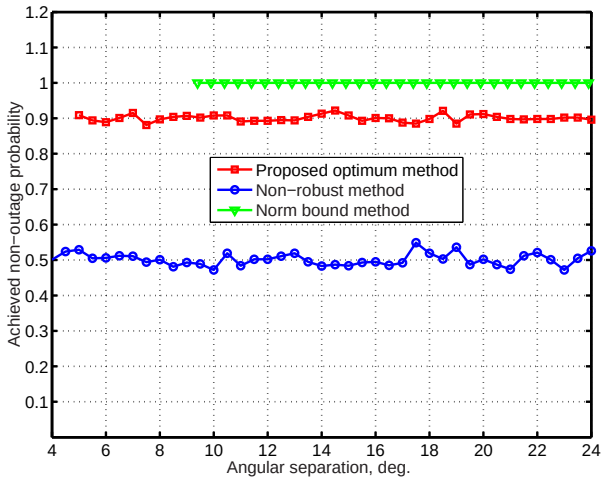

Figure 6.7: Non-outage probability (second MS) with different beamforming methods

As shown in Fig. 6.7, although the non-robust method (6.4) shows the best performance in terms of transmit power, it never achieves the target $p = 0.9$. It can be seen that with the non-robust method the SINR value of the MS remains above the target threshold value γ_{th} with a probability of less than 0.5. This means that the achieved non-outage probability is much less than the target non-outage probability $p = 0.9$. However, the proposed optimum robust method (6.18) always achieves the target $p = 0.9$ by using some more BS transmit power than the non-robust method. The norm bound method (6.2) always maintains the target p to a value of 1, but it uses BS transmit power which is many times higher than that of the non-robust and the proposed methods. Thus the proposed method performs better in terms of achieved non-outage probability while an acceptable compromise with the total BS transmit power is made.

6.5 Summary

We propose a new robust downlink beamforming method based upon minimization of the total BS transmit power while keeping the non-outage probability of all the MSs in the downlink above a threshold value. Our approach leads to a relaxation of a Semidefinite optimization problem that can be solved efficiently using the available optimization toolboxes like SeDuMi 1.02. Simulation results show that our method is robust against the uncertainties of the spatial covariance matrix, although this robustness is achieved with a slight increase in the BS transmit power when compared to the non-robust method. Although non-robust method requires least transmit power, its performance in terms of achieved non-outage probability is worse than that of the proposed robust optimum

method. On the other hand, the norm bound method (based upon worst-case performance optimization) achieves best non-outage probability but needs very high transmission power. Moreover, the computational complexity of our approach is similar to that of the norm bound method. As a part of the future work we are trying to evaluate the performance of downlink beamforming based upon non-outage probability criterion for the UMTS-FDD scenario using a dynamic system level simulator of [18].

Chapter 7

Robust MIMO Design and Optimum Power Control for MIMO Beamforming

In this chapter we first analyze a single user MIMO link where the transmitter has only partial information about the channel. A transmitter which is robust against the errors in the available channel estimate is designed for such a MIMO space diversity system. The design is based on the minimization of the outage probability while keeping the total transmit power constant. This leads to an exploitation of all eigenmodes of the estimated MIMO channel by the transmitter whereas in classical beamforming only the strongest eigenmode of the MIMO channel is used for transmission. We compare the performance of our method with that of the robust MIMO design based upon worst-case performance optimization [58]. Simulation results confirm that the proposed method outperforms the worst-case performance optimization method. Moreover, the proposed technique avoids the necessity to know the norm bound of the error in channel estimate that is required for worst-case performance optimization.

The second part of this chapter is extended to a multiuser MIMO system with beamforming. The analysis is carried out for a MRT system in a Rayleigh fading environment. A simple closed and compact form expression for the outage probability of the downlink of such a system is obtained by considering the scenario where a MS of interest receives the signals transmitted from the BS to other MSs of the same cell. This is known as intracell interference. An interesting observation of the analysis is that an optimum power control problem can be formulated based upon the outage probability of each user in the

downlink because the outage probability computation can easily be simplified for a single cell environment. The optimization problem is non-convex and non-linear. We show how the Evolutionary Strategy (EV)[85](see Appendix 9.5) can be used to solve such a non-convex problem.

7.1 Introduction

Although initial interest in SAs has mainly focused on receiver diversity, nowadays MIMO systems with both transmit and receive diversity are receiving a lot of attention. Recently, the proposal of several transmission schemes [35, 95] based on multiple antennas at both the transmitter and the receiver has been introduced in order to improve the system performance of wireless communication systems significantly. Wireless MIMO systems are able to provide a high spectral efficiency in a rich and quasi-static scattering environment. They combine the signals received from multiple independent channels to mitigate fading and suppress interference.

Space-time block codes [93] and linear processing or beamforming are some of the transmission techniques used for MIMO systems. The former is used if no CSI is available at the transmitter and the latter is used when the transmitter knows the channel. Zhou et. al [108] proposed the combination of eigen-beamforming and space-time block coding for the design of an optimal transmitter. In a realistic environment, the transmitter has only an estimate of the channel [107] and hence if this estimate deviates far from the actual channel, the performance in terms of BER or capacity degrades significantly. Therefore so-called robust techniques are necessary in order to take into account the errors in the channel estimate. A robust MIMO design which combines OSTBC and beamforming with minimum transmission power requirements is proposed in [58]. This approach is based on maximization of the SNR for the worst channel estimate and needs to clearly define the upper bound of the channel estimate error. In this robust transmitter design, a random error with bounded norm is added to the available channel estimate. In wireless systems, it is not practical to find the upper bound of the norm of this channel estimation error. As the channel varies randomly, it is logical to use the statistical distribution of the estimation error. Robust uplink and downlink beamforming methods based on outage probability were proposed in **Chapters 5, 6**. In this chapter, we use a similar approach for the MIMO transmission.

Power control for interference limited wireless systems with single transmit and single receive antennas has been proposed in [63] where the total transmit power is minimized subject to outage probability constraints. A scheme which couples power control with a minimum outage probability receiver is proposed in [74]. It extends the results of [63] by finding tight bounds for the outage probability that also includes receiver noise. However, both of the previous works [63, 74] are limited to multiuser wireless systems with single antennas at the receivers and transmitters, respectively. A simple and popular scheme called MRT [68] maximizes the system output SNR in MIMO systems. An outage probability expression for MRT based multi-cellular MIMO systems was derived in [96]. The outage probability expression was derived by considering equal power intracell interferers and intercell interferers with distinct powers for the uplink which is not the case in a realistic system. In a realistic scenario, the MSs that are power controlled by the same BS transmit with different powers because of the different channel gains. Moreover, an optimum power control scheme based on this outage probability becomes highly complicated. In this work, we consider a downlink of MRT based multiuser MIMO system. First, we derive a simple expression for outage probability of a MS in the downlink and then formulate an optimum power control problem based on outage probability constraints. The objective is to minimize the total BS transmit power by keeping the outage probability of all MSs in the system below a certain threshold value. Although, this optimization problem is nonlinear and non-convex, stochastic ranking based on EV [85] can be used to solve it efficiently.

The chapter is organized as follows. A robust MIMO transmitter for a single user system is presented in Section 7.2. Here, we describe the system and signal models for the single user transmission, the Maxmin robust design proposed in [58] and finally our formulation of the robust MIMO design based upon minimization of the outage probability. In Section 7.3, a multiuser MIMO system with beamforming is presented. We first provide preliminaries for MIMO system with beamforming, then the outage probability of a MS in the downlink is investigated, and finally a power control scheme is formulated based on this outage probability. Section 7.4 presents simulation results for a single user MIMO system, where the performance of the proposed method is compared with the robust Maxmin approach based upon worst-case performance optimization. In Section 7.5, simulation results for multiuser MIMO beamforming are presented in order to compare with analytical results. The results for the optimum power for the constrained optimization

problem are also discussed. Finally, the chapter is summarised in Section 7.6.

7.2 Robust MIMO Transmitter

7.2.1 System and Signal Models

We consider a single user flat fading spatially uncorrelated Rayleigh MIMO channel with n_t transmit and n_r receive antennas. The channel response matrix $\mathbf{H} \in \mathcal{C}^{n_r \times n_t}$ consists of independent, complex and circularly symmetric Gaussian random variables with zero mean and unknown variance $\tilde{\sigma_h^2}$. The gain factor between the jth transmit and ith receive antenna is represented by the (i, j)th component of the random matrix $\mathbf{H}$. It is assumed that the transmitter knows the channel matrix $\mathbf{H}$ with a certain uncertainty according to the following model: $\mathbf{H} = \hat{\mathbf{H}} + \mathbf{E} \in \mathcal{C}^{n_r \times n_t}$, where the channel estimate $\hat{\mathbf{H}}$ (elements are complex i.i.d. Gaussian with known variance σ_h^2) is availabe at the transmitter and $\mathbf{E}$ represents the error in the channel estimate. The elements of $\mathbf{E}$ are also i.i.d. complex, circularly symmetric Gaussian random variables with variance σ_e^2 and independent from $\mathbf{H}$. In the absence of CSI at the transmitter, it is possible to achieve

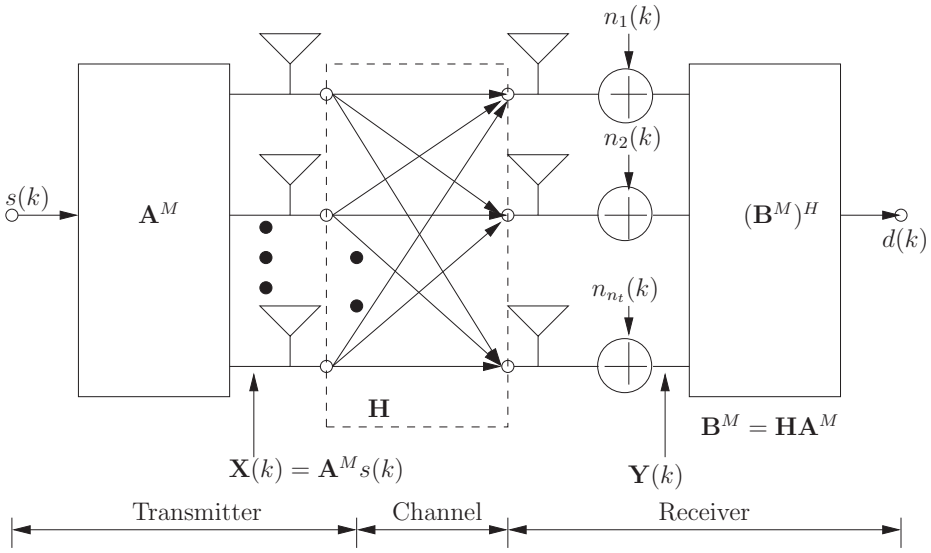

Figure 7.1: Matrix modulation and matched filter

transmit diversity by transmitting the same symbol $s(k)$ during n_t channel periods using different transmission weight vectors $\{\mathbf{a}_n\}_{n=1}^{n_t}$. The matrix $\mathbf{A}^M = [\mathbf{a}_1, \cdots, \mathbf{a}_{n_t}]$ in this case is known as a modulation matrix, upon which the transmission is based as shown in Fig. 7.1. This transmission technique is perhaps one of the simplest examples [65] of a linear Space-Time Block Codes (STBC). A linear STBC code matrix takes the following

form:

$$\mathbf{X}' = \sum_{q=1}^{N_s} (\bar{s}_q \mathbf{A}'_q + \mathrm{j}\tilde{s}_q \mathbf{B}'_q), \tag{7.1}$$

where $\{s_1, \cdots, s_{N_s}\}$ is a set of complex symbols to be transmitted, N_s is the total number of symbols, and $\left\{\mathbf{A}'_q, \mathbf{B}'_q\right\}$ are in general fixed complex-valued code matrices of dimension $n_t \times N_T$ where N_T is the number of time intervals. Note that $\bar{s}_q$ and $\tilde{s}_q$ are the real and imaginary parts of the symbol s_q. It can be easily seen that for the transmission structure of Fig. 7.1, we have $N_s = 1$, $\mathbf{A}'_1 = \mathbf{A}^M$ and $\mathbf{B}'_1 = \mathbf{A}^M$.

In order to transmit a symbol $s(k)$, the following signal is transmitted; $\mathbf{X}(k) = \mathbf{A}^M s(k)$, where the matrix $\mathbf{A}^M \in \mathcal{C}^{n_t \times n_t}$ contains the factors that multiply the symbol $s(k)$ before the signal is transmitted through n_t transmit antennas during n_t channel uses. The received samples at all the receive antennas during n_t periods of time corresponding to transmission of the symbol $s(k)$ is expressed as

$$\mathbf{Y}(k) = \left\{\mathbf{H}\mathbf{A}^M s(k) + \mathbf{N}(k)\right\} \in \mathcal{C}^{n_r \times n_t}, \tag{7.2}$$

where $\mathbf{N}(k)$ has i.i.d. complex Gaussian random variables with zero mean and variance σ_n^2 and represents an additive white Gaussian noise channel. It is assumed that the receiver knows perfectly the channel matrix $\mathbf{H}$ and the transmitter type i. e. matrix $\mathbf{A}^M$. In this context, the optimum receiver is the matched filter which carries out the detection based on the following statistic; $d(k) = \mathrm{tr}((\mathbf{B}^M)^H \mathbf{Y})$, where $\mathbf{B}^M = \mathbf{H}\mathbf{A}^M$, which can be expressed as

$$d(k) = \mathrm{tr}((\mathbf{A}^M)^H \mathbf{H}^H \mathbf{H} \mathbf{A}^M) s(k) + \mathrm{tr}((\mathbf{A}^M)^H \mathbf{H}^H \mathbf{N}(k)). \tag{7.3}$$

This receiver maximizes the received SNR which is given by [58]

$$\mathrm{SNR} = \frac{\sigma_s^2}{\sigma_n^2} \mathrm{tr}((\mathbf{A}^M)^H \mathbf{H}^H \mathbf{H} \mathbf{A}^M), \tag{7.4}$$

where $\sigma_s^2 = E(s(k)s^*(k))$ and $\sigma_n^2 \mathbf{I} = E(\mathbf{N}(k)\mathbf{N}(k)^H)$ represent the symbol and correlation matrix of the noise, respectively. The power constraint in terms of the modulation matrix $\mathbf{A}^M \in \mathcal{C}^{n_t \times n_t}$ is $||\mathbf{A}^M||^2 = \mathrm{tr}((\mathbf{A}^M)^H \mathbf{A}^M) = P_t$. We use the same transmitter structure as of [58] and thus $\mathbf{A}^M$ is forced to have the following structure

$$\begin{aligned} \mathbf{A}^M &= \sqrt{P_t} \sum_{n=1}^{n_t} \sqrt{p_n} \hat{\mathbf{u}}_n \mathbf{c}_n^H \\ &= \sqrt{P_t} \hat{\mathbf{U}} \mathbf{P} \mathbf{C}^H, \end{aligned} \tag{7.5}$$

where

$$\hat{\mathbf{H}}^H\hat{\mathbf{H}} = \hat{\mathbf{U}}\mathbf{D}\hat{\mathbf{U}}^H, \quad \hat{\mathbf{U}}^H\hat{\mathbf{U}} = \mathbf{I}, \quad \hat{\mathbf{U}} = [\hat{\mathbf{u}}_1, \cdots, \hat{\mathbf{u}}_{n_t}]$$
$$\mathbf{D} = \text{diag}(\lambda_1, \cdots, \lambda_{n_t}), \quad \lambda_1 \geq \cdots \geq \lambda_{n_t} \geq 0$$
$$\mathbf{P} = \text{diag}(\sqrt{p_1}, \cdots, \sqrt{p_{n_t}}), \quad \mathbf{C}^H\mathbf{C} = \mathbf{I}. \tag{7.6}$$

It can be observed from (7.5) and (7.6) that different eigenmodes of the estimated channel are used for signal transmission. $\hat{\mathbf{U}}$ represents the matrix of eigenvector obtained from the eigenvalue decomposition of $\hat{\mathbf{H}}^H\hat{\mathbf{H}}$ and $\mathbf{D}$ is the diagonal matrix (note the notation 'diag') with corresponding eigenvalues. A set of n_t orthonormal temporal signatures $\mathbf{c}_n \in \mathcal{C}^{n_t \times 1}, \quad n = 1, \cdots, n_t$ decouple the transmission and form the unitary matrix $\mathbf{C} = [\mathbf{c}_1, \cdots, \mathbf{c}_{n_t}]$. The powers ($p_n \geq 0, \quad n = 1, \cdots, n_t$) are used to weight different eigenmodes. With this transmission scheme, the SNR from (7.4) can be expressed as

$$\text{SNR} = P_t\frac{\sigma_s^2}{\sigma_n^2}\text{tr}(\hat{\mathbf{U}}^H\mathbf{H}^H\mathbf{H}\hat{\mathbf{U}}\mathbf{P}^2), \tag{7.7}$$

with the power constraint $\sum_{n=1}^{n_t} p_n = 1$. As can be seen from this signal model, n_t channel uses or periods are needed to transmit a single symbol. This means that there is a reduction of the useful signal rate by a factor of n_t. If a full rate transmission system is required, then n_t different symbols $\{s_n(k)\}_{n=1}^{n_t}$ have to be transmitted simultaneously, according to the following scheme

$$\mathbf{X}(k) = \sum_{n=1}^{n_t}\mathbf{A}_n^M s_n(k) = \sqrt{P_t}\sum_{n=1}^{n_t}\hat{\mathbf{U}}\mathbf{P}\mathbf{C}_n^H s_n(k)$$
$$= \sqrt{P_t}\hat{\mathbf{U}}\mathbf{P}\underbrace{\sum_{n=1}^{n_t}\mathbf{C}_n^H s_n(k)}, \tag{7.8}$$

where the same importance is given to the estimated eigenmodes for all the symbols, but different temporal signatures are applied. It is clear that the problem consists in decoupling the detection of the symbols at the receiver without decreasing the SNR. In case of real constellations, this can be done by using unitary matrices deduced for OSTBC [38, 93]. Note that, an OSTBC is a linear STBC (see eq: 7.1) that has the following unitary property

$$\mathbf{X}'\mathbf{X}'^H = \sum_{q=1}^{N_s}|s_q|^2 \cdot \mathbf{I}, \tag{7.9}$$

where the identity matrix on the right hand side of (7.9) can be scaled by an arbitrary constant factor. However, only a 1/2 rate transmission can be achieved for any number of transmit antennas for the case of complex symbols. The underbraced term on the right hand side of (7.8) can be obtained by using the code matrix $\mathbf{X}'$ that can be expressed as (7.1) and fulfills the property (7.9). Therefore, the transmitter architecture presented in this section is based on concatenation of an OSTBC and a set of n_t beamformers [60, 107], each one corresponding to an eigenmode of the estimated channel and applied to an output of the OSTBC as shown in Fig. 7.2.

If the channel estimate is perfect i.e. the uncertainty $\mathbf{E}$ is negligible to have $\mathbf{H} = \hat{\mathbf{H}}$, a non-robust classical design is obtained. The SNR (7.7) in this case can be simply expressed as

$$\begin{aligned} \text{SNR} &= P_t \frac{\sigma_s^2}{\sigma_n^2} \text{tr}(\hat{\mathbf{U}}^H \hat{\mathbf{H}}^H \hat{\mathbf{H}} \hat{\mathbf{U}} \mathbf{P}^2) \\ &= P_t \frac{\sigma_s^2}{\sigma_n^2} \sum_{n=1}^{n_t} \lambda_n p_n. \end{aligned} \tag{7.10}$$

Here, the power distribution among the eigenmodes is optimized in order to maximize the SNR. Therefore, the non-robust optimization problem can be formulated as

$$\begin{aligned} &\max_{\mathbf{p}} \lambda^T \mathbf{p} \\ &\text{subject to } \sum_{n=1}^{n_t} p_n = 1, \quad p_n \geq 0 \end{aligned} \tag{7.11}$$

where $\lambda^T = (\lambda_1, \cdots, \lambda_{n_t})$, and $\mathbf{p} = (p_1, \cdots, p_{n_t})^T$. The solution of this constrained optimization problem is $p_1 = 1$ and $p_n = 0$, $\forall n > 1$, corresponds to classical beamforming in which no space-time coding is applied. When compared to combined OSTBC and beamforming transmission [108], this is a transmission scheme in which only the first output of the OSTBC is transmitted via the strongest eigenmode of the MIMO channel estimate.

7.2.2 Maxmin Robust Approach

This section briefly deals with the robust method [58] for the design of the power parameters p_n, $n = 1...n_t$ under a maximin perspective. The objective is to first find the worst channel that minimizes the SNR for a fixed power distribution and then to maximize the SNR for this worst channel by designing the power parameters adequately. Thus

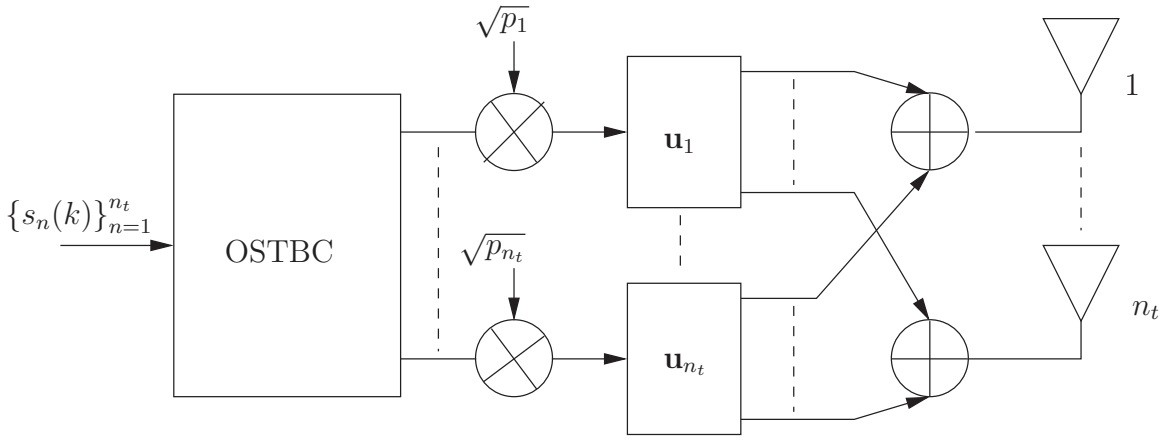

Figure 7.2: Transmission scheme with OSTBC and beamforming [58]

the performance i.e. SNR is maximized according to worst-case scenario. The problem formulation is repeated here as

$$\max_{\mathbf{P}} \min_{||\mathbf{E}|| \leq \sqrt{\epsilon}} \text{tr}(\hat{\mathbf{U}}^H \mathbf{H}^H \mathbf{H} \hat{\mathbf{U}} \mathbf{P}^2), \tag{7.12}$$

where $||\mathbf{E}||^2 \leq \epsilon$ represents that Frobenius norm of the error matrix is upper-bounded with a positive constant ϵ. According to the result of [58], the Maxmin problem of (7.12) is changed to the following convex optimization

$$\begin{aligned} &\max_{\mathbf{p}} \left\{ \lambda^T \mathbf{p} - 2\sqrt{\epsilon} ||\mathbf{Q}\mathbf{p}|| \right\} \\ &\text{subject to} \quad \sum_{n=1}^{n_t} p_n = 1, \quad p_n \geq 0, \end{aligned} \tag{7.13}$$

where matrix $\mathbf{Q}^H$ is constructed by choosing only the rows $1+n(1+n_t),\ n = 0, \cdots, n_t - 1$ of $\hat{\mathbf{U}}^T \otimes \left(\hat{\mathbf{U}}^H \hat{\mathbf{H}}^H \right)$. Here $\otimes$ represents the 'Kronecker' product.

7.2.3 Minimum Outage Probability Approach

In this section we propose a design of a robust MIMO transmitter based on the outage probability which is defined as the probability that the received SNR falls below the threshold value γ_0. The objective is to minimize the outage probability under the condition that the power constraint is satisfied at the transmitter. Mathematically, the problem can be formulated as

$$\begin{aligned} &\min_{p_n} \left(P_{\text{out}}(\gamma_0) = \text{pr}(\text{SNR} \leq \gamma_0) \right) \\ &\text{subject to} \ \sum_{n=1}^{n_t} p_n = 1. \end{aligned} \tag{7.14}$$

Omitting the constant term $P_t\frac{\sigma_s^2}{\sigma_n^2}$, the expression for the SNR (7.7) can be further expressed as

$$\begin{aligned}\text{SNR} &= \text{tr}(\hat{\mathbf{U}}^H\hat{\mathbf{H}}^H\hat{\mathbf{H}}\hat{\mathbf{U}}\mathbf{P}^2) + \text{tr}(\hat{\mathbf{U}}^H\hat{\mathbf{H}}^H\mathbf{E}\hat{\mathbf{U}}\mathbf{P}^2) + \\ &\quad \text{tr}(\hat{\mathbf{U}}^H\mathbf{E}^H\hat{\mathbf{H}}\hat{\mathbf{U}}\mathbf{P}^2) + \text{tr}(\hat{\mathbf{U}}^H\mathbf{E}^H\mathbf{E}\hat{\mathbf{U}}\mathbf{P}^2), \end{aligned} \tag{7.15}$$

where the quadratic term of the error $\mathbf{E}$ in the channel estimate is negligible for the usual values of σ_h^2 and σ_e^2. Noting that $\text{Re}\left(\text{tr}(\hat{\mathbf{U}}^H\hat{\mathbf{H}}^H\mathbf{E}\hat{\mathbf{U}}\mathbf{P}^2)\right) = \text{Re}\left(\text{tr}(\hat{\mathbf{U}}^H\mathbf{E}^H\hat{\mathbf{H}}\hat{\mathbf{U}}\mathbf{P}^2)\right)$ and $\text{Im}\left(\text{tr}(\hat{\mathbf{U}}^H\hat{\mathbf{H}}^H\mathbf{E}\hat{\mathbf{U}}\mathbf{P}^2)\right) = -\text{Im}\left(\text{tr}(\hat{\mathbf{U}}^H\mathbf{E}^H\hat{\mathbf{H}}\hat{\mathbf{U}}\mathbf{P}^2)\right)$, and considering that the other terms of (7.15) are real, the expression (7.14) for outage probability can be written as

$$\begin{aligned}P_{\text{out}}(\gamma_0) &= \text{pr}\left(b\text{tr}(\hat{\mathbf{U}}^H\hat{\mathbf{H}}^H\hat{\mathbf{H}}\hat{\mathbf{U}}\mathbf{P}^2) + 2b\text{tr}(\hat{\mathbf{U}}^H\hat{\mathbf{H}}^H\mathbf{E}\hat{\mathbf{U}}\mathbf{P}^2) \leq \gamma_0\right) \\ &= \text{pr}\left(\text{tr}(\hat{\mathbf{U}}^H\hat{\mathbf{H}}^H\mathbf{E}\hat{\mathbf{U}}\mathbf{P}^2) \leq \frac{\gamma_0 - b\text{tr}(\mathbf{D}\mathbf{P}^2)}{2b}\right), \end{aligned} \tag{7.16}$$

where $\mathbf{D} = \hat{\mathbf{U}}^H\hat{\mathbf{H}}^H\hat{\mathbf{H}}\hat{\mathbf{U}}$, $b = P_t\frac{\sigma_s^2}{\sigma_n^2}$ and $\text{tr}(\hat{\mathbf{U}}^H\hat{\mathbf{H}}^H\mathbf{E}\hat{\mathbf{U}}\mathbf{P}^2) = \text{Re}\left(\text{tr}(\hat{\mathbf{U}}^H\hat{\mathbf{H}}^H\mathbf{E}\hat{\mathbf{U}}\mathbf{P}^2)\right)$. Let us define a random variable

$$\begin{aligned}y &= \text{tr}(\hat{\mathbf{U}}^H\hat{\mathbf{H}}^H\mathbf{E}\hat{\mathbf{U}}\mathbf{P}^2) \\ &= \text{tr}(\hat{\mathbf{U}}\mathbf{P}^2\hat{\mathbf{U}}^H\hat{\mathbf{H}}^H\mathbf{E}), \end{aligned} \tag{7.17}$$

where $\mathbf{E}$ is the random matrix and all other matrices are deterministic because the channel estimate $\hat{\mathbf{H}}$ is available at the transmitter.

Using the result of **Lemma 1 (Chapter 5)**, we can write $y \sim \text{N}(0, \sigma_e^2||\hat{\mathbf{U}}\mathbf{P}^2\hat{\mathbf{U}}^H\hat{\mathbf{H}}^H||^2)$ i. e. y is a Gaussian distributed random variable with zero mean and variance $\sigma_e^2||\hat{\mathbf{U}}\mathbf{P}^2\hat{\mathbf{U}}^H\hat{\mathbf{H}}^H||^2$. The outage probability can thus be written as

$$\begin{aligned}P_{\text{out}}(\gamma_0) &= \text{pr}\left(y \leq \frac{\gamma_0 - b\text{tr}(\mathbf{D}\mathbf{P}^2)}{2b}\right) \\ &= \int_{-\infty}^{\frac{\gamma_0 - b\text{tr}(\mathbf{D}\mathbf{P}^2)}{2b}} \frac{1}{\sqrt{2\pi}\sigma_y}\exp\left(-\frac{y^2}{2\sigma_y^2}\right)\,dy, \end{aligned} \tag{7.18}$$

where $\sigma_y = \sigma_e||\hat{\mathbf{U}}\mathbf{P}^2\hat{\mathbf{U}}^H\hat{\mathbf{H}}^H||$. With the help of error function

$$\text{erf}(z) = \frac{2}{\sqrt{\pi}}\int_0^z \exp\left(-u^2\right)\,du, \tag{7.19}$$

the outage probability can be expressed as

$$P_{\text{out}}(\gamma_0) = \begin{cases} \frac{1}{2} + \frac{1}{2}\text{erf}\left(\frac{\gamma_0 - b\text{tr}(\mathbf{D}\mathbf{P}^2)}{2\sqrt{2}\sigma_e||\hat{\mathbf{U}}\mathbf{P}^2\hat{\mathbf{U}}^H\hat{\mathbf{H}}||b}\right), & \text{for } \gamma_0 \geq b\text{tr}(\mathbf{D}\mathbf{P}^2), \\ \frac{1}{2} - \frac{1}{2}\text{erf}\left(\frac{b\text{tr}(\mathbf{D}\mathbf{P}^2) - \gamma_0}{2\sqrt{2}\sigma_e||\hat{\mathbf{U}}\mathbf{P}^2\hat{\mathbf{U}}^H\hat{\mathbf{H}}||b}\right), & \text{for } \gamma_0 \leq b\text{tr}(\mathbf{D}\mathbf{P}^2) \end{cases} \tag{7.20}$$

Using the following property of the error function; $\text{erf}(-z) = -\text{erf}(z)$, the upper equation of (7.20) can be changed into lower equation and vice-versa. Note that for a reliable link in a wireless communication system, the outage probability $P_{\text{out}}(\gamma_0)$ must be close to zero. The objective is now to find out the diagonal matrix $\mathbf{P}$ that minimizes the outage probability (lower equation of (7.20)) with the power constraint. It can be observed that $P_{\text{out}}(\gamma_0)$ with respect to $\mathbf{P}$ approaches its minimum value of zero, when erf( ) of (lower equation of (7.20)) takes the value of 1. This means the argument of the error function erf( ) must tend to infinity which is made possible by maximizing its numerator and keeping its denominator to a constant value. The minimization problem after substituting $\mathbf{P}' = \mathbf{P}^2$ into the lower equation of (7.20) is expressed as

$$\begin{aligned} &\min_{\mathbf{P}'} \left(\frac{\gamma_0}{b} - \text{tr}(\mathbf{D}\mathbf{P}')\right) \\ &\text{subject to} \quad ||\hat{\mathbf{U}}\mathbf{P}'\hat{\mathbf{U}}^H\hat{\mathbf{H}}|| = \frac{1}{2\sqrt{2}\sigma_e} \\ &\qquad\qquad \text{tr}(\mathbf{P}') = 1, \end{aligned} \tag{7.21}$$

where $\mathbf{P}' = \text{diag}(p_1, \cdots, p_{n_t})$. Since $\mathbf{P}'$ and $\mathbf{D}$ are both diagonal matrices, the optimization problem can be rewritten as

$$\begin{aligned} &\min_{\mathbf{p}} \tilde{\lambda}^T\mathbf{p} \\ &\text{subject to} \quad ||\hat{\mathbf{U}}^H\hat{\mathbf{H}}^H\hat{\mathbf{U}}\mathbf{P}'|| = \frac{1}{2\sqrt{2}\sigma_e} \\ &\qquad\qquad \sum_{n=1}^{n_t} p_n = 1, \end{aligned} \tag{7.22}$$

where $\tilde{\lambda} = \left(\frac{\gamma_0}{b} - \lambda_1, \cdots, \frac{\gamma_0}{b} - \lambda_{n_t}\right)$. This is a convex optimization problem with a linear objective, and equality constraints that are non-linear and linear in optimization variable $\mathbf{p}$, respectively. It can be solved using iterative and powerful algorithms such as the interior point methods [15].

7.3 Multiuser MIMO

7.3.1 Background

We consider a cellular system with a single cell having a BS with n_t antenna elements. The BS serves K MSs each having n_r antenna elements. A flat fading spatially uncorrelated Rayleigh MIMO channel is considered for the downlink communication between the BS and MSs. The channel response matrix $\mathbf{H} \in \mathcal{C}^{n_r \times n_t}$ consists of the components that

are i.i.d. complex and circularly symmetric Gaussian random variables with zero mean and variance σ_h^2. The gain factor between the jth transmit and ith receive antenna is represented by the (i, j)th component of the random matrix $\mathbf{H}$. As shown in the block

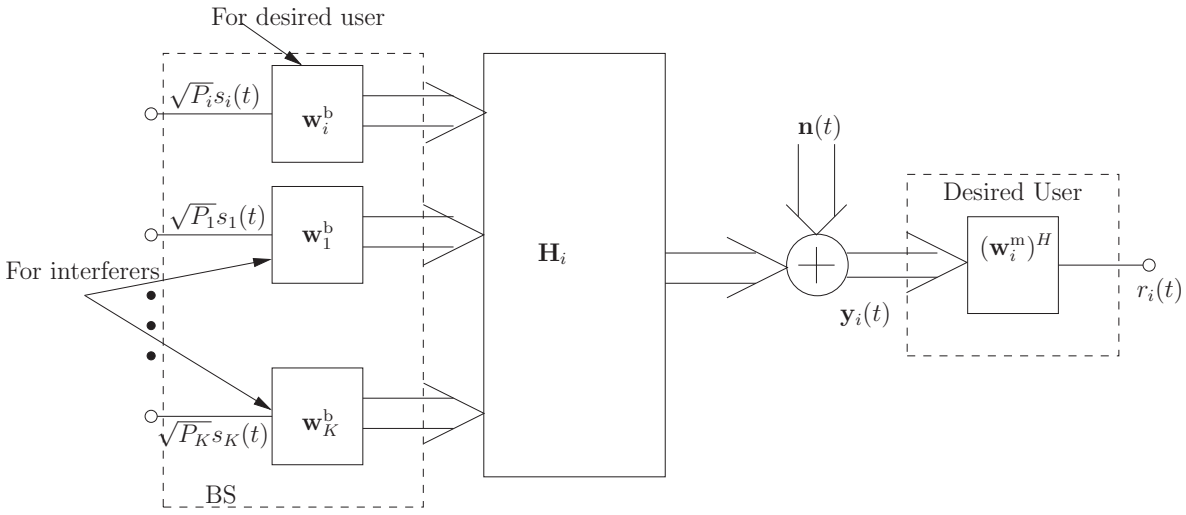

Figure 7.3: Downlink beamforming for a MIMO system

diagram (Fig. 7.3) of downlink beamforming for a MIMO system, the received signal at the ith desired MS is given by

$$\mathbf{y}_i(t) = \sqrt{P_i}\mathbf{H}_i\mathbf{w}_i^{\mathrm{b}}s_i(t) + \sum_{k=1,\ k\neq i}^{K} \sqrt{P_k}\mathbf{H}_i\mathbf{w}_k^{\mathrm{b}}s_k(t) + \mathbf{n}(t), \tag{7.23}$$

where $\mathbf{H}_i \in \mathcal{C}^{n_r \times n_t}$ is the channel matrix between the BS and ith MS, $\mathbf{w}_i^b \in \mathcal{C}^{n_t \times 1}$ is the beamforming vector used by the BS for ith MS, P_i is the total power transmission to i th MS and $s_i(t)$ is the information signal intended for ith MS, where $i = 1, \cdots, K$. It is assumed that the channel matrices $\mathbf{H}_i,\ i = 1, \cdots, K$, are independent from each other. The ith MS weights the signal received at each of its antennas with elements of the vector $\mathbf{w}_i^m \in \mathcal{C}^{1 \times n_r}$ and combines the resulting output (see Fig. 7.4) to give the following signal

$$r_i(t) = (\mathbf{w}_i^{\mathrm{m}})^H\mathbf{y}_i(t), \tag{7.24}$$

where $\mathbf{w}_i^{\mathrm{m}} \in \mathcal{C}^{n_r \times 1}$ indicates beamforming vector used by MS. Using (7.23) and (7.24), the received signal after beamforming at ith MS is

$$r_i(t) = \sqrt{P_i}(\mathbf{w}_i^{\mathrm{m}})^H\mathbf{H}_i\mathbf{w}_i^{\mathrm{b}}s_i(t) + \sum_{k=1,\ k\neq i}^{K} \sqrt{P_k}(\mathbf{w}_i^{\mathrm{m}})^H\mathbf{H}_i\mathbf{w}_k^{\mathrm{b}}s_k(t) + (\mathbf{w}_i^m)^H\mathbf{n}(t), \tag{7.25}$$

where first term of the right-hand side represents the desired signal and the other two terms contribute to interference and noise, respectively. We assume that the BS transmits

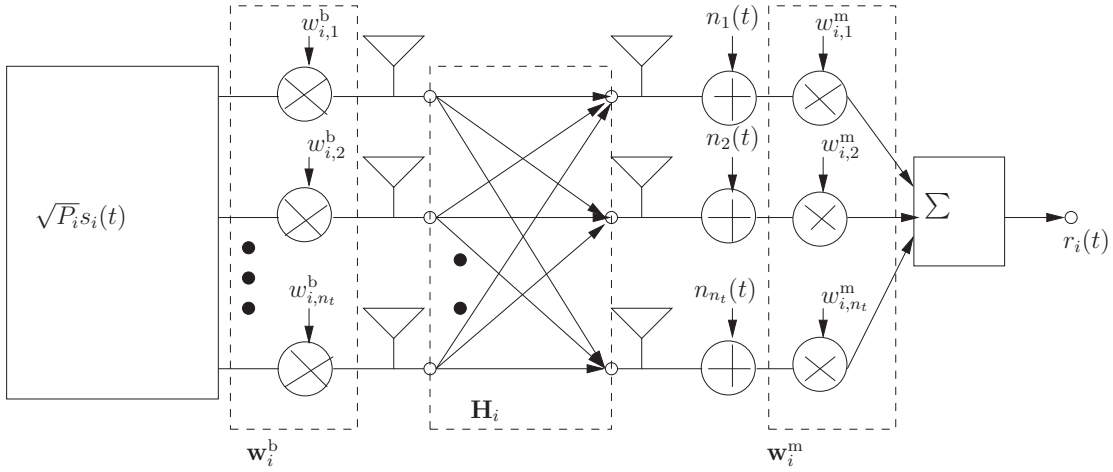

Figure 7.4: Beamforming for a desired user

statistically independent information bearing signals $s_i(t)$ with average power given by $\mathrm{E}(s_i(t)s_i(t)^*) = 1$. Thus signal power S and interference power I are written as

$$S = P_i|(\mathbf{w}_i^{\mathrm{m}})^H \mathbf{H}_i \mathbf{w}_i^{\mathrm{b}}|^2 \tag{7.26}$$

$$I = \sum_{k=1,\ k\neq i}^{K} P_k|(\mathbf{w}_i^{\mathrm{m}})^H \mathbf{H}_i \mathbf{w}_k^{\mathrm{b}}|^2. \tag{7.27}$$

The singular value decomposition of $\mathbf{H}_i$ allows us to write the channel matrix as $\mathbf{H}_i = \sum_{r=1}^{R} \sigma_i^r \mathbf{u}_i^r (\mathbf{v}_i^r)^H$, where R is the rank of the matrix $\mathbf{H}_i$, σ_i^r are singular values, $\mathbf{u}_i^r$ and $\mathbf{v}_i^2$ are left and right singular vectors, respectively. In a MRT system, the beamforming vectors at the BS and MSs are selected in order to maximize the SINR. In this case the optimum beamforming vectors are the largest left and right singular vectors of the channel matrix $\mathbf{H}_i$, i. e. $\mathbf{w}_i^{\mathrm{m}} = \mathbf{u}_i^1$ and $\mathbf{w}_i^{\mathrm{b}} = \mathbf{v}_i^1$. The resulting signal and interference powers can be written as

$$\begin{aligned} S &= P_i|(\mathbf{u}_i^1)^H \sigma_i^1 \mathbf{u}_i^1 (\mathbf{v}_i^1)^H \mathbf{v}_i^1|^2 \\ &= P_i|\sigma_i^1|^2 \end{aligned} \tag{7.28}$$

$$\begin{aligned} I &= \sum_{k=1,\ k\neq i}^{K} \sqrt{P_k}|(\mathbf{u}_i^1)^H \sigma_i^1 \mathbf{u}_i^1 (\mathbf{v}_i^1)^H \mathbf{v}_k^1|^2 \\ &= |\sigma_i^1|^2 \sum_{k=1,\ k\neq i}^{K} P_k|(\mathbf{v}_i^1)^H \mathbf{v}_k^1|^2, \end{aligned} \tag{7.29}$$

where $|\sigma_i^1|$ is also called largest eigenvalue of the complex matrix $\mathbf{H}_i^H \mathbf{H}_i$, whose elements are Wishart distributed [73]. If the noise power at the ith MS is negligible compared to

the interference, the SIR is given by

$$\mathrm{SIR}_i = \frac{P_i}{\sum\limits_{k=1,\ k\neq i}^{K} P_k |(\mathbf{v}_i^1)^H \mathbf{v}_k^1|^2}. \tag{7.30}$$

7.3.2 Outage Probability

The outage probability is defined as the probability that the SIR of ith MS in the downlink remains smaller than a threshold value of the SIR.

$$\begin{aligned} P_{\mathrm{out}}^i(\gamma_{th}) &= \mathrm{pr}\left\{\mathrm{SIR}_i \leq \gamma_{th}\right\} \\ &= \mathrm{pr}\left\{ \sum_{k=1,\ k\neq i}^{K} P_k |(\mathbf{v}_i^1)^H \mathbf{v}_k^1|^2 \geq \frac{P_i}{\gamma_{th}} \right\}. \end{aligned} \tag{7.31}$$

It is important to note that since $\mathbf{H}_i,\ (i = 1, \cdots, K)$ are independent with elements that are zero mean i.i.d. complex Gaussian random, the singular vectors $(\mathbf{v}_i^1)^H$ and $(\mathbf{v}_k^1)^H$ are also zero mean complex Gaussian. The term $\rho_k = |(\mathbf{v}_i^1)^H \mathbf{v}_k^1|^2$ represents the correlation coefficient which for $n_t > 2$ follows the beta distribution [61] with following probability density function

$$\begin{aligned} f_{\rho_k}(x) &= (n_t - 1)(1 - x)^{n_t - 2}, \quad (0 \leq x \leq 1) \\ &= 0, \quad \text{elsewhere.} \end{aligned} \tag{7.32}$$

Fig. 7.5 compares the probability distribution function (pdf) $f_{\rho_k}(x)$ of the random variable ρ_k with the simulation results for different numbers of transmit antennas n_t. As the number of transmit antennas increases, the pdf of ρ_k approaches to an exponential distribution. Let us define a random variable,

$$\begin{aligned} z &= \sum_{k=1,\ k\neq i}^{K} P_k |(\mathbf{v}_i^1)^H \mathbf{v}_k^1|^2 \\ &= \sum_{k=1,\ k\neq i}^{K} P_k \rho_k, \end{aligned} \tag{7.33}$$

which is the weighted sum of the beta distributed random variables ρ_k. The closed form expression for pdf of the random variable z is not known. However, as seen from Fig. 7.5, the pdf of ρ_k can be approximated for the higher values of n_t (generally $n_t > 4$), with an exponential distribution $f_{\rho_k}(x) \approx n_t \exp^{-n_t x}$, for $0 \leq x \geq 1$. With this assumption, the closed form expression for the pdf of random variable z can be derived (see Appendix

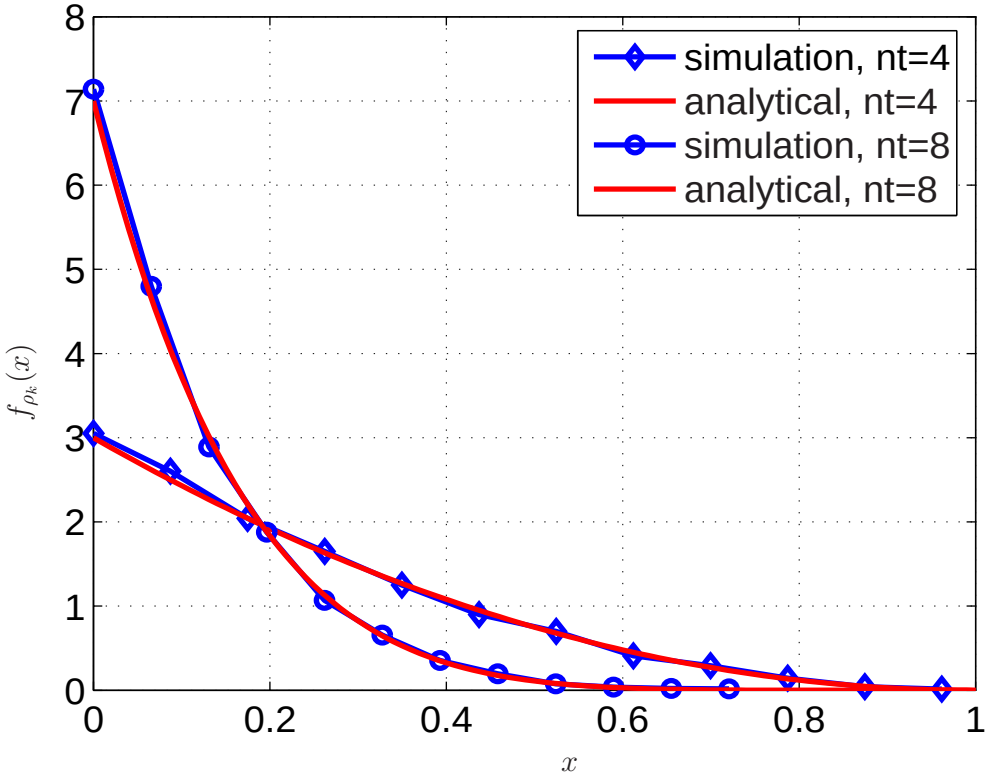

Figure 7.5: Comparison of analytical pdf $f_{\rho_k}(x)$ with the simulated one

9.4) as

$$f_Z(K, P_k, z) = n_t \sum_{k=1, k\neq i}^{K} \frac{a_k}{P_k} \mathrm{e}^{-\frac{n_t z}{P_k}}, \tag{7.34}$$

where $P_j \neq P_k$'s and

$$a_k = \prod_{j=1, j\neq k, i}^{K} \frac{P_k}{P_k - P_j}. \tag{7.35}$$

With the knowledge of probability density function (7.34 and 7.35) of the random variable z, the outage probability (7.31) can be computed as

$$\begin{aligned} P^i_{\text{out}}(\gamma_{th}) &= \text{pr}\left\{ z \geq \frac{P_i}{\gamma_{th}} \right\} \\ &= n_t \int_{\frac{P_i}{\gamma_{th}}}^{\infty} \sum_{k=1, k\neq i}^{K} \frac{a_k}{P_k} \mathrm{e}^{-\frac{n_t z}{P_k}} \, dz \\ &= \sum_{k=1, k\neq i}^{K} a_k \mathrm{e}^{-\frac{n_t P_i}{\gamma_{th} P_k}}. \end{aligned} \tag{7.36}$$

It can be observed from (7.36) that for given P_i and P_k's, the outage probability decreases with increasing n_t and increases with increasing threshold value γ_{th} of SIR. The outage probability is independent of n_r because of the fact that the MSs choose their receive beamforming weights according to the channel between them and their power controlling BS, which is the same for all MSs in case of a single cell scenario.

7.3.3 Power Control

The objective of power control in downlink beamforming is to minimize the total BS transmit power by fulfilling the QoS requirements of all MSs. The outage probability is one of the parameters that can be used as a measure of QoS. In this section we formulate the optimum power control method based upon the outage probability criterion. In this method, the objective is to minimize the total BS transmit power by keeping the outage probability below a certain value. Mathematically, the optimization problem can be expressed as,

$$\begin{aligned} &\min_{P_k} \sum_{k=1}^{K} P_k \\ &\text{subject to } \; P^i_{\text{out}}(\gamma_{th}) \leq q_i, \quad i = 1, \cdots, K. \end{aligned} \tag{7.37}$$

Substituting $P^i_{\text{out}}(\gamma_{th})$ of (7.36) in (7.37), the constrained optimization problem can be written as,

$$\begin{aligned} &\min_{P_k} \sum_{k=1}^{K} P_k \\ &\text{subject to } \sum_{k=1, k\neq i}^{K} a_k \mathrm{e}^{-\frac{n_t P_i}{\gamma_{th} P_k}} \leq q_i, \quad i = 1, \cdots, K \\ &\qquad\qquad P_j \neq P_k, \forall k. \end{aligned} \tag{7.38}$$

The optimization problem consists of a linear objective function but its constraints are non-linear and non-convex. Penalty functions are often used to solve this type of constrained optimization, although it is very difficult to find the correct balance between the objective and penalty functions. Without introducing complicated and specialized variation operators, stochastic ranking method as proposed in [85] provides improved search performance. The algorithm for stochastic ranking using a bubble-sort like procedure is also given in [85] (see Appendix 9.5), which is used for the solution of the optimization problem (7.38).

7.4 Simulation Results: Single User MIMO

We illustrate the performance of the proposed robust design (7.22) for a single user 4×4 MIMO link in a simulated scenario by comparing with the robust method based on the worst-case channel estimate [58]. The performance evaluation is done for a Rayleigh flat fading environment. For any channel realization, the minimum transmit power required to guarantee a minimum QoS in terms of threshold SNR is computed. We use SeDuMi 1.02 [91] (see Appendix 9.2) to solve the convex optimization problem of (7.22). In all simulations, it is assumed that signal and noise power are $\sigma_s^2 = \sigma_n^2 = 1$ and $\sigma_h^2 = 1$.

The comparison between the analytical expression for outage probability (7.20) and

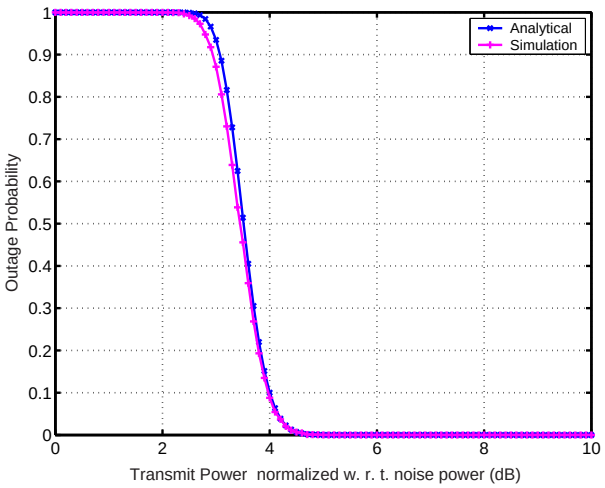

Figure 7.6: Analytical and simulated outage probabilities for the proposed method

simulation is shown in Fig. 7.6 for $\sigma_e^2 = 0.01$. The target SNR is fixed to 10 dB. It can be observed that the outage probability curve from simulation matches with that from analytical expression. The outage probabilty decreases as the transmit power increases.

The comparison of the proposed method (7.22) with the Maxmin approach [58] is shown in Fig. 7.7 by evaluating the outage probability for different transmit powers and changing the target SNR values. We consider 4×4 MIMO system with variance $\sigma_e^2 = 0.05$ of error in the channel estimate. An adhoc approach [58] is used to determine the norm bound of the error matrix $\mathbf{E}$ for the robust Maxmin method. It can be observed that the proposed robust method outperforms Maxmin method for all target values of SNR. For example, to guarantee an SNR of 10 dB with an outage probability of 0.3, the proposed method needs 0.6 dB less transmit power than the Maxmin method. As expected, when the target SNR increases, more transmit power is required to maintain the same outage probability.

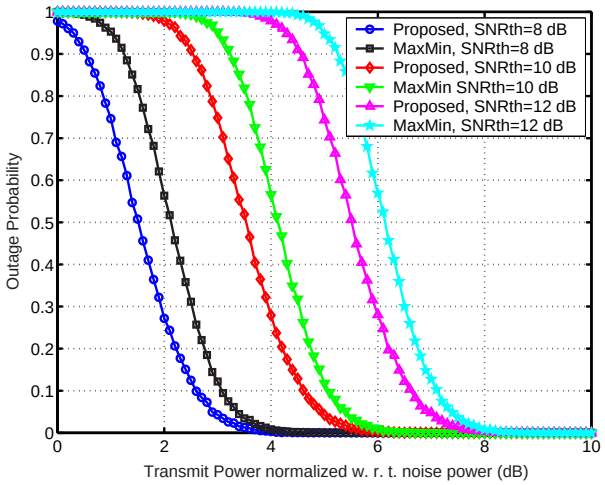

Figure 7.7: Outage probability with new minimum outage probability approach and Maxmin approach as a function of the total transmit power

Fig. 7.8 compares the two robust methods by finding the minimum transmit power

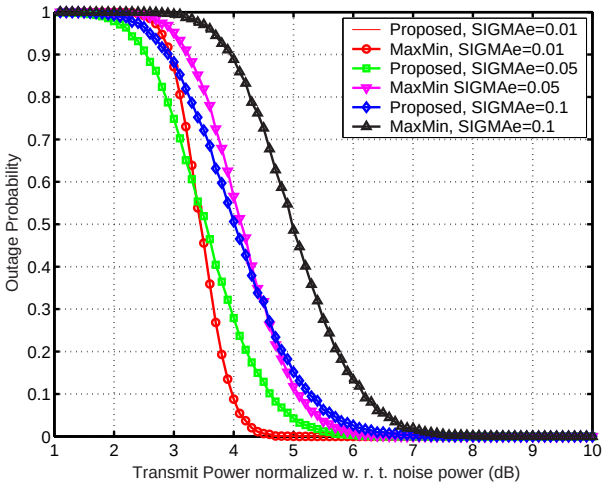

Figure 7.8: Outage probability with the proposed and Maxmin approaches as a function of the total transmit power

required to maintain the SNR of 10 dB for different values of σ_e^2. For $\sigma_e^2 = 0.01$, there is no difference between the outage probability computed by the two robust methods. As σ_e^2 increases this difference increases significantly. As an example when $\sigma_e^2 = 0.1$, the robust method based on outage probability minimization requires almost 1 dB less transmission power than the Maxmin method to keep the outage probability less than 0.3. When $\sigma_e^2 = 0.05$, the proposed robust design needs about 4 dB transmission power whereas the Maxmin robust method requires about 4.6 dB to maintain the outage probability of 0.3. This clearly indicates the importance of the proposed method when channel estimate

errors are significant.

7.5 Simulation Results: Multiuser MIMO

First we check the approximate expression of the outage probability we have derived (7.36) using Monte Carlo simulations. An analysis of the effects of an increasing number of antennas on the system performance is carried out. As expected, Fig 7.9 shows that as the threshold value of the SIR increases, the outage probability of the desired MS also increases. Here, we have considered 10 intracell interferers with arbitrarily taken fixed power levels $\{3.3, 2.8, 2.4, 2.1, 1.8, 1.6, 1.5, 0.8, 0.5, 0.2\}$. The power P_1 for the desired user is assumed to be 1. Note that these power levels have no relation to the optimum power levels that can be obtained from the solution of (7.38). We have assumed that $\sigma_h^2 = \sigma_s^2 = 1$. The MIMO channels between these intracell interferers and the BS are flat fading spatially uncorrelated Rayleigh as described in section 7.3.1. As the number of transmit antennas increases, the agreement between the analytical (7.36) and simulation results improves. As an example for $n_t = 4$, the difference between the analytical and simulation results is higher than compared with the case of $n_t = 12$. This is because of the approximation of (7.32) with an exponential distribution which is a good one only for higher values of n_t. For a given value of the SIR threshold, as the number of transmit antenna increases, the outage probability decreases.

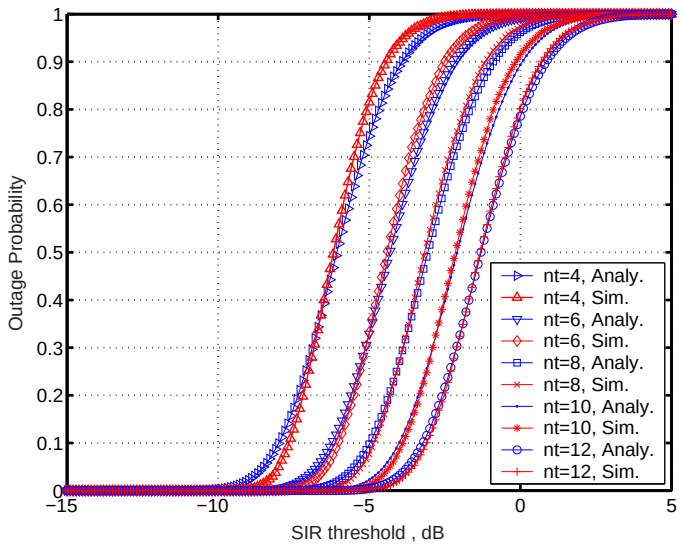

Figure 7.9: Outage probability for different numbers of transmit antennas versus the SIR threshold γ_{th}

Figure 7.10 shows the total transmit power required by the BS for different SIR threshold values where the probability $q_i,\ i \neq k, i = 1, \cdots, K$ that the SIR at all MSs considered in the system remains below the threshold SIR is fixed to 0.2. For this purpose, we find the optimum transmit power levels $P_k,\ k = 2, \cdots, K$ (P_1 is fixed to 0.5) by solving the constrained optimization problem (7.38) using a stochastic ranking method [85]. Here, the total BS transmit power is normalized with reference power $P_0 = 1$. Simulation results are presented for the system with 4 MSs. As expected, as the threshold SIR for MSs increases, the required BS transmit power also increases. It is important to note that the optimum set of transmit powers is not always feasible. As an example when $n_t = 4$ and threshold SIR is greater than -1 dB, an optimum solution does not exist. The required BS transmit power for different SIR threshold values is shown in Fig.

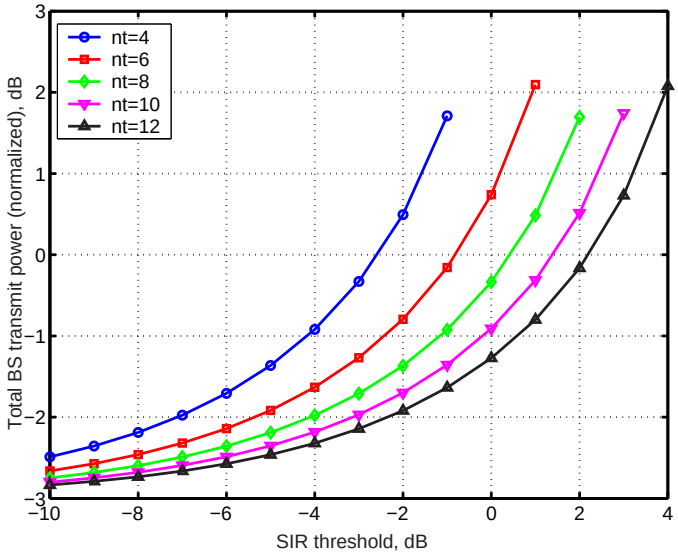

Figure 7.10: Total BS transmit power for $q_i = 0.2$

7.11, where q_i is now fixed to 0.4 $\forall i$. Again the total BS transmit power is normalized with reference power $P_0 = 1$. As before, we find the optimum transmit power levels $P_k,\ \ k = 2, \cdots, K$ (P_1 is fixed to 0.5) by solving the constrained optimization problem (7.38) using stochastic ranking method [85]. Simulation results are again presented for the system with only 4 MSs. As the threshold SIR for the MSs increases, the required BS transmit power also increases. The required BS transmit power for a given SIR threshold value and number of transmit antennas, decreases with increasing value of target outage probability q_i. This can be observed by comparing the simulation results with $q_i = 0.2$ to that with $q_i = 0.4$. Increasing the value of q_i indicates that the probability that a MS falls in outage increases.

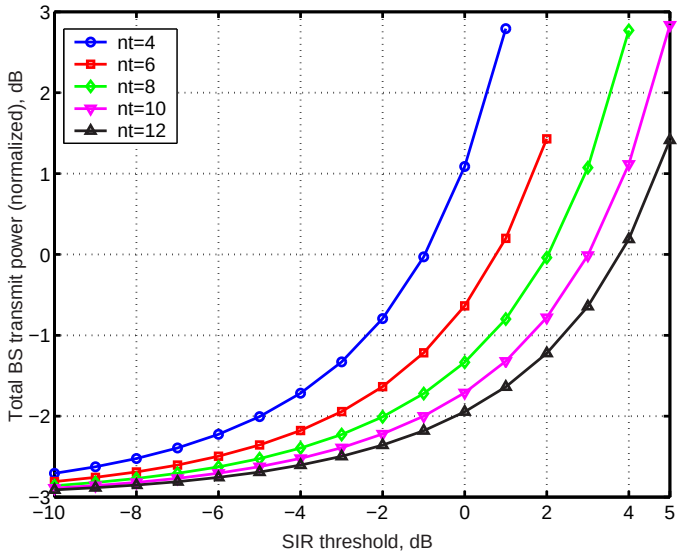

Figure 7.11: Total BS transmit power for $q_i = 0.4$

7.6 Summary

A robust MIMO transmitter based on minimization of the outage probability with a transmit power constraint is proposed in this chapter. Our approach leads to a convex optimization problem that can be solved efficiently using an optimization toolbox like SeDuMi 1.02. Simulation results confirm that our proposed method is robust against errors in channel estimate and performs better than the Maxmin method [58] especially for cases of large uncertainty. The computational complexity of our approach is similar to that of the robust Maxmin method. The knowledge of the upper bound of the Frobenius norm of the error in the channel estimate is not required.

We also analyzed a multiuser MIMO system with a MRT based beamforming for downlink communications. A simple approximate expression for the outage probability is derived for a single cell case. Based on this outage probability, a constrained optimization problem is solved in order to find the optimum set of power levels for downlink transmission. For downlink transmission in a single cell scenario, the use of the multiple antennas at MSs does not improve the system performance (e.g. the outage probability). Multiple antennas at MSs are helpful only if interference from other BSs is taken into consideration. However, an optimum power control scheme for such cases becomes practically infeasible because the BSs need information about the channels of the MSs which are power controlled by other BSs.

Chapter 8

Conclusion and Perspectives

This dissertation focusses on the optimization of the system level performance of multiple antenna cellular wireless communication systems that employ beamforming. QoS parameters like the SINR and outage probability are used for the analysis of the system level performance of both SA and MIMO systems. Many optimum as well as suboptimum algorithms that provide robustness against various types of channel uncertainty are proposed. The performance of these algorithms is evaluated using deterministic as well as probabilistic propagation environment.

In **Chapter 3**, the performance improvement (in terms of system capacity) that can be achieved from the use of the SAs is investigated for the 3G systems like UMTS-FDD. For this purpose, a novel and dynamic system level simulator that takes into account the realistic propagation environment has been developed.

In **Chapter 4**, the performance of uplink to downlink spatial covariance transformation methods has been investigated for the UMTS-FDD system by using the dynamic system level simulator. A new robust algorithm that gives an optimum linear transformation matrix for the case of erroneous uplink steering vectors has been proposed. The performance of this robust method is compared with non-robust methods.

In **Chapter 5**, a new robust uplink beamforming algorithm that provides robustness against errors in the estimate of the uplink spatial covariance matrices has been proposed. This method is based on the minimization of the outage probability of the MS in the uplink. Simulation results carried out in deterministic as well as in stochastic propagation environments show that the proposed method is computationally efficient

and performs better than a robust method based on worst-case performance optimization and the non-robust method based on maximization of the received SINR.

A new optimum robust downlink beamforming method based on stochastic programming is presented in **Chapter 6**. A computationally efficient suboptimum solution has also been presented and solved using a convex optimization toolbox. The performance of the proposed optimum robust method is compared with a robust method based on worst-case performance optimization as well as a centralized non-robust method [8] based on minimization of the total BS transmit power with the received SINR constraints. Simulation results show that the proposed robust optimum method performs better in terms of outage probability although some more BS transmit power is required than the non-robust method proposed in [8].

Finally in **Chapter 7**, a new method for the design of a MIMO transmitter is proposed. This MIMO transmitter combines beamforming with OSTBC and provides robustness against errors in the channel estimate available at the transmitter. The design criterion is to optimally distribute the power of each eigenmode of the channel estimate such that the outage probability at the receiver is minimized. Simulation results show that the proposed method performs significantly better than the Maxmin method proposed in [58]. Moreover, a multiuser MIMO system with beamforming based on MRT scheme is also analyzed in this chapter. A simple and an approximate expression for the outage probability of the MS in the downlink is derived. With the help of this outage probability, a power control optimization problem for the downlink transmission is formulated and solved using a stochastic ranking method [85].

8.1 Future Work

Several considerations for future work are presented below.

- As seen from **Chapter 3**, only circular adaptive antenna arrays have been used to evaluate the system level performance of UMTS-FDD system without taking into account sectorization of the cells. As a part of future work, it is interesting to investigate the performance improvement that can be obtained by the use of sectored antennas as well as simple beamforming methods such as beam switching.

- In **Chapter 4**, uncertainty can also be introduced to the downlink steering vectors and a robust transformation matrix can be derived on the basis of the TLS solution.
- In **Chapter 5**, the assumption that the elements of the error matrix $\mathbf{E}$ are i.i.d. complex Gaussian can be relaxed to a more general type of distribution.
- The complexity of the robust optimum as well as the suboptimum downlink beamforming algorithms presented in **Chapter 6** has to be reduced so that they can be practically implemented and introduced into the dynamic system level simulator presented in **Chapter 3**.
- The robust MIMO transmitter based upon minimization of the outage probability and proposed in **Chapter 7**, can be improved to support full-rate transmission. The power control optimization problem proposed in the same chapter can be extended for a multi-cellular environment, although the complexity of such a problem will be very high.

Chapter 9

Appendix

9.1 Spatial Fading Correlation for UCA

When deriving the spatial fading correlation for a UCA, let us start by substituting $b = \frac{\sigma_\theta}{\sqrt{2}}$ in (2.33) as

$$\mathbf{R}_s(m,n) = \int_{-\pi+\mu}^{\mu} \mathrm{e}^{-\mathrm{j}A_c \sin(\alpha+\theta)} \frac{1}{2b} \mathrm{e}^{\frac{\theta-\mu}{b}}\, d\theta + \int_{\mu}^{\pi+\mu} \mathrm{e}^{-\mathrm{j}A_c \sin(\alpha+\theta)} \frac{1}{2b} \mathrm{e}^{\frac{-\theta+\mu}{b}}\, d\theta. \quad (9.1)$$

Let

$$I_1 = \frac{1}{2b} \mathrm{e}^{-\frac{\mu}{b}} \int_{-\pi+\mu}^{\mu} \mathrm{e}^{-\mathrm{j}A_c \sin(\alpha+\theta)} \mathrm{e}^{\frac{\theta}{b}}\, d\theta. \quad (9.2)$$

Substituting $\xi = \alpha + \theta$, (9.2) can be rewritten as

$$I_1 = \frac{1}{2b} \mathrm{e}^{-\frac{\mu+\alpha}{b}} \int_{-\pi+\alpha+\mu}^{\mu+\alpha} \mathrm{e}^{-\mathrm{j}A_c \sin(\xi)} \mathrm{e}^{\frac{\xi}{b}}\, d\xi, \quad (9.3)$$

where the term $\mathrm{e}^{-\mathrm{j}A_c \sin(\xi)}$ can be expressed as

$$\mathrm{e}^{-\mathrm{j}A_c \sin(\xi)} = \cos\left(A_c \sin\xi\right) - \mathrm{j} \sin\left(A_c \sin\xi\right). \quad (9.4)$$

With the help of following well known series of Bessel function coefficients

$$\begin{aligned} \cos\left(A_c \sin\xi\right) &= J_0(A_c) + 2\sum_{k=1}^{\infty} J_{2k}(A_c) \cos\left(2k\xi\right) \\ \sin\left(A_c \sin\xi\right) &= 2\sum_{k=1}^{\infty} J_{(2k-1)}(A_c) \sin\left((2k-1)\xi\right), \end{aligned} \quad (9.5)$$

(9.3) can be expressed as

$$\begin{aligned} I_1 = {} & BJ_0(A_c) \int_{-\pi+\alpha+\mu}^{\mu+\alpha} \mathrm{e}^{\frac{\xi}{b}}\, d\xi + 2B \sum_{k=1}^{\infty} J_{2k}(A_c) \int_{-\pi+\alpha+\mu}^{\mu+\alpha} \cos\left(2k\xi\right) \mathrm{e}^{\frac{\xi}{b}}\, d\xi - \\ & 2\mathrm{j}B \sum_{k=1}^{\infty} J_{(2k-1)}(A_c) \int_{-\pi+\alpha+\mu}^{\mu+\alpha} \sin\left((2k-1)\xi\right) \mathrm{e}^{\frac{\xi}{b}}\, d\xi, \end{aligned} \quad (9.6)$$

where $B = \frac{1}{2b}\mathrm{e}^{-\frac{\mu+\alpha}{b}}$. The following three terms I_{11}, I_{12}, and I_{13} in (9.6) have to be evaluated

$$\begin{aligned} I_{11} &= BJ_0(A_c)\int_{-\pi+\alpha+\mu}^{\mu+\alpha} \mathrm{e}^{\frac{\xi}{b}}\, d\xi \\ &= BJ_0(A_c)b\mathrm{e}^{\frac{\alpha+\mu}{b}}\left(1-\mathrm{e}^{-\frac{\pi}{b}}\right) \\ &= \frac{1}{2}J_0(A_c)\left(1-\mathrm{e}^{-\frac{\pi}{b}}\right), \end{aligned} \tag{9.7}$$

$$\begin{aligned} I_{12} &= 2B\int_{-\pi+\alpha+\mu}^{\mu+\alpha} \cos(2k\xi)\,\mathrm{e}^{\frac{\xi}{b}}\, d\xi \\ &= 2B\frac{b}{1+4b^2k^2}\left[\mathrm{e}^{\frac{\xi}{b}}\left(\cos(2k\xi)+2bk\sin(2k\xi)\right)\right]_{-\pi+\alpha+\mu}^{\alpha+\mu} \\ &= \frac{1}{1+4b^2k^2}\left\{\left(1+\mathrm{e}^{-\frac{\pi}{b}}\right)\left(\cos(2k(\alpha+\mu))+2kb\sin(2k(\alpha+\mu))\right)\right\}, \end{aligned} \tag{9.8}$$

and

$$\begin{aligned} I_{13} &= 2B\int_{-\pi+\alpha+\mu}^{\mu+\alpha} \sin((2k-1)\xi)\,\mathrm{e}^{\frac{\xi}{b}}\, d\xi \\ &= 2B\frac{b}{1+b^2(2k-1)^2}\left[\mathrm{e}^{\frac{\xi}{b}}\left(\sin(2k-1)\xi)-b(2k-1)\cos((2k-1)\xi)\right)\right]_{-\pi+\alpha+\mu}^{\alpha+\mu} \\ &= \frac{1}{1+b^2(2k-1)^2}\left\{\left(1+\mathrm{e}^{-\frac{\pi}{b}}\right)\left(\sin((2k-1)(\alpha+\mu))-(2k-1)b\cos((2k-1)(\alpha+\mu))\right)\right\}. \end{aligned} \tag{9.9}$$

I_{12} and I_{13} are evaluated with the help of following indefinite integrals

$$\int \mathrm{e}^{ax}\cos b'x\, dx = \frac{\mathrm{e}^{ax}\left(a\cos(b'x)+b'\sin(b'x)\right)}{a^2+b'^2} \tag{9.10}$$

and

$$\int \mathrm{e}^{ax}\sin b'x\, dx = \frac{\mathrm{e}^{ax}\left(a\sin(b'x)-b'\cos(b'x)\right)}{a^2+b'^2}, \tag{9.11}$$

respectively. Substituting I_{11}, I_{12} and I_{13}, we get I_1 from (9.6) as

$$I_1 = I_{11} + \sum_{k=1}^{\infty} J_{2k}(A_c)I_{12} - \mathrm{j}\sum_{k=1}^{\infty} J_{(2k-1)}I_{13}. \tag{9.12}$$

Similarly let us define

$$I_2 = \frac{1}{2b}\mathrm{e}^{\frac{\mu}{b}}\int_{\mu}^{\mu+\pi} \mathrm{e}^{-\mathrm{j}A_c\sin(\alpha+\theta)}\mathrm{e}^{-\frac{\theta}{b}}\, d\theta. \tag{9.13}$$

Using similar steps as carried out for computation of I_1, we can express I_2 as

$$I_2 = I_{21} + \sum_{k=1}^{\infty} J_{2k}(A_c)I_{22} - \mathrm{j}\sum_{k=1}^{\infty} J_{(2k-1)}(A_c)I_{23}, \tag{9.14}$$

where

$$I_{21} = \frac{1}{2} J_0(A_c) \left[1 - \mathrm{e}^{-\frac{\pi}{b}}\right], \tag{9.15}$$

$$I_{22} = \frac{1}{1+4k^2b^2} \left[\left(1 + \mathrm{e}^{-\frac{\pi}{b}}\right)\left(\cos(2k(\alpha+\mu)) - 2kb\sin(2k(\alpha+\mu))\right)\right], \tag{9.16}$$

and

$$I_{23} = \frac{1}{1+b^2(2k-1)^2} \left[\left(1 + \mathrm{e}^{-\frac{\pi}{b}}\right)\left(\sin((2k-1)(\alpha+\mu)) + (2k-1)b\cos((2k-1)(\alpha+\mu))\right)\right]. \tag{9.17}$$

Finally, the spatial fading correlation $\mathbf{R}_s(m,n)$ between mth and nth elements of the UCA is given by

$$\begin{aligned} \mathbf{R}_s(m,n) &= \left(1 - \mathrm{e}^{-\frac{\pi}{b}}\right) J_0(A_c) + 2\left(1 + \mathrm{e}^{-\frac{\pi}{b}}\right) \sum_{k=1}^{\infty} \frac{1}{1+4b^2k^2} J_{2k}(A_c) \cos\left(2k(\alpha+\mu)\right) \\ &\quad -2\mathrm{j}\left(1 + \mathrm{e}^{-\frac{\pi}{b}}\right) \sum_{k=1}^{\infty} \frac{J_{(2k-1)}(A_c)}{1+b^2(2k-1)^2} \sin\left((2k-1)(\alpha+\mu)\right), \end{aligned} \tag{9.18}$$

where $b = \frac{\sigma_\theta}{\sqrt{2}}$.

9.2 Convex Optimization Toolbox

The convex optimization problems that appear in this dissertation have been solved using SeDuMi 1.02 [91] which is a MATLAB toolbox for optimization over symmetric cones. SeDuMi allows to solve optimization problems with linear, quadratic and semidefinite constraints. Even large scale optimization problems can be solved efficiently by exploiting sparsity. A convex optimization problem with different types of constraints can be solved using either standard primal or dual form of SeDuMi. The standard primal form for such optimization problem is written as

$$\begin{aligned} \text{minimize} \quad & \mathbf{c}^T\mathbf{x} \\ \text{such that} \quad & \mathbf{A}\mathbf{x} = \mathbf{b} \\ & \mathbf{x} \in \mathcal{K}, \end{aligned} \tag{9.19}$$

where the optimization variable $\mathbf{x}$ belongs to a symmetric-cone $\mathcal{K}$. A symmetric cone is a Cartesian product of a nonnegative orthant, quadratic cones and cones of positive semidefinite constraints.
Similarly the standard dual form is

$$\begin{aligned} \text{maximize} \quad & \mathbf{b}^T\mathbf{y} \\ \text{such that} \quad & \mathbf{c} - \mathbf{A}^\mathbf{T}\mathbf{y} \in \mathcal{K}, \end{aligned} \tag{9.20}$$

where $\mathbf{y}$ is the optimization variable and $\mathbf{c} - \mathbf{A^T y}$ belongs to symmetric-cone $\mathcal{K}$. The dual equality, linear, quadratic, rotated quadratic and semidefinite constraints are arranged in as symmetric cone $\mathcal{K}$ as

$$\mathcal{K} = \mathcal{R}^{\text{K.f}} \times \mathcal{R}_{+}^{\text{K.l}} \times (\text{Qcone} \times \cdots \times \text{Qcone}) \times (\text{Rcone} \times \cdots \times \text{Rcone}) \times (\text{Scone} \times \cdots \times \text{Scone}), \tag{9.21}$$

where $\mathcal{R}_{+}^{\text{K.l}}$ represents a linear constraint for K.l non-negative variables. The quadriatic cone Qcone by definition is a cone of the form

$$\text{Qcone} = \{(x_1, \mathbf{x}_2) \in \mathcal{R} \times \mathcal{C}^{\text{K.q}-1} | x_1 \geq ||\mathbf{x}_2||_2\}, \tag{9.22}$$

where $\mathcal{C}^n$ denotes the space of complex n-tuples and $||\cdot||_2$ represents the Euclidean norm. The quadriatic cone is often known as a SOC. SeDuMi supports another form of cone which is

$$\text{Rcone} = \{(x_1, x_2, \mathbf{x}_3) \in \mathcal{R} \times \mathcal{R} \times \mathcal{C}^{\text{K.r}-2} | x_1 x_2 \geq \frac{1}{2}||\mathbf{x}_3||_2^2, x_1 + x2 \geq 0\}. \tag{9.23}$$

Geometrically, Rcone is a rotation of a quadratic cone. Scone represents semidefinte constraints which is a constraint that a symmetric $m \times m$ matrix $\mathbf{X}$ is a positive semidefinite. Scone for primal components is defined as

$$\text{Scone} = \{\mathbf{x} \in \mathcal{C}^{\text{K.s}^2} | \text{mat}(\mathbf{x}) \text{ is a Hermitian positive semidefinite}\}, \tag{9.24}$$

where K.s represents a list of orders of positive semidefinite constraints. Similarly, for dual components $\mathbf{z} = \mathbf{c} - \mathbf{A^T y}$, the definition of Scone is given as

$$\text{Scone} = \{\mathbf{z} \in \mathcal{C}^{\text{K.s}^2} | \text{mat}(\mathbf{z}) + \text{mat}(\mathbf{z})' \text{ is a Hermitian positive semidefinite}\}. \tag{9.25}$$

All the convex optimization problems must be first transformed into either standard primal or dual forms of SeDuMi before calling the optimization routine of SeDuMi. The calling sequence for solving primal-dual pair of SeDuMi is

$$[\mathbf{x}, \mathbf{y}, \text{info}] = \text{sedumi}(\mathbf{A}, \mathbf{b}, \mathbf{c}, \mathbf{K}, \mathbf{pars}), \tag{9.26}$$

where $\mathbf{K}$ is a MATLAB structure for defining the symmetric cone $\mathcal{K}$ which consists of following fields:

- K.f: The number of dual equality constraints
- K.l: The number of non-negativity constraints
- K.q: A list of dimensions of quadriatic cone constraints

- K.r: A list of dimensions of rotated quadriatic cone constraints
- K.s: A list of orders of positive semidefinite constraints
- K.xcomplex: A list of primal variables in the f, l, q and r blocks that are allowed to have nonzero imaginary parts
- K.scomplex: A list of matrix variables that are restricted to Hermitian positive semidefinite
- K.ycomplex: This field is not related to $\mathcal{K}$. It lists the components of the $\mathbf{y}$ variables that are complex valued.

9.3 Proof of the Invalidity of the Constraint (6.21)

We start with the constraint (6.21), in which we substitute $||\mathbf{W}_i|| = \mathrm{tr}(\mathbf{W}_i)$, because $\mathbf{W}_i$ are rank-one matrices. Then the constraint (6.21) can be expressed as

$$\mathrm{tr}\left(\left(\mathbf{R}_i - c_i\mathbf{I}\right)\mathbf{W}_i\right) - \gamma_{th}\sum_{k\neq i,k=1}^{K}\mathrm{tr}\left(\left(\mathbf{R}_i + c_i\mathbf{I}\right)\mathbf{W}_k\right) \leq \gamma_{th}\sigma_i^2, \tag{9.27}$$

which is equivalent to

$$\frac{\mathrm{tr}\left(\left(\mathbf{R}_i - c_i\mathbf{I}\right)\mathbf{W}_i\right)}{\sum_{k\neq i,k=1}^{K}\mathrm{tr}\left(\left(\mathbf{R}_i + c_i\mathbf{I}\right)\mathbf{W}_k\right) + \sigma_i^2} \leq \gamma_{th}. \tag{9.28}$$

Note that the left-hand side of (9.28) represents the actual SINR at the i-th MS. This means that if the constraint (6.21) is fulfilled, the actual SINR remains below its threshold value γ_{th}. By keeping the SINR below this threshold value, we cannot maintain the non-ouatge probability $\tilde{P}_{\mathrm{out}}^{i}(\gamma_{th})$ of (6.7) above a certain threshold p_i, where $p_i \geq 1/2$. Thus, the constraint (6.21) contradicts to the objective of the optimization problem (6.6).

9.4 Probability Density Function of a Weighted Sum of Statistically Independent Exponentially Distributed Random Variables

Probability density function (7.34) of random variable z is derived in this section. We have $z_1 = P_1\rho_1 + P_2\rho_2$ for $K = 2$ where $f_{\rho_1}(x) \approx n_t\mathrm{e}^{-n_t x}$ and $f_{\rho_2}(y) \approx n_t\mathrm{e}^{-n_t y}$, for

$0 \leq x \leq 1$ and $0 \leq y \leq 1$. Then the probability density functions of $P_1\rho_1$ and $P_2\rho_2$ are $\frac{n_t}{P_1}\mathrm{e}^{-\frac{n_t}{P_1}x}$ and $\frac{n_t}{P_2}\mathrm{e}^{-\frac{n_t}{P_2}y}$, respectively. Since the two random variables are independent, the probability density function of z_1 is given by convolution

$$\begin{aligned} f_{\mathbf{z}_1}(z) &= \int_0^z f_{\rho_1}(z-y) f_{\rho_2}(y)\, dy \\ &= \int_0^z \frac{n_t^2}{P_1 P_2} \mathrm{e}^{-\frac{n_t}{P_1}(z-y)} \mathrm{e}^{-\frac{n_t}{P_2}y}\, dy \\ &= \int_0^z \frac{n_t^2}{P_1 P_2} \mathrm{e}^{-\frac{n_t}{P_1}z} \mathrm{e}^{-n_t y(\frac{P_1-P_2}{P_1 P_2})}\, dy \\ &= \frac{n_t}{P_1 - P_2}\left\{\mathrm{e}^{-\frac{n_t}{P_1}z} - \mathrm{e}^{-\frac{n_t}{P_2}z}\right\}. \end{aligned} \tag{9.29}$$

Now consider another random variable $P_3\rho_3$ with probability density function $\frac{n_t}{P_3}\mathrm{e}^{-\frac{n_t}{P_3}y}$, then we can write $z_2 = z_1 + P_3\rho_3$ whose density function is given as

$$\begin{aligned} f_{\mathbf{z}_2}(z) =& \int_0^z \frac{n_t^2}{(P_1-P_2)P_3} \mathrm{e}^{-\frac{n_t}{P_3}y}\left(\mathrm{e}^{-\frac{n_t}{P_1}(z-y)} - \mathrm{e}^{-\frac{n_t}{P_2}(z-y)}\right) dy \\ =& \frac{n_t^2}{(P_1-P_2)P_3}\left\{\mathrm{e}^{-\frac{n_t}{P_1}z}\int_0^z \mathrm{e}^{-n_t y(\frac{P_1-P_3}{P_1 P_3})}\, dy - \mathrm{e}^{-\frac{n_t}{P_2}z}\int_0^z \mathrm{e}^{-n_t y(\frac{P_2-P_3}{P_2 P_3})}\, dy\right\} \\ =& \frac{n_t P_1}{(P_1-P_2)(P_1-P_3)}\mathrm{e}^{-\frac{n_t}{P_1}z} + \frac{n_t P_2}{(P_2-P_1)(P_2-P_3)}\mathrm{e}^{-\frac{n_t}{P_2}z} \\ &+ \frac{n_t P_3}{(P_3-P_1)(P_3-P_2)}\mathrm{e}^{-\frac{n_t}{P_3}z} \\ =& \sum_{k=1}^{3} \frac{a_k n_t}{P_k}\mathrm{e}^{-\frac{n_t}{P_k}z}, \end{aligned} \tag{9.30}$$

where

$$\begin{aligned} a_k &= \prod_{j=1,\ j\neq k}^{3} \frac{P_k}{P_k - P_j} \\ & P_k \neq P_j. \end{aligned} \tag{9.31}$$

Therefore the probability density function of random variable z which is the weighted sum of the exponentially distributed independent random variables ρ_ks can be expressed as (7.34).

9.5 Stochastic Ranking for Constrained Optimization

A general nonlinear programming problem can be formulated as solving the objective function

$$\min \ \ f(\mathbf{x}), \ \ \mathbf{x} = (x_1, \cdots, x_n) \in \mathcal{R}^n, \tag{9.32}$$

where $\mathbf{x} \in \mathcal{S} \bigcap \mathcal{F},\ \mathcal{S} \subseteq \mathcal{R}^n$ defines the search space which is a n-dimensional space bounded by parametric constraints

$$x_i^l \leq x_i \leq x_i^u,\ i \in \{1, \cdots, n\} \tag{9.33}$$

and the feasible region $\mathcal{F}$ is defined as

$$\mathcal{F} = \{\mathbf{x} \in \mathcal{R}^n | g_j(\mathbf{x}) \leq 0\ \forall\ j \in \{1, \cdots, m\}\}, \tag{9.34}$$

where $g_j(\mathbf{x}),\ j \in \{1, \cdots, m\}$ are the constraints. By introducing penalty terms in order to penalize the constraint violations, the constrained optimization problem can be transformed into an unconstrained one, which is given by

$$\psi(\mathbf{x}) = f(\mathbf{x}) + r_g \phi(g_j(\mathbf{x});\ j = 1, \cdots, m), \tag{9.35}$$

where $\phi \geq 0$ is a real valued function which imposes a penalty controlled by a sequence of penalty coefficients $\{r_g\}_0^G$, where g is the generation counter. The penalty function method may work quite well for some problems, however, finding an optimal value of r_g becomes a difficult optimization problem itself. If r_g is too small, an infeasible solution may not be penalized enough. If r_g is too large, a feasible solution is very likely to be found but could be of poor quality. An adaptive approach where r_g are adjusted dynamically and automatically by an evolutionary algorithm itself, appears to be most promising for tackling different constrained optimization problems. The stochastic ranking method for evolutionary strategy ranks fit individuals [85] according to their objectives and penalty values without specifying an r_g value.

Bibliography

[1] 3GPP, "RF system scenarios - Technical specification (TS) 25.942," *http://www.3gpp.org/*, 2000.

[2] Intel, "Understanding WiMAX and 3G for portable/mobile broadband wireless," *Technical White Paper*, Dec. 2004.

[3] S. M. Alamouti, "A simple transmit diversity for wireless communications," *IEEE Transactions on Communications*, vol. 16, no. 8, Oct. 1998.

[4] S. Andersson, M. Millnert, M. Viberg and B. Wahlberg, "An adaptive array for mobile communications," *IEEE Transactions on Vehicular Technology*, vol. 40, pp. 230-236, Jan. 1991.

[5] T. Aste, P. Forster, L. Fety, and S. Mayrargue, "Downlink beamforming avoiding DOA estimation for cellular mobile communications," *In Proceedings of IEEE ICASSP'98*, Seattle, USA, pp. 3313-3316, May 1998.

[6] T. Baumgartner, T. Neubauer and E. Bonek, "Performance of DL beam switching for UMTS FDD in the presence of angular spread," *IEEE International Conference on Communications (ICC 2002)*, New York, USA, April 2002.

[7] K. L. Bell, Y. Ephraim and H. L. Van Trees, "A Bayesian approach to robust adaptive beamforming," *IEEE Transactions on Signal Processing*, vol. 48, pp. 386-398, Feb. 2000.

[8] M. Bengtsson and B. Ottersten, "Optimal downlink beamforming using semidefinite optimization," *In Proceedings of 37th Annual Allerton Conference on Communication, Control and Computing*, pp. 987-996, Sept. 1999.

[9] M. Bengtsson and B. Ottersten, "Optimum and suboptimum transmit beamforming," *Handbook of Antennas in Wireless Communications*, Chap. 18, CRC Press, 2001.

[10] O. Besson and P. Stoica, "Decoupled estimation of DOA and angular spread for a spatially distributed source," *IEEE Transactions on Signal Processing*, vol. 48, pp. 1872-1882, July 2000.

[11] M. Biguesh, S. Shahbazpanahi and A. B. Gershman, "Robust downlink power adjustment in cellular communication systems with antenna arrays at BSs," *In Proceedings of IEEE Signal Processing for Wireless Communications (SPWAC)*, Rome, Italy, June 2003.

[12] H. Boche and M. Schubert, "Theoretical and experimental comparisons of optimization criteria for downlink beamforming," *European Transactions on Telecommunications, Special Issue on Smart Antennas* , vol. 12, no. 5, pp. 417-426, 2001.

[13] H. Boelcskei, D. Gesbert and A. J. Paulraj, "On the capacity of OFDM based spatial multiplexing systems," *IEEE Transactions on Communications*, vol. 50, pp. 225-234, Feb. 2002.

[14] A. O. Boukalov and S.-G. Haeggman, "System aspects of smart-antenna technology in cellular wireless communications- An overview," *IEEE Transactions on Microwave Theory and Techniques*, vol. 48, no. 6, June 2000.

[15] S. Boyd and L. Vandenberghe, "Convex optimization," *Cambridge University Press*, ISBN 0521833787, 2004.

[16] L. E. Brennan, J. D. Mallet and I. S. Reed, "Adaptive arrays in airborne MTI radar," *IEEE Transactions on Antennas Propagation*, vol. 24, Sept. 1976.

[17] B. D. Carlson, "Covariance matrix estimation errors and diagonal loading in adaptive arrays," *IEEE Trans. Aerospace Electronic System*, vol. 24, pp. 397-401, July 1988.

[18] B. K. Chalise, L. Haering and A. Czylwik, "Robust uplink to downlink spatial covariance transformation method for downlink beamforming," *In the Proceedings of IEEE International Conference on Communications (ICC)*, Paris, France, June 2004.

[19] S. Chandrasekaran, G. H. Golub, M. Gu, A. H. Sayed, "Efficient algorithms for least squares type problems with bounded uncertainities," *http://www.ee.ucla.edu/asl/publications/book_chapters/siam_1997.pdf*, 1997.

[20] S. Chandrasekaran, G. H. Golub, M. Gu and A. H. Sayed, "An efficient algorithm for a bounded errors-in-variables model," *SIAM Journal of Matrix Analysis and Applications*, vol. 20, no. 4, pp. 839-859, July 1999.

[21] L. Chang and C. C. Yeh, "Performance of DMI and eigenspace-based beamformers," *IEEE Trans. Antennas and Propagation*, vol. 40, pp. 1336-1347, Nov. 1992.

[22] M. Chiani, M. Win, A. Zanella and J. H. Winters, "Exact symbol error probability for optimum combining in the presence of multiple co-channel interferers and thermal noise," *IEEE Global Telecommunications Conference (GLOBECOM'01)*, San Antonio, Texas, USA, no. 1, pp. 1182-1186, Nov. 2001.

[23] M. Chiani, M. Z. Win and A. Zanella, "On the capacity of spatially correlated MIMO Rayleigh fading channels," *IEEE Transactions on Information Theory*, vol. 49, no. 10, pp. 2363-2371, Oct. 2003.

[24] H. Cox, "Resolving power and sensitivity to mismatch of optimum array processors," *Journal of Acoustics Society of America* vol. 54, pp. 771-785, 1973.

[25] H. Cox, R. M. Zeskind and M. H. Owen, "Robust adaptive beamforming," *IEEE Trans. Acoust., Speech, Signal Processing*, vol. 35, pp. 1365-1376, Oct. 1987.

[26] A. Czylwik and A. Dekorsy, "Optimization of downlink beamforming for systems with frequency division duplex," *COST 259 Technical Document TD (00)34*, 2000.

[27] A. Czylwik and T. Matsumoto, "Downlink beamforming for frequency-duplex systems in frequency-selective fading," *In proceedings of the IEEE Vehicular Technology Conference VTC 2000 Spring*, Tokyo, Japan, pp. 695-699, May 2000.

[28] A. Czylwik and A. Dekorsy, "Optimization of downlink beamforming for systems with frequency division duplex," *IEEE Globecom 2001*, San Antonio, Texas, USA, Nov. 2001.

[29] L. Dong, G. Xu and H. Ling, "Predictive downlink beamforming for wideband CDMA over Rayleigh fading channels," *IEEE Transactions on Wireless Communications*, vol. 4, no. 2, pp. 410-421, Mar 2005.

[30] F. R-Farrokhi, L. Tassiulas and K. J. Ray Liu, "Joint optimal power control and beamforming in wireless networks using antenna arrays," *IEEE Transactions on Communications*, vol. 46, No. 10, Oct. 1998.

[31] C. Farsakh and J. A. Nossek, "Spatial covariance based downlink beamforming in an SDMA mobile radio system," *IEEE Trans. on Vehicular Technology*, vol. 48, pp. 333-341, 1999.

[32] C. Farsakh and J. A. Nossek, "Application of SDMA to mobile radio," *In Proceedings of Int. Symp. Personal, Indoor Mobile Radio Communications (PIMRC'94)*, The Hague, Netherlands, pp. 736-739, Sept. 1994.

[33] D. D. Feldman and L. J. Griffiths, "A projection approach to robust adaptive beamforming," *IEEE Trans. Signal Processing*, vol. 42, pp. 867-876, Apr. 1994.

[34] D. Filho, C. Panazio, F. Cavalcanti and J. Romano, "On downlink beamforming techniques for TDMA/FDD Systems," *XIX Symposium on Brazilian Telecommunications (SBRT 2001)*, Fortaleza-CE, Brazil, Sept. 2001.

[35] G. J. Foschini, "Layered space-time architecture for wireless communication in a fading environment using multiple antennas," *Bell Labs Technical Journal*, vol. 1, no. 2, pp. 41-59, Autumn 1996.

[36] G. J. Foschini, "On limits of wireless communications in a fading environment when using multiple antennas," *Wireless Personal Communications*, vol. 6, pp. 311-335, 1998.

[37] G. J. Foschini and Z. Miljanic, "A simple distributed autonomous power control algorithm and its convergence," *IEEE Transactions on Vehicular Technology*, vol. 42, pp. 641-646, 1993.

[38] G. Ganesan and P. Stoica, "Space-time block codes: A maximum SNR approach," *IEEE Transactions on Information Theory*, vol. 47, no. 4, pp. 1650-1656, May 2001.

[39] A. B. Gershman, "Robust adaptive beamforming in sensor arrays," *AEU, International Journal of Electronics and Communications*, vol. 53, No. 6, pp. 305-314, 1999.

[40] A. B. Gershman, V. I. Turchin and V. A. Zverev, "Experimental results of localization of moving underwater signal by adaptive beamforming," *IEEE Transactions on Signal Processing*, vol. 43, pp. 2249-2257, Oct. 1995

[41] D. Gesbert, M. Shafi, D. Shiu and P. J. Smith, "From theory to practice: An overview of MIMO space-time coded wireless systems," *IEEE Journal on Selected Areas in Communications*, vol. 21, no. 3, pp. 281-302, Apr. 2003.

[42] L. E. Ghaoui and H. Lebret, "Robust solutions to least-squares problems with uncertain data matrices," *SIAM Journal on Matrix Analysis and Applications*, vol. 18, no. 4, pp. 1035-1064, Oct. 1996.

[43] S. A. Ghorashi, E. Homayounvala, F. Said and A. H. Aghvami, "Dynamic simulator for studying WCDMA based hierarchical cell structures," *12th IEEE International Symposium on Personal, Indoor and Mobile Radio Communications 2001*, San Diego, USA, vol. 1, pp. 32-37, Sept. 2001.

[44] L. C. Godara, "Applications of antenna arrays to mobile communications, part I: performance improvement, feasibility and system considerations," *In Proceedings of the IEEE*, vol. 85, no. 7, pp. 1031-1060, July 1997.

[45] L. C. Godara, "Applications of antenna arrays to mobile communications, part II: performance improvement, feasibility and system considerations," *In Proceedings of the IEEE*, vol. 85, no. 8, pp. 1195-1245, August 1997.

[46] L. C. Godara, "Handbook of antennas in wireless communications," *CRC Press*, 2002.

[47] J. Goldberg and J. R. Fonollosa, "Downlink beamforming for cellular mobile communications," *In Proceedings of IEEE Vehicular Technology Conference*, Phoenix, Arizona, USA, pp. 632-636, May 1997.

[48] G. H. Golub and C. F. Van Loan, "Matrix computations," *MD: John Hopkins Univ. Press*, Baltimore, 1996.

[49] M. Gudmundson, "Correlation model for shadow fading in mobile radio systems," *IEE Electronics Letters*, vol. 23, pp. 2145-2146, Nov. 1991.

[50] J. R. Guerci, "Theory an application of covariance matrix tapers for robust adaptive beamforming," *IEEE Trans. Signal Processing*, vol. 47, pp. 997-985, Apr. 1999.

[51] Y. Hara, D. K. Park and Y. Kamio, "Downlink beamforming method for multimedia CDMA/TDD systems," *Proceedings of European Wireless*, Florence, Italy, Feb. 2002.

[52] L. Häring, B. K. Chalise and A. Czylwik, "Dynamic system level simulator for W-CDMA with smart antennas," *COST 273 Technical Document TD (03)18*, 2003.

[53] B. M. Hochwald and T. L. Marzetta, "Adapting a downlink array from uplink measurements," *IEEE Transactions on Signal Processing*, vol. 49, pp. 642-653, Mar. 2001.

[54] H. Holma and A. Toskala, *WCDMA for UMTS*, John Wiley and Sons, ISBN 0471720518.

[55] K. Hugl, J. Laurila and E. Bonek, "Downlink beamforming for frequency-duplex systems," *IEEE Global Telecommunications Conference Globecom'99*, Rio de Janerio, Brazil, pp. 2097-2101, Dec. 1999.

[56] K. Hugl, K. Kalliola and J. Laurila, "Spatial reciprocity of uplink and downlink radio channels in FDD systems," *COST 273 Technical Document TD(02) 066*, 2002.

[57] S. Hyakin, "Adaptive filter theory," *Engelwood Cliffs*, NJ: Prentice-Hall, 2nd. edition, 1991.

[58] A. Pascual-Iserte, A. Perez-Neira and M. A. Lagunas, "A maxmin approach for robust MIMO design: combining OSTBC and beamforming with minimum transmission power requirements ," *In Proceedings of ICASSP 2004*, Montreal, Canada, May 2004.

[59] W. C. Jakes, *Microwave mobile communications*, John Wiley, New York, 1974.

[60] G. Joengren, M. Skoglund and B. Ottersten, "Combining beamforming and orthogonal space-time block coding," *IEEE Transactions on Information Theory*, vol. 48, no. 3, pp. 611-627, March 2002.

[61] N. L. Johnson and S. Kotz, *Continuous univariate distributions*, John Wiley, New York, 1970.

[62] Y. Kameda and J. Ohga, "Adaptive microphone-array system for noise-reduction," *IEEE Trans. Acous., Speech, Signal Processing*, vol. 34, pp. 1391-1400, Dec. 1986.

[63] S. Kandukuri and S. Boyd, "Optimal power control in interference-limited fading wireless channels with outage-probability specifications," *IEEE Transactions on Wireless Communications*, vol. 1, no. 1, Jan. 2002.

[64] K. Kopsa, R. Weinmann, V. Braun and M.Tangemann, "Performance of multiple antenna combining algorithms in the uplink of UTRA/FDD," *European Conference on Wireless Technology (ECWT 2000)*, Paris, France, pp. 122-125, Oct. 2000.

[65] E. G. Larsson and P. Stoica,*Space-time block coding for wireless communications*, Cambridge University Press, 2003.

[66] J. C. Liberti, Jr. and T. S. Rappaport, "Smart antennas for wireless communications: IS-95 and Third Generation CDMA Applications," *Prentice Hall*, New-Jersey, 1999.

[67] H. Liu and G. Xu, "Multiuser blind channel estimation and spatial channel preequalization," *In Proc. IEEE Int. Conf. Acoust. Speech and Signal Processing (ICASSP'95)*, Detroit MI, USA, pp. 1756-1760, May 1995.

[68] T. K. Y. Lo, "Maximum ratio transmission," *IEEE Transactions on Communications*, vol. 47, no. 10, pp. 57-60, Oct. 1999.

[69] R. Lorenz and S. Boyd, "Robust minimum variance beamforming," *IEEE Transactions on Signal Processing* vol. 53, no. 5, pp. 1684-1696, May 2005.

[70] D. J. Love and R. W. Heath, "Equal gain transmission in Multiple Input Multiple Output wireless systems," *IEEE Transactions on Communications*, vol. 51, no. 7, July 2003.

[71] D. R. Morgan, "Downlink adaptive array algorithms for cellular mobile communications," *IEEE Transactions on Communications*, vol. 51, no. 3, Mar. 2003.

[72] R. A. Monzingo and T. W. Miller, "Introduction to adaptive arrays," Wiley, NY, 1980.

[73] R. J. Muirhead, "Aspects of multivariate statistical theory," *Wiley Series in Probability and Mathematical Statistics*, Feb. 1982.

[74] J. Papandriopoulos, J. Evans and S. Dey, "A framework for joint power control and multiuser detection with outage probability specifications," *In Proceedings of IEEE Globecom 2003*, San Francisco, USA, Dec. 2003.

[75] A. Paulraj, B. Ottersten, R. Roy, A. Swindelhurst, G. Xu and T. Kailath, "Subspace methods for direction finding and parameter estimation," *in Handbook of Statistics Volume 10 "Signal Processing and its Applications"*, Elsevier Science Publishers B. V., 1992.

[76] A. Paulraj and C. B. Papadias, "Array processing for mobile communications," Chapter in CRC *Handbook on Signal Processing*, Ed. M. Kaveh, CRC Press, 68.1-16, December 1997.

[77] A. J. Paulraj and C. B. Papadias, "Space-time processing for wireless communications," *IEEE Signal Processing Magazine*, pp. 49-83, Nov. 1997.

[78] K. I. Pedersen, P. E. Mogensen, "The downlink orthogonality factors influence on WCDMA system performance," *In Proceedings of IEEE Vehicular Technology Conference VTC'02 Fall*, Vancouver, Canada, Sept. 2002.

[79] M. Pettersen, L. E. Braten and A. G. Spilling, "An evaluation of adaptive antennas for UMTS FDD by system simulations," *In Proceedings of IEEE Vehicular Technology Conference VTC'03 Fall*, Orlando, USA, March 2003.

[80] J. G. Proakis, "Digital communications," *McGraw-Hill International Edition*, 2001.

[81] G. G. Raleigh, S. N. Diggavi, V. K. Jones and A. Paulraj, "A blind adaptive transmit antenna algorithm for wireless communication," *IEEE International Conference on Communications (ICC 95)*, Seattle, USA, vol. 3, pp. 1494-1499, June, 1995 .

[82] G. Raleigh and J. M. Cioffi, "Spatial-temporal coding for wireless communications," *IEEE Transactions on Communications*, vol. 46, pp. 357-366, 1998.

[83] T. S. Rappaport, "Wireless communications - principles and practice," *Prentice Hall*, 2002.

[84] J. Riba, J. Goldberg and G. Vazquez, "Robust beamforming for interference rejection in mobile communications," *IEEE Trans. Signal Processing*, vol. 45, pp. 271-275, Jan. 1997.

[85] T. P. Runarsson and X. Yao, "Stochastic ranking for constrained evolutionary optimization," *IEEE Transactions on Evolutionary Computation*, vol. 4, no. 3, pp. 284-294, Sept. 2000.

[86] S. Shahbazpanahi, A. B. Gershman, Z-Q. Luo and K. M. Wong, "Robust adaptive beamforming for general-rank signal models," *IEEE Transactions on Signal Processing*, vol. 51, no. 9, pp. 2257-2269, Sept. 2003.

[87] J. Salz and J. H. Winters, "Effect of fading correlation of adaptive arrays in digital mobile radio," *IEEE Transactions on Vechicular Technology*, pp. 1049-1057, Nov. 1994.

[88] M. Schacht, A. Dekorsy and P. Jung, "Downlink beamforming concepts in UTRA FDD," *KleinheubacherTagung*, Germany, 2003.

[89] B. Sklar, "Rayleigh fading channels in mobile digital communication systems part I: characterization," *IEEE Communications Magazine*, July, 1997.

[90] M. R. Sturgill, Siavash M. Alamouti, *Simulator-based design methodology for wireless communications systems*, http://www.cadence.com.

[91] J. F. Sturm, "Using SeDuMi 1.02, A MATLAB toolbox for optimization over symmetric cones," *http://fewcal.kub.nl/ sturm*, 2001.

[92] S. C. Swales, M. A. Beach, D. J. Edwards and J. P. McGreehan, "The perfromance enhancement of multibeam adaptive BS antennas for cellular land mobile radio systems," *IEEE Transactions on Vehicular Technology*, vol. 39, pp. 56-67, Feb. 1990.

[93] V. Tarokh, H. Jafharkani and A. R. Calderbank, "Space-time block codes from orthogonal designs," *IEEE Transactions on Information Theory*, vol. 45, no. 5, pp. 1456-1467, July 1999.

[94] V. Tarokh, N. Seshadri and A. R. Calderbank, "Space-time codes for high data rates wireless communication: performance criterion and code construction," *IEEE Transactions on Information Theory*, vol. 44, no. 2, pp. 744-765, March 1998.

[95] E. Telatar, "Capacity of multi-antenna Gaussian channels," *European Transactions on Telecommunications*, vol. 10, pp. 585-595, Nov.-Dec. 1999.

[96] Y. Tokgoz and B. D. Rao, "Outage probability of multi-cellular MIMO systems in Rayleigh fading," *In Proceedings of IEEE ICASSP'04*, Montreal, Canada, May 2004.

[97] J. Tsai and B. D. Woerner, "The fading correlation function of a circular antenna array in mobile radio environment," *In Proceedings of IEEE Global Telecommunications Conference (GLOBECOM'01)*, San Antonio, Texas, USA, vol. 5, Nov. 2001.

[98] W. Utschick and J. A. Nossek, "Downlink beamforming for FDD mobile radio systems based on spatial covariances," *In Proceedings of the European Wireless 99 and ITG Mobile Communications*, Munich, Germany, pp. 65-67, 1999.

[99] E. Visotsky and U. Madhow, "Optimum beamforming using transmit antenna arrays," *IEEE In Proceedings of IEEE Vehicular Technology Conference VTC'99*, Amsterdam, Netherlands, vol. 1, pp. 851-856, Sept. 1999.

[100] S. A. Vorobyov, A. B. Gershman and Z-Q. Luo , "Robust adaptive beamforming using worst-case performance optimization: A solution to the signal mismatch problem," *IEEE Transactions on Signal Processing*, vol. 51, no. 2, Feb. 2003.

[101] S. Widrow and B. Stearns, "Adaptive signal processing," *Engelwood Cliffs*, NJ: Prentice-Hall, 1985.

[102] B. Wild and A. Majumdar, "A novel solution to the optimum transmit beamforming problem," *http://citeseer.nj.nec.com/574896*.

[103] J. H. Winters, "Smart antennas for wireless systems," *IEEE Personal Communications*, pp. 23-27, Feb. 1998.

[104] J. H. Winters, "Optimum combining in digital mobile radio with Co-channel interference," *IEEE Tranactions on Vehicular Technology*, vol. 33, no. 3, pp. 144-155, Aug. 1984.

[105] A. Zanella, M. Chiani and M. Z. Win, "On the convergence of steepest descent and least mean-square algorithms for MIMO Systems," *In Proceedings of IEEE International Conference on Communications, ICC'04*, Paris, France, June 2004.

[106] P. Zetterberg, *Mobile cellular communications with base station antenna arrays: spectrum efficiency, algorithms and propagation models*, Ph.D. Thesis, Royal Institute of Technology, Stockholm, Sweden, 1997.

[107] S. Zhou and G. B. Giannakis, "Adaptive modulation for multi-antenna transmissions with channel mean feedback," *In Proceedings of IEEE International Conference on Communications, ICC'03*, Seattle, USA, May 2003.

[108] S. Zhou and G. B. Giannakis, "Optimal transmitter eigen-beamforming and space-time block coding based on channel mean feedback," *IEEE Transactions on Signal Processing*, vol. 50, no. 10, Oct 2002.

[109] M. D. Zoltowski, "On the performance of the MVDR beamformer in the presence of correlated interference," *IEEE Transactions on Acoustics, Speech, Signal Processing*, vol. 36, pp. 945-947, June 1998.